TITLE Electron Transport in Systems of Reduced Dimensionality

AUTHOR Philip Keith Milsom

UNIVERSITY University of Warwick (1987)

Electron Transport in Systems of Reduced Dimensionality

by

Philip Keith Milsom

A Thesis
presented to the University of Warwick
in partial fulfilment of the requirements
for entry to the degree of
Doctor of Philosophy
Department of Physics
June 1987

ABSTRACT

The Boltzmann equation is modified to examine the effects of a range of scattering mechanisms on the DC conductivity of semiconductor material in the form of thin sheets and fine wires.

This is solved exactly for elastic scattering mechanisms by introducing a set of momentum relaxation times which are relevant to the occupied sub-bands. These times are calculated for alloy scattering, surface roughness scattering and the acoustic phonon mechanisms at high temperatures.

At low temperatures the inelasticity of the acoustic phonon mechanisms is taken into account and a variational method is employed. At very low temperatures we show that the acoustic deformation potential gives rise to a mobility which varies at T^{-5}.

We use an iterative method to examine the strongly inelastic polar optic phonon scattering mechanism in a wire. Ridley has suggested that the momentum relaxation time may be negative in this system. We introduce a time relevant to transport measurements and this is found to be positive. It is shown that the time derived by Ridley may be of relevance to time resolved transport measurements.

CONTENTS

ACKNOWLEDGEMENTS

There are many people who have helped me to reach this stage. I would like to thank some of them here.

My parents for support and encouragement.

Professor P N Butcher for excellent supervision and patient guidance.

My colleagues at Warwick, for their friendship and conversation.

Professor A J Forty for use of the facilities of the Physics Department and the SERC for financial support.

Finally, to Mrs C Edge for her dedication to the typing of this thesis.

DECLARATION

This thesis contains an account of my own independent research work performed in the Department of Physics at the University of Warwick between October 1983 and October 1986 under the supervision of Professor Paul N Butcher.

Some of the work has previously been published:

"Phonon Limitations to the metallic conductivity of a quasi two-dimensional semiconductor structure", P K Milsom and P N Butcher, Journal of Semiconductor Science and Technology 1, 58 (1986).

CHAPTER 1

INTRODUCTION

In bulk semiconductors, when the de Broglie wavelength λ_B is much smaller than the size of the sample, the electron is considered to behave as a classical particle and the transport properties of the material are normally calculated with the Boltzmann transport equation (Butcher (1973)). Reasonable agreement is obtained with experiment (Rode (1975)). However, classical arguments are not valid if the de Broglie wavelength is no longer small when compared to some typical constraining dimension. For example, when λ_B becomes large when compared to a cyclotron orbit in a material it is necessary to modify the Boltzmann equation (Bridges (1980)) to explain experimental data.

In this thesis we consider a similar problem although the dimensional constraint does not arise from the application of a field but from the structure of the material. Advanced fabrication techniques, eg molecular beam epitaxy (MBE) and metal organic chemical vapor deposition (MOCVD) can produce samples in which one or more dimensions are comparable with the electron wavelength. The scale of these systems means that the bandstructure is no longer just a function of the material but it is also dependent on the device dimensions. This has given rise to a new branch of technology termed "bandstructure engineering". Esaki and Chang exploited this with their pioneering work on superlattices (1974). It was found that these devices possessed some unusual properties by virtue of their regularity and scale. Transport measurements perpendicular to the layers which make up the superlattice are difficult. Attention has been focussed on the motion of the electrons parallel to the interfaces in thin films and also in fine semiconductor wires. Typical examples include the MOSFET (see Figure 1.1a) and quantum well (see Figure (1.2). In both of

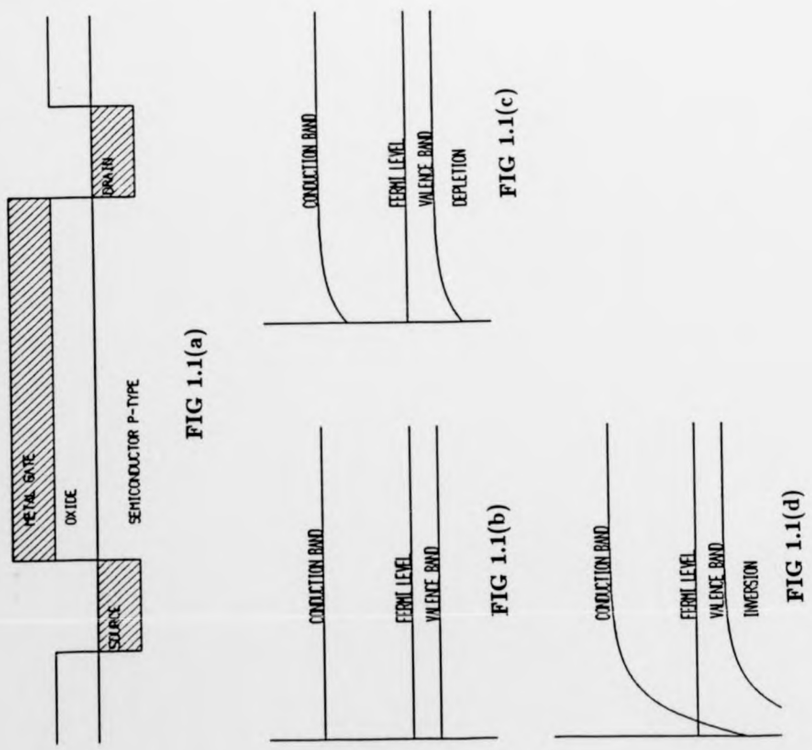

FIG 1.1(a)

FIG 1.1(c)

FIG 1.1(b)

FIG 1.1(d)

FIG 1.1

The p-type M.O.S.F.E.T. and the effect of applying a gate voltage. Fig 1.1(d) shows the inverted state.

these examples the electrons behave as if they are dynamically two-dimensional. We concentrate on the parallel transport problem in this thesis.

Historically, the MOSFET has an importance which ranks it alongside the bipolar transistor, indeed Shockley and Pearson produced the first patents (Ando (1982)) and this device can now possess extremely large electronic mobilities ($\sim 10^6 cm^2/Vsec$, Di Lorenzo (1982)). It also lends itself to planar integration and research in this area has increased because of the drive to large scale integration. Experimentally it is interesting because the areal electron density can be varied at will by the application of a gate voltage to the surface plane of the device, enabling a range of experiments to be carried out on one sample, removing uncertainties in device reproducibility which arise when measurements are taken from a device batch.

When a positive gate voltage is applied to a p-type MOSFET (see Figure 1.1), electrons are drawn through the p-type semiconductor and are held at the oxide/semiconductor interface, where they neutralise the holes, giving rise to a depletion region. Eventually enough electrons reside near the surface to neutralise the holes completely in a narrow region. The p-type semiconductor then begins to behave as if it had an n-type surface and an inversion layer is formed. Classically, we would expect the charge density to decay exponentially as we move away from the semiconductor/insulator surface. However the length scale of this decay is so short that quantum effects are important and a proper description of the problem involves a self-consistent solution of the Shroedinger and Poisson equations (Ando (1982)).

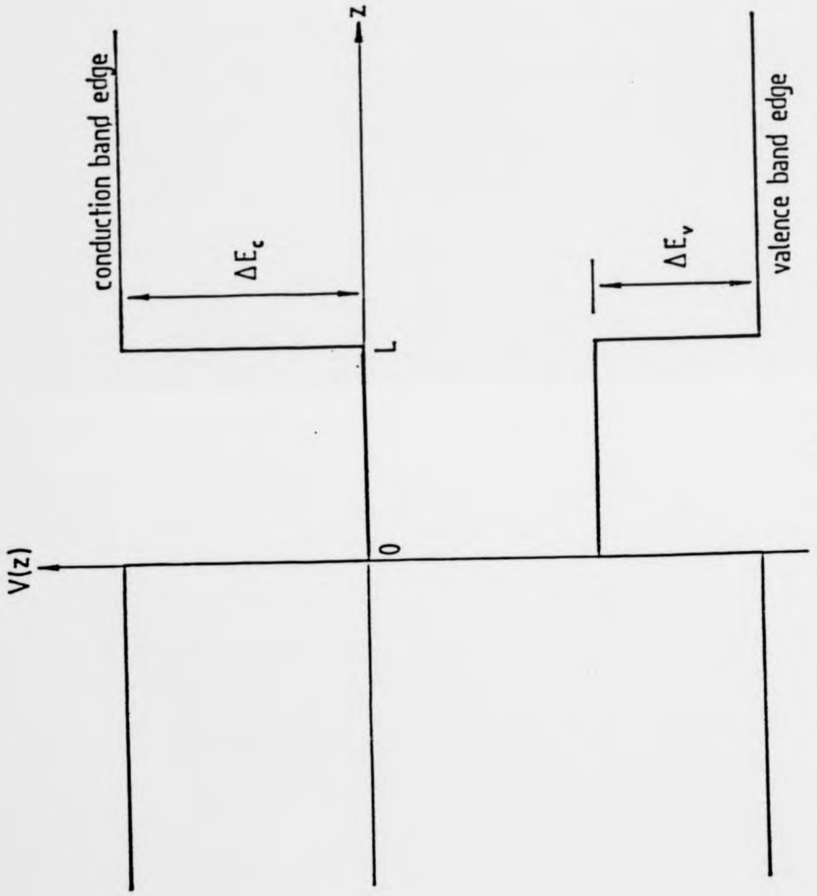

FIG 1.2 The quantum well indicating the conduction band offsets for the GaAs/GaAlAs system.

The applied gate voltage can also be considered to bend the bandstructure of the semiconductor near the interface. In figure 1.1b we see the situation when the gate voltage is zero. As it is increased the conduction band edge can be considered to bend towards the Fermi-level which still lies in the band-gap (Figure 1.1c). Eventually the band is bent to such an extent that it dips below the Fermi level (Figure 1 1d) and electrons can travel freely in a direction parallel to the surface, but motion away from the surface is inhibited by the transverse potential well. This is the inverted state.

As well as producing a two-dimensional electron gas by applying an electric field to a material it is also possible to produce a quantum well by introducing an artificial conduction band edge discontinuity. The classic example is the GaAs/$Al_xGa_{1-x}As$ quantum well, see Figure 1.2. The similarity in atomic size between Ga and Al makes it possible to fabricate high purity quantum wells which are relatively free from surface strain fields (Adachi (1985)). In this case the materials have different band gaps and it is now well known that when the materials are in close electronic contact the conduction band edges align in such a way that an electron residing in the GaAs sees a potential barrier as it tunnels into the $Al_xGa_{1-x}As$ and this is typically equal to 831xmeV (Okumura (1985)). If the well is narrow enough then electrons with energies lower than this will behave as a two-dimensional electron gas (2-DEG).

Work is also being carried out on quantum well wires which can be produced in free standing form (Kelly (1984)). In this case both of the wires dimensions (they usually have rectangular cross-section) are small enough for the electrons to behave as a one-dimensional electron gas (1-DEG). The finite (but small) dimensions of both types of system (1-DEG and 2-DEG) means that they are, strictly speaking, quasi-one-dimensional and quasi-two-dimensional, it is often this feature which gives rise to the major effects

considered in this thesis.

In Chapter 2 we show that the energy eigenstates in these systems can be described in terms of two-dimensional and one-dimensional bandstructures. The dimensional constraints split the usual three-dimensional bands into two-dimensional bands (Ridley (1982)) and one-dimensional bands which are usually termed sub-bands, and this has severe consequences for the transport coefficients. In the case of the 2-DEG we introduce a two-dimensional Boltzmann equation for each sub-band (Chapter 3). These are subsequently coupled together by inter-sub-band scattering off impurities and imperfections. These ideas naturally extend to the one-dimensional systems. In using the Boltzmann equation we neglect localisation effects which have excited a great deal of interest in recent years (Lee and Ramakrishnan (1985)). Nevertheless, these effects appear as small corrections to the Boltzmann conductivity and it is therefore important to appreciate the magnitude of the latter before any estimate of the localisation effects can be obtained from the experimental data.

Similar problems have been considered by previous authors. The earliest examples stem from conductivity measurements on thin films of Bismuth (Ogrin (1966)). Ogrin observed a non-monatonic resistivity variation with film thickness and this was explained by Freeman et al (1977) in terms of the quantum confinement of the electrons. As the films get thicker it is possible for the electrons to occupy more than one sub-band and inter-sub-band scattering also becomes possible. This drastically reduces the mobility and this manifests itself in conductivity dips: the so called quantum size effects.

It was only recently that MBE and MOCVD have made it possible to construct

semiconductor devices in which these effects are easily seen (Stormer (1981)). This has led to a detailed theoretical investigation in two-dimensions and one-dimension of the relative importance of the scattering mechanisms which are known to be important in bulk semiconductors. Ridley (1982, 1983, see also Riddoch (1985)) has provided an insight into these problems with the aid of his scattering rate formulae and he has considered various mechanisms including the acoustic deformation potential, piezoelectric and polar optic phonon scattering in both one and two-dimensional systems. Johnson and Vassell (1984) have adopted a similar approach in 1-DEG's. Basu and Nag (1981) have looked at the extreme quantum limit when only one sub-band is occupied and have considered a strictly two-dimensional system.

Siggia and Kwok (1970) solved the Boltzmann equation exactly for elastic scattering in two-dimensional systems using a relaxation time approach. The solution was presented as a formal framework and the equations were not applied to specific scattering mechanisms. We use the equations of Siggia and Kwok to reconsider acoustic phonon scattering, alloy scattering and surface roughness scattering in 2-DEG's. The model for the rough interface was suggested by Bruce Joyce (Philips, Redhill) and is considered in detail in section 5.2.3. This is an improvement on previous attempts which used simple Gaussian autocorrelation models for the interface (Ando (1982)). A set of relaxation times similar to those of Siggia and Kwok are derived for one-dimensional systems and these are applied to the acoustic phonon mechanisms. The effects of inter-sub-band scattering are found to be particularly important in one-dimension.

The Siggia and Kwok equations are only valid for elastic scattering mechanisms. They fail for inelastic mechanisms but approximate solutions may be found using a variational method (see Chapter 6). This is applied to the acoustic phonon mechanism at low temperatures in both one and two-dimensional systems. This method should be of general applicability to inelastic mechanisms but it is not applied to the polar optic phonon mechanism in two-dimensions as Vinter (1984) presents an exact solution using an iterative approach (see Rode (1970)). The iterative approach is extended to the 1-DEG and an effective relaxation time is derived for polar optic phonon scattering. This is compared to the momentum relaxation rate due to Ridley (1983), which was derived by weighting the scattering rate by the fractional change in electron momentum. Ridley's approach neglects the electron statistics and predicts that in some circumstances the momentum relaxation time may be negative. We find that our effective relaxation time is positive.

In Chapter 2 we discuss the form of the wavefunctions in one and two-dimensional electron gases, and the concept of a sub-band structure is introduced. Chapter 3 is devoted to the transport equations describing the dynamics of the electrons. The behaviour of the electrons under the influence of elastic points scatterers is considered in Chapter 4. In Chapter 5 we derive momentum relaxation times for extended defect scatterers. In Chapter 6 we introduce a variational method to describe the effects of inelasticity. The transformation between elastic scattering and inelastic scattering is considered and the equations are applied to the acoustic phonon mechanisms at low temperatures. An analytic form for the low temperature phonon limited mobility is derived in both one and two-dimensions. In Chapter 7 we use an exact method to look at momentum relaxation in a 1-DEG when only one sub-band is occupied and the dominant scattering mechanism is due to polar optic phonons. In Chapter 8 we

consider approximations involved in the Boltzmann equation and, in particular, consider ways in which lifetime broadening and screening effects may be included in the analysis. The structure of the potential responsible for alloy scattering is also considered in some detail.

CHAPTER 2

SMALL SYSTEMS WITHOUT SCATTERING

2.1 Wavefunctions

In this chapter we consider the form of the wavefunctions in small scale systems. We do not look at the details but use approximations which make the calculations simpler whilst still embodying the physics. In solving these problems it is usual to use the effective mass approximation (see Ridley (1982), Okumura (1985), Warren (1986) and Appendix 1). We consider the simplest case where we have a thin sheet of semiconducting material containing the electrons. We suppose that the electrons in the layer behave as if they have a scalar effective mass m* which is taken to have the same value as in bulk GaAs (0.066-Rode (1975)). The electrons are strongly confined in the semiconductor layer and we approximate this potential by an infinitely deep square potential well. The effective mass Schroedinger equation can then be written as (Collins (1985))

$$\frac{-\hbar^2}{2}\,\underline{\nabla}\cdot\frac{\underline{\underline{1}}}{m^*}\cdot\nabla\psi_n + V\psi_n = \epsilon_n\psi_n \qquad (2.1)$$

where V is the square potential

$$V(\underline{r},z) = 0 \qquad 0 < z < L$$
$$= \infty \qquad z < 0, z > L \qquad (2.2)$$

with $\underline{r} = (x,y)$ and L is the thickness of the sheet.

Hence we may write,

$$\epsilon_n(\underline{k}) = E_n + \epsilon(\underline{k}) \qquad (2.3)$$

where

$$E_n = \frac{\hbar^2}{2m^*}\left[\frac{n\pi}{L}\right]^2 \qquad \text{and} \qquad \epsilon(\underline{k}) = \frac{\hbar^2\underline{k}^2}{2m^*} \qquad (2.4)$$

FIG 2.1

The two-dimensional sub-band ladder and density of states, the envelope of the staircase gives the energy behaviour of the 3-D density of states.

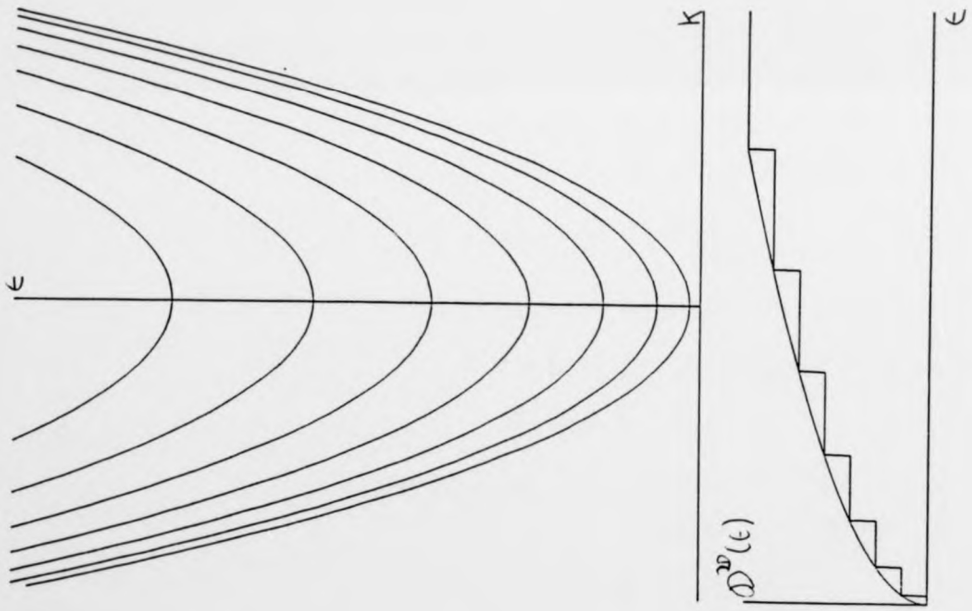

Where E_n is the energy marking the bottom of the n'th sub-band and $\epsilon(\underline{k})$ defines the two-dimensional sub-band parabolas. The sub-band wavefunctions have the form

$$\psi_n(\underline{k},\underline{x},z) = \left[\frac{2}{V}\right]^{\frac{1}{2}} \sin \frac{n\pi z}{L} \; e^{i\underline{k}\cdot\underline{x}} \qquad (2.5)$$

where $\underline{k}$ is a two-dimensional wave-vector and V is the volume of the electron cavity. Throughout we shall assume that periodic boundary conditions apply in the plane of the layer, restricting the values of $\underline{k}$ in a square of semiconductor of area B^2 to

$$\underline{k} = \left[\frac{2\pi n}{B}, \frac{2\pi m}{B}\right] \qquad (2.6)$$

where n and m are integers. The energies in 2.3 can be plotted to give a sub-band ladder (see Figure 2.1). We shall see later that the sub-band structure has severe consequences for the transport properties of small devices.

By analogy with the two-dimensional result the electrons confined in one-dimensional wire with rectangular cross-section (width a, depth b) will have eigenvalues given by

$$\epsilon_{nm}(k) = \frac{\hbar^2}{2m^*}\left[k^2 + \left[\frac{n\pi}{a}\right]^2 + \left[\frac{m\pi}{b}\right]^2\right] \qquad (2.7)$$

where n and m are sub-band labels and k is a one-dimensional wavenumber. The sub-band wavefunctions being given by (Ridley (1983))

$$\psi_n(\underline{k},x,y,z) = \frac{2}{V^{\frac{1}{2}}} \sin \frac{n\pi x}{a} \sin \frac{m\pi y}{b} \; e^{ikz} \qquad (2.8)$$

If we allow the wavefunctions to leak out of a two-dimensional well, then a solution of the Schroedinger equation may still be effected using the separation of variables method, but care must be taken in conserving the quantum-mechanical current at the boundary and this results in matching $\frac{1}{m^*}\nabla\psi$ and ψ (Collins (1985)). In a one-dimensional system, however, this requirement at the corners of any square-well model means that the separation of variables method is no longer useful and the wavefunctions for the system are complicated. Throughout we shall use sinusoidal wavefunctions in order to discuss phonon scattering and the leaky wavefunctions when we are considering surface roughness and alloy scattering in two-dimensional systems. This choice reflects the symmetry of the situation in a quantum well but may not accurately represent the wavefunctions in a heterojunction or a MOSFET. Here the situation is inherently asymmetric because of the presence of only one material interface. The other potential barrier is due either to the application of a gate voltage in the case of a MOSFET (Ando (1982)) or to the electrostatic attraction of the carriers for the donors in the case of a heterojunction. A full treatment of this problem involves the self-consistent solution of the Schroedinger and the Poisson equation, (Ando (1982), Vinter (1984) and Bastard (1983)). The numerical methods which this necessitates tend to obscure the physics of the problem. Fang and Howard (1966) appreciated this point and proposed a form for the wavefunction in the lowest sub-band.

$$\zeta_1(z) = \left[\frac{b^3}{2}\right]^{\frac{1}{2}} z e^{-bz} \qquad z > 0$$

$$= 0 \qquad z < 0 \qquad (2.9)$$

where b is determined by a variational calculation. This functional form is expected to represent the wavefunction in a MOSFET fairly accurately. It vanishes at z=0 (the oxide/semiconductor interface) and tends to zero as z tends to infinity. The form (2.9) is only useful when electrons are in the lowest sub-band and is not useful for treating inter-sub-band scattering,

which we discuss in Chapter 3. Most of the structure in the transport coefficients involves inter-sub-band scattering and sinusoidal sub-band wavefunctions provide a convenient first approach to calculating the sort of structure that may be expected to arise.

2.2 Density of States in Reduced Dimensionality Systems

In three dimensions the density of states is defined as the number of states in $\underline{k}$ space per unit energy range per unit volume. In three dimensions this vanishes for $\epsilon < 0$ and is proportional to $\epsilon^{1/2}$ for $\epsilon > 0$. In two dimensions the density of states per unit area for the lowest sub-band can be written as

$$D(\epsilon) = \frac{2}{(2\pi)^2} \times 2\pi k \frac{dk}{d\epsilon} \theta(\epsilon - E_1)$$

$$= \frac{m^*}{\pi\hbar^2} \theta(\epsilon - E_1) \qquad (2.10)$$

where we have included spin degeneracy and the sub-band has been assumed to be "circular and parabolic". When more than one sub-band is occupied the density of states is

$$D(\epsilon) = \sum_n \frac{m^*}{\pi\hbar^2} \theta(\epsilon - E_n) \qquad (2.11)$$

where θ denotes the unit step function. The main difference between three-dimensional and two-dimensional systems is seen in this functional form. In three dimensions the density of states is a continuous function of energy. In two dimensions it is constant over a range of energies but it possesses abrupt step-like discontinuities (see Figure 2.1). The envelope of this staircase increases as $\epsilon^{1/2}$ and this is an indication that these systems behave with a three-dimensional character when a large number of sub-bands are occupied.

Scattering can smooth out the discontinuities in the density of states (see

FIG 2.2
The one-dimensional sub-band structure and density of states indicating the $\epsilon^{-\frac{1}{2}}$ discontinuities.

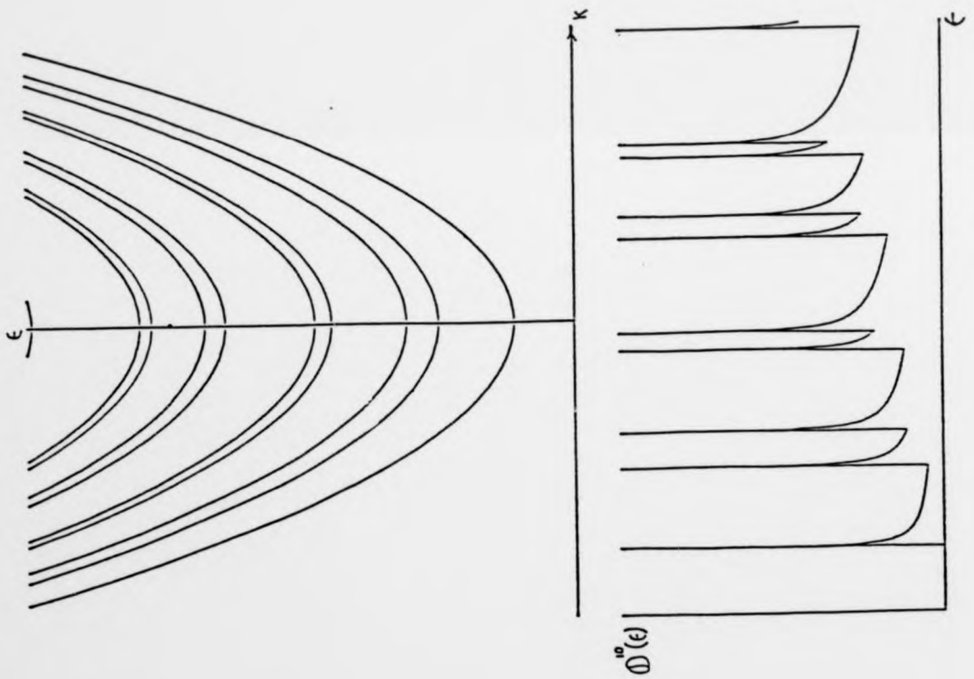

Cantrell and Butcher (1985) and Chapter 8). This is a second order effect due to the finite lifetime of the carriers which we neglect here. This approach is the only one which is viable if realistic scattering mechanisms are to be included. So far as we are aware smoothing has only been taken into account for delta function scattering centres.

In one-dimensional systems the density of states has the form (see Figure 2.2)

$$D(\epsilon) = \sum_{nm} \frac{1}{\pi\hbar} \left[\frac{m^*}{2(\epsilon - E_{nm})}\right]^{\frac{1}{2}} \theta(\epsilon - E_{nm}) \qquad (2.12)$$

and shows square-root singularities at the sub-band energies, consequently inter-sub-band scattering is particularly important in this case (see Chapter 4).

CHAPTER 3

SYSTEMS WITH SCATTERING

3.1 Introduction

Throughout we shall work within the Boltzmann framework. We shall not be concerned with the detailed behaviour of the individual electrons in the system but with macroscopic averages over their phase space trajectories. We shall be satisfied with determining the average density of electrons in the phase space of each sub-band and to do this we modify the three-dimensional Boltzmann equation to take account of the sub-band structure.

3.2 The Boltzmann Equation in Two-Dimensional Systems

We introduce a distribution function $f(\underline{k},n,\underline{r},t)$ which is defined as the probability of finding an electron in sub-band n with momentum $\underline{k}$ at time t with spin up. This concept violates the uncertainty principle but if we assume $\underline{r}$ is known to an accuracy $\Delta\underline{r}$ and the electron wavepacket has momentum $\underline{k}$ with a spread $\Delta\underline{k}$ such that $\Delta\underline{r}\Delta\underline{k} \sim \hbar$, then this specification is correct within $\Delta\underline{r}$ and $\Delta\underline{k}$ and is sufficient for our needs (Butcher (1973)).

Since electrons are conserved we can equate the increase of $f(\underline{k},n,\underline{r},t)$ to the four-dimensional divergence plus a term which corresponds to the rate of increase of f due to collisions (see Rode (1975) for three-dimensional arguments).

$$\frac{\partial f^n}{\partial t} = - \underline{\nabla}.(f^n\underline{v}^n) - \underline{\nabla}_{\underline{k}}\cdot(f^n\underline{F}'^n) + \left[\frac{\partial f^n}{\partial t}\right]_c \qquad (3.1)$$

where we have used the shorthand notation $f^n = f(\underline{k},n,\underline{r},t)$ and $\underline{v}^n$ is the velocity of an electron in sub-band n with momentum $\underline{k}$.

$\underline{F}'$ is defined as

$$\underline{F}' = \frac{-e}{\hbar}\left[\underline{E} + \underline{v}^n \wedge \underline{B}\right] \qquad (3.2)$$

Equation (3.1) is very similar to the usual three-dimensional Boltzmann equation except that this takes scattering between bands into account. Inter-band scattering is usually neglected in elementary treatments of electron transport in three-dimensions. It is important in the conduction bands of Silicon and Germanium which have several equivalent minima (Ando (1982)), and it is important in GaAs at fields which are high enough for the electrons to transfer to satellite valleys (**Ridley & Watkins** (1961)). In our two-dimensional problem we shall see that the scattering of electrons between sub-bands is very important. Transport in each sub-band is described by a separate Boltzmann equation (3.1) and these are coupled together by inter-sub-band scattering terms in $\left[\frac{\partial f^n}{\partial t}\right]_c$. Let us look at the form of $\left[\frac{\partial f^n}{\partial t}\right]_c$ in detail.

We consider our two-dimensional semiconducting layer to have a surface area A. The number of electrons which may be scattered per unit time from $\underline{dk}$ around $\underline{k}$ in sub-band n to $\underline{dk'}$ around $\underline{k'}$ in sub-band m is given by

$$2\left[\frac{A}{4\pi^2}\right]^2 f(\underline{k},n,\underline{r},t)\left[1-f(\underline{k'},m,\underline{r},t)\right]P(\underline{k},n,\underline{k'},m)\,dkdk' \qquad (3.3)$$

where we are assuming that the spin of the electrons remains unchanged in the collision process and $P(\underline{k},n;\underline{k'},m)$ is the transition rate. The reverse process is also possible so the rate of increase of the number of electrons in $\underline{dk}$, around $\underline{k}$ per unit area of sub-band n is

$$-\frac{1}{2\pi^2}\,\frac{A}{4\pi^2}\sum_{mn}\int_{k'}\Big[f(\underline{k},n,\underline{r},t)[1-f(\underline{k'},m,\underline{r},t)]P(\underline{k},n,\underline{k'},m)$$

$$-f(\underline{k'},m,\underline{r},t)[1-f(\underline{k},n,\underline{r},t)]P(\underline{k'},m,\underline{k},n)\Big]dkdk' \qquad (3.4)$$

All transitions are assumed to take place instantaneously and as we are not applying a magnetic field the distribution function is independent of electron spin. The scattering rate is given by

$$\left[\frac{\partial f(\underline{k},n,\underline{r},t)}{\partial t}\right]_c = \frac{-A}{4\pi^2}\sum_m \int_{k'} \Big[f(\underline{k},n,\underline{r},t)[1-f(\underline{k}',m,\underline{r},t)]P(\underline{k},n;\underline{k}',m) - f(\underline{k}',m,\underline{r},t)[1-f(\underline{k},n,\underline{r},t)]P(\underline{k}',m';\underline{k},n)\Big] dk' \tag{3.5}$$

The Boltzmann equations for the sub-bands form a set of coupled integro-differential equations which can only be solved approximately. If we assume the scattering rates $P(\underline{k},n;\underline{k}',m)$ and $P(\underline{k}',m;\underline{k},n)$ correspond to the energies $\epsilon_n(\underline{k})$ and $\epsilon_m(k')$ then detailed balance implies that (Butcher (1973))

$$P(\underline{k},n;\underline{k}',m)\exp\frac{-\epsilon_n(\underline{k})}{K_B T} = P(\underline{k}'m;\underline{k},n)\exp\frac{-\epsilon_m(\underline{k}')}{K_B T} \tag{3.6}$$

where K_B is Boltzmann's constant and T is the temperature. In the absence of applied fields in equilibrium the integrand in (3.5) must be zero. Hence

$$\frac{f'}{1-f'}\exp\frac{\epsilon'}{K_B T} = \frac{f}{1-f}\exp\frac{\epsilon}{K_B T} \tag{3.7}$$

Both sides of (3.7) must equal a constant which gives

$$f = f_o \equiv \frac{1}{e^{(\epsilon-\epsilon_F)/k_B T}+1} \tag{3.8}$$

The Fermi-Dirac function is the zeroth order solution to the Boltzmann equation. This solution is only the solution if there exists some inelastic mechanism for which $\epsilon \neq \epsilon'$. We assume the Fermi-Dirac distribution function has been established and we look at small deviations away from this due to

the application of an electric field to an homogeneous system. We consider the electric field to be small so that the new distribution function is only slightly different from f_o. We write

$$f^n(\underline{k}) = f_o(\epsilon_n(\underline{k})) + f_1^n(\underline{k}) \tag{3.9}$$

where f_1^m is of first order in smallness. If we substitute (3.9) into (3.5) we find that to first order the collision term may be written in the linearised form

$$\left[\frac{\partial f_1^n}{\partial t}\right]_c$$

$$= \sum_m \int \Big[f_1^m(\underline{k}') \Big[\left[1-f_o(\epsilon_n(\underline{k}))\right] P(\underline{k}',m;\underline{k},n) + f_o(\epsilon_n(\underline{k}))P(\underline{k},n;\underline{k}',m) \Big]$$

$$- f_1^n(\underline{k}) \Big[\left[1-f_o(\epsilon_m(\underline{k}'))\right] P(\underline{k},n;\underline{k}',m) + f_o(\epsilon_m(\underline{k}'))P(\underline{k}',m;\underline{k},n) \Big] \Big] \frac{A}{4\pi^2} \, d^2k' \tag{3.10}$$

After some manipulation we find that, in the absence of magnetic fields, the linearised steady state Boltzmann equation reads

$$-\frac{e}{\hbar} \underline{E}\cdot\underline{\nabla}_{\underline{k}} f_o(\epsilon^n(k)) = \left[\frac{\partial f_1^n}{\partial t}\right]_c \tag{3.11}$$

The value of f_1 determined from (3.11) can be used to determine the low field transport coefficients relevant to two-dimensional systems. We define a current flux per unit length $\underline{J}$ which describes the flow of electrons in the channel. This current is carried by the electrons in the different sub-bands, to obtain the value of $\underline{J}$ we must sum over all these contribution

so that, taking spin degeneracy into account,

$$\underline{J} = \frac{-e}{2\pi^2} \sum_n \int f^n(\underline{k}) \underline{V}^n(\underline{k}) d^2k \qquad (3.12)$$

where $\underline{V}^n(\underline{k})$ is the velocity of an electron in the n'th sub-band with wave-vector $\underline{k}$. Now, f_o is of even parity in $\underline{k}$ and $\underline{V}^n(\underline{k})$ is odd, so to first order

$$\underline{J} = \frac{-e}{2\pi^2} \sum_n \int f_1^n(\underline{k}) \underline{V}^n(\underline{k}) d^2k \qquad (3.13)$$

Now that we have laid the framework we have to consider how specific mechanisms influence the value of f_1^n to limit the conductivity of the 2-DEG. We could solve equations (3.10) and (3.1) exactly with an iterative method (Rode (1975), Fletcher and Butcher (1972)) for all mechanisms, but it transpires that these equations can be solved exactly for elastic mechanisms (Siggia and Kwok (1970)) and approximate solutions may be found for quasi-elastic ones (Milsom and Butcher (1986)).

3.2.1 Isotropic Elastic Scattering

We have considered our sub-bands to be "circular and parabolic", if there exists some elastic scattering mechanism, then we may define a relaxation time for each sub-band (Siggia and Kwok (1970)). These relaxation times can be shown to be a function of energy and sub-band number alone. As we can only scatter to states with the same energy we see from (3.6) that

$$P(\underline{k}',m;\underline{k},n) = P(\underline{k},n;\underline{k}',m) \qquad (3.14)$$

(3.10) then reduces to

$$\left[\frac{\partial f_1^n}{\partial t}\right]_c = \sum_m \int [f_1^m(\underline{k}') - f_1^n(\underline{k})] P(\underline{k},n;\underline{k}',m) \frac{A}{4\pi^2} d^2k' \qquad (3.15)$$

The perturbed part of the distribution function, f_1^n decays away in each sub-band when the electric field is turned off and this process will have some characteristic time $\tau_n(\epsilon)$. We model this process by writing

$$\frac{\partial f_1^n(\underline{k})}{\partial t} = -\frac{f_1^n(k)}{T_n(\epsilon_n(k))} \tag{3.16}$$

which implies from (3.1)

$$\left[\frac{\partial f_1^n(\underline{k})}{\partial t}\right]_c = \frac{-f_1^n(\underline{k})}{T_n(\epsilon_n(\underline{k}))} \tag{3.17}$$

we assume that this is true when the electric field is present and we find from (3.11) that

$$f_1^n(\underline{k}) = \frac{e}{\hbar} \underline{E}\cdot\underline{\nabla}_k f_o(\epsilon_n(\underline{k}))T_n$$

$$= e\underline{E}\cdot\underline{V}^n(\underline{k})\frac{df_o}{d\epsilon} T_n \tag{3.18}$$

If we substitute (3.18) into (3.15) divide through by $f_1^n(\underline{k})$ and substitute the expression for f_1^n, we find that

$$\frac{-1}{T_n} = -\sum_m \int \left[\frac{\underline{E}\cdot\underline{V}^m T_m}{\underline{E}\cdot\underline{V}^n T_n} P(\underline{k}',m;\underline{k},n) - P(\underline{k}',m;\underline{k},n)\right] \frac{A}{4\pi^2} d^2k' \tag{3.19}$$

In the case of circular band the quotient in (3.19) may be reduced to $\frac{|K'|}{|K|}\cos\theta$ where θ is the angle between $\underline{k}'$ and $\underline{k}$. Hence multiplying (3.19) through by τ_n

we find that

$$1-T_n\sum_m \int P(\underline{k}',m;\underline{k},n)\frac{A}{4\pi^2}\,d^2k' - \sum_m T_m \int \frac{|\underline{k}'|}{|\underline{k}|}\cos\theta P(\underline{k}',m;\underline{k},n)\frac{A}{4\pi^2}\,d^2k' \tag{3.20}$$

These are the equations first derived by Siggia and Kwok (1970). Their solution exactly satisfies the linearised Boltzmann equation for elastic scattering mechanisms. We see that the guess for the form of the relaxation (3.16) is exact as the relaxation times derived from (3.20) are dependent on the sub-band number and electronic energy alone. The coupled equations (3.20) are independent of the distribution function f_o^n, this is a peculiarity of elastic scattering, however the statistics do come into the expression for the conductivity. In the extreme quantum limit when only one sub-band is occupied it is only necessary to calculate one relaxation time τ_1. This is given by

$$\frac{1}{T_1} = \int (1-\cos\theta)\ P\ (\underline{k}',m;\underline{k},n)\ \frac{A}{4\pi^2}\,d^2k' \tag{3.21}$$

which is the two-dimensional analogue of the usual three-dimensional result.

To evaluate the electrical conductivity σ we substitute (3.18) into (3.13) to obtain

$$\underline{J} = \frac{e^2}{2\pi^2\hbar}\sum_n \int \underline{E}\cdot\underline{v}_{\underline{k}}\ f_o\ T_n\ \underline{v}^n d^2k = \underline{\sigma}\cdot\underline{E} \tag{3.22}$$

where

$$\sigma_{ij} = \frac{-e^2}{2\pi^2} \sum_n \int V_i^n \frac{df_o}{d\epsilon} T_n(\epsilon) V_j^n d^2k \qquad (3.23)$$

The cylindrical symmetry of the system under consideration implies that $\sigma_{ij} = 0$ $i \neq j$ and $\sigma_{xx} = \sigma_{yy} = \sigma_o$. Hence

$$\sigma_o = \frac{-e^2}{4\pi^2} \sum_n \int V^{n2} T_n(\epsilon) \frac{df_o}{d\epsilon} d^2k \qquad (3.24)$$

at low temperatures this reduces to

$$\sigma_o(\epsilon_F) = \sum_n \frac{N_n(\epsilon_F) e^2 T_n(\epsilon_F) \theta(\epsilon_F - E_n)}{m^*} \qquad (3.25)$$

where N_n is the areal electron density in sub-band n. At finite temperatures the conductivity is equal to the expression for the low temperature conductivity multiplied by $df_c/d\epsilon$ and integrated over energy, ie

$$\sigma(T) = \int \sigma_o(\epsilon) \frac{df_o}{d\epsilon} d\epsilon \qquad (3.26)$$

Together equations (3.26) and (3.20) give the low field Boltzmann conductivity in a 2-DEG when the dominant scattering mechanism is elastic. We can derive similar equations for a 1-DEG.

3.3 One-Dimensional Systems (isotropic elastic scattering)

Johnson and Vassell (1984) and Ridley (1983) have considered conduction in one-dimensional wires, both used a relaxation time which was sub-band number independent. We have seen that this is insufficient in two dimensions and the same is true in one-dimensional systems. In one dimension we can write

the linearised steady state Boltzmann equation as

$$\frac{-e}{\hbar} E \frac{\partial f_o}{\partial k} = \left[\frac{\partial f_1^{nm}(k)}{\partial t}\right]_c \tag{3.27}$$

where E is the electric field directed along the wire which defines the z-axis, k is the wavenumber describing the free electron motion along the length of the wire and

$$\left[\frac{\partial f_1^{nm}(k)}{\partial t}\right]_c = -\sum_{n'm'} \int \Big[f_1^{n'm'}(k') \Big[[1-f_o(\epsilon_{nm}(k))] P(k,n,m;k',n',m') + f_o(\epsilon_{nm}(k)) P(k',n',m';k,n,m) \Big]$$

$$- f_1^{nm}(k) \Big[[1-f_o(\epsilon_{n'm'}(\underline{k}'))] P(k',n'm';k,n,m) + f_o(\epsilon_{n'm'}(k')) P(k,n,m;k',n',m') \Big] \Big] \times \frac{L}{2\pi} dk' \tag{3.28}$$

where L is the length of the wire and the P(k,n,m;k',n',m') give the transition probabilities. The equivalent to a current flux per unit area in three dimensions and a current flux per unit length in two dimensions is simply a current in one dimension. Here

$$J = \frac{-e}{\pi} \sum_{nm} \int f_1^{nm}(k) V^{nm}(k) dk \tag{3.29}$$

In the elastic scattering approximation we can define a relaxation time by

$$\left[\frac{\partial f_1^{nm}(k)}{\partial t}\right]_c = \frac{-f_1^{nm}(k)}{T_{nm}(\epsilon_{nm}(k))} \tag{3.30}$$

The Boltzmann equation in one dimension can be solved exactly with the techniques used above for two dimensions and we find that the relaxation times are given by a set of coupled algebraic equations similar to those of Siggia and Kwok, ie

$$T_{nm}\sum_{n'm'}\int P(k',n'm';k,n,m,)\frac{L}{2\pi}dk' - \sum_{n'm'} T_{n'm'}\int \frac{k'}{k}P(k',n',m';k,n,m) \times \frac{L}{2\pi}dk' = 1 \tag{3.31}$$

and at low temperatures the conductivity of this system is given by the expected form

$$\sigma_o(\epsilon_F) = \sum_{nm} \frac{N_{nm}e^2T_{nm}}{m^*} \quad \theta(\epsilon_F - E_{nm}) \tag{3.32}$$

and at finite temperatures

$$\sigma(T) = \int \sigma_o(\epsilon)\frac{df_o}{d\epsilon}\, d\epsilon \tag{3.33}$$

3.4 Changes in Dimensionality

Now that we have looked at the conductivity in 1-DEG's and 2-DEG's (in the elastic scattering approximation) it is natural to ask how the various relaxation time formulae transform into one another as the constraining dimensions are increased in size.

The one-dimensional conductivity must transform into the two-dimensional form in the limit of large width. This two-dimensional result must reduce to the three-dimensional form in the limit of large channel depth. Each transition to higher dimensionality results in the bunching of the sub-bands until in the three-dimensional limit they are all quasi-continuous. This degeneracy in sub-band structure makes the $\tau_{n,m}$ or the τ_n independent of one of their subscripts. We look at a one to two-dimensional transition due

to the conducting wire becoming wide in the y direction, k_y then becomes a good quantum number and we can convert the sum over m to an integral over k_y. If we convert to cylindrical polars we can transform equation (3.31) to the Siggia and Kwok two-dimensional result.

$$T_n \sum_m \int P(\underline{k},n;\underline{k}',m) \frac{A}{4\pi^2} d^2k' - \sum_m T_m \int \frac{|\underline{k}'|}{|\underline{k}|} \cos\theta P(\underline{k},n;\underline{k}',m) \frac{A}{4\pi^2} d^2k' = 1 \tag{3.34}$$

When we expand our conducting channel in the x-direction and perform a similar co-ordinate transformation we obtain the three-dimensional result.

$$\frac{1}{T} = \int P(\underline{k};\underline{k}')(1-\cos\theta) \frac{V}{8\pi^3} d^3k' \tag{3.35}$$

Which is the result for a single three-dimensional band (Mott (1936)). Here θ is the angle between the wavevectors in question. Thus the relaxation times carry smoothly over into one another. The expressions for the conductivity change in a similar way. In two dimensions we had

$$\sigma = \sum_m \frac{N_m e^2 T_m}{m^*} \tag{3.36}$$

In our case the T m's are equal and we may take them outside the summation to obtain

$$\sigma = \frac{e^2 T}{m^*} \sum_m N_m \tag{3.37}$$

In the two-dimensional formalism $\underline{J}$ was introduced as a current flux per unit length, to obtain the three-dimensional current flux per unit area we divide by the well width to obtain

$$\sigma_{3D} = \frac{ne^2T}{m^*} \tag{3.38}$$

where n is the number of electrons per unit volume.

CHAPTER 4

ELASTIC SCATTERING BY POINT DEFECTS

We turn now to a discussion of the transition rates $P(\underline{k},n;\underline{k}',m)$. These are usually evaluated in a Golden Rule Calculation (Butcher (1973), Nag (1972))

$$P(\underline{k},n:\underline{k}',m)= \frac{2\pi}{\hbar} |\langle n,\underline{k}|V_p|\underline{k}',m\rangle|^2 \delta(\epsilon_{final}-\epsilon_{initial}) \qquad (4.1)$$

where V_p is the perturbing potential, due to deviations away from the perfect periodic system, and $\epsilon_{initial}$ and ϵ_{final} are the initial and final electron state energies. In three dimensions the evaluation of expression (4.1) yields the Fourier transform of the scattering potential. In one and two dimensions however this is modified because of the standing wave components of the wavefunction. Whereas crystal momentum conservation is a good concept in three-dimensional systems, it is no longer good to think in these terms for reduced dimensionality systems and "momentum" conservation is fuzzy in the constrained dimensions (Ridley (1982)). The simplest scattering potential that we can substitute into (4.1) to reveal the properties of the relaxation time formulae is the delta function. This makes the integrals particularly easy to perform.

4.1 Delta function scattering in two-dimensional systems

We can represent a sharply confined potential, or potential spike by a delta function and obtain reasonable results out of the Siggia and Kwok equations (3.20) if the range of the potential is small compared to the reciprocal of the Fermi momentum, ie, if the wavefunctions (2.5) change little over the total extent of the scattering potential V_p (Rode and Fedders (1983)). If these delta scatterers are arranged at random and their density is sufficiently low, then we may express the scattering effect of the ensemble as the sum of the scattering from all the individuals (Kearney (1986)).

We consider one δ-scatterer of strength V_o, at position $(\underline{r}_o, z_o)$, ie

$$V_p = V_o \delta(z-z_o)\delta(\underline{r}-\underline{r}_o) \tag{4.2}$$

where δ is the Dirac delta function. The probability per unit time that an electron will scatter from a state $|\underline{k},n\rangle$ to a state $|\underline{k}',m\rangle$ is obtained by substituting (4.2) into (4.1) giving

$$P(\underline{k},n;\underline{k}',m) = \frac{2\pi}{\hbar} \left| \frac{V_o}{A} \zeta_n(z_o)\zeta_m(z_o) \right|^2 \delta(\epsilon_n(\underline{k})-\epsilon_m(\underline{k}')) \tag{4.3}$$

Where the $\zeta n(z)$ are the localised wavefunctions in the quantum well.

The total transition rate $P_{TOT}(\underline{k},n;\underline{k}',m)$ will be due to a sum over all scatterers. If we define a density of scatterers ρ which is taken to be independent of $\underline{r}$ and z then we find

$$P_{TOT}(\underline{k},n;\underline{k}',m) = \rho\int dz_o \int d^2r_o \frac{2\pi}{\hbar} \frac{V_o^2}{A^2} |\zeta_n(z_o)\zeta_m(z_o)|^2 \delta(\epsilon_n(\underline{k})-\epsilon_m(\underline{k}')) \tag{4.4}$$

now if we take $\zeta_n(z_o)$ from equation (2.5) we have

$$P_{TOT}(\underline{k},n;\underline{k}',m) = \frac{2\pi}{\hbar} \frac{V_o^2\rho}{A} \int_o^L \frac{4}{L^2} \sin^2 \frac{n\pi z_o}{L} \sin^2 \frac{m\pi z_o}{L} \delta(\epsilon_n(k)-\epsilon_m(k')) \, dz_o$$

$$= \frac{2\pi}{\hbar} \frac{V_o^2\rho}{A} \frac{1}{2L} [2+\delta_{n,m}] \delta(\epsilon_n(k)-\epsilon_m(k')) \tag{4.5}$$

(see Arora and Awad (1981))

where $\delta_{n,m}$ is the Kronecker delta, so the inter-sub-band scattering rate is 2/3 of the intra-sub-band rate. It is also worth noting that both intra and the inter-sub-band scattering rates are independent of the sub-band indices.

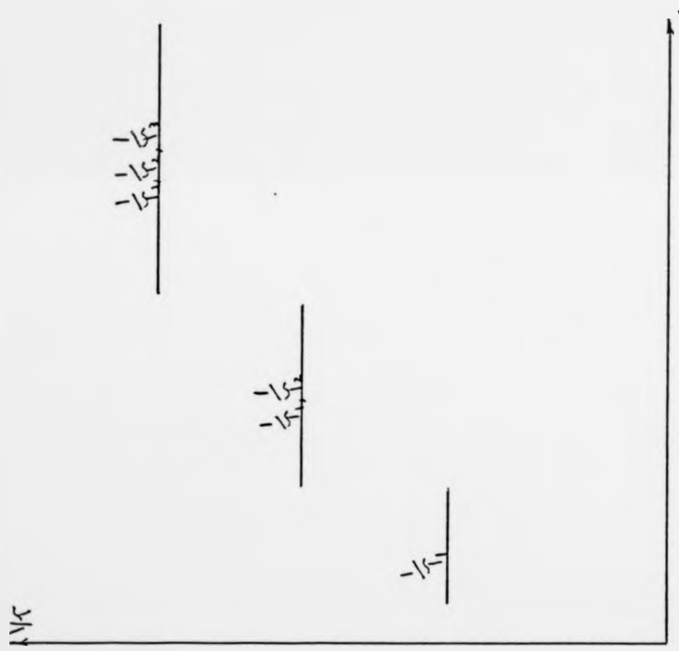

FIG 4.1 The momentum relaxation rate staircase for delta function scattering in the infinite square well limit.

As the density of states is flat the Siggia and Kwok momentum relaxation time equations now take a particularly simple form. The second integral in (3.20) is zero and we obtain

$$\frac{1}{\tau_n} = \sum_m \int P_{TOT}(k,n;k',m)\frac{A}{4\pi^2}\, d^2k' \tag{4.6}$$

The Siggia and Kwok equations decouple and we are left with a momentum relaxation time which is identical to the scattering rate. Inserting (4.5) into (4.6) we find, finally

$$\frac{1}{\tau_n} = \sum_m \frac{V_o^2 \rho m^*}{2\hbar^3 L}\,[2+\delta_{n,m}]\theta(\epsilon - E_m) \tag{4.7}$$

The τ_n take the staircase form shown in Figure 4.1. The τ_n are also independent of n, but they possess step-like discontinuites due to the staircase nature of the density of states. The n independence is an artifact of the sinusoidal wavefunctions in general the τ_n can be n dependent for δ function scatterers. The discontinuities in the τ_n produce sudden drops in σ (see equation (3.25)).

4.2 Delta function scatterers (one-dimensional systems)

In a one-dimensional wire we can carry out the same procedure as that in 4.1 and we find

$$P_{TOT}(k,n,m;k',n',m') = \frac{2\pi}{\hbar}\frac{V_o^2\rho}{4AL}\,[2+\delta_{n,n'}][2+\delta_{m,m'}]\delta(\epsilon_{nm}(k)-\epsilon_{n'm'}(k')) \tag{4.8a}$$

when n'=n and m'=m the product of the square brackets is 9. Relaxing one of these conditions gives 6 and relaxing both gives 4. The distinction between the inter and intra-sub-band scattering rates is not as clear as it is in two dimensions as three numbers are needed to define the problem. If (4.8a)

is substituted into (3.31) we find that the relaxation times are different for different sub-bands because the density of states in one-dimensional systems is not constant. A set of curves representative of delta function scattering in one-dimensional wires are shown in Figure 5.5. Again we see from the scattering rate formula (4.8) that the transition rate and hence the mobility can be engineered by changing the characteristic dimensions of these low dimensionality systems. The singularity in the density of states also results in singular scattering rates and infinite momentum relaxation rates, consequently the conductivity will drop to zero for all well dimensions when the Fermi energy corresponds to a sub-band energy ϵ_{nm}.

4.3 Scattering by ionised impurities (two-dimensional systems)

In an extrinsic bulk semiconductor the dopants increase the conductivity by supplying carriers but reduce the mobility by acting as scattering centres. In the bulk the two effects are inseparable, and the carriers are always influenced by this scattering mechanism. In a two-dimensional system where the electrons are confined to a thin conducting channel it is always possible to introduce carriers from remote dopants, by doping the material surrounding the quantum well (Stormer (1979)). It is energetically favourable for electrons to fall into the well where they are held in the quantum levels described in Chapter 2, very little charge extends beyond the walls of the channel and so the scattering is drastically reduced. With this "modulation doping" technique (Dohler (1983)) it is also possible to introduce a large number of carriers to the system so that many of the states in the sub-bands are filled, the system can then behave as a degenerate electron gas. This is better able to screen the impurities that may be lying in the channel. The scattering efficiency of the ionised impurities is also dependent on the speed of the impacting carriers and this leads to an additional reduction in the scattering because the only important velocity in the system is the Fermi velocity which can be

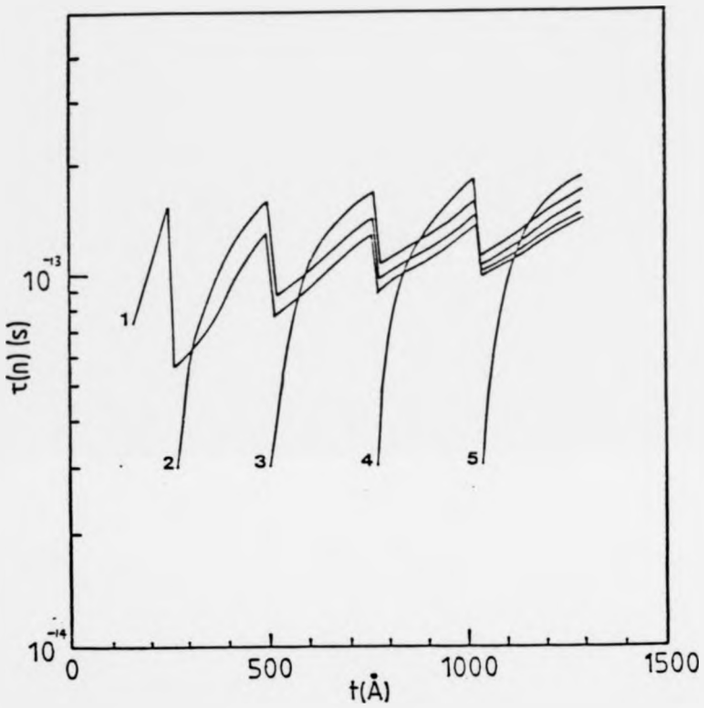

FIG 4.2

Momentum relaxation times for ionised impurity scattering as a function of the well width (after Sernelius(1985)).

controlled and made to be large (N Apsley (1986)).

The mobility in modulation doped systems can increase in consequence of all these factors. Sernelius, Bergrenn and Tomak (1985) have looked at ionised impurity scattering in some depth, but instead of looking at modulation doped structures they considered scattering off ionised impurities in the well. The impurities were distributed at random across the well and correlation effects were ignored. Their treatment includes the effects of screening and inter-sub-band scattering using the Siggia and Kwok equations. This approach is correct within the Boltzmann framework. The results are shown in Figure 4.2. The matrix element for scattering off unscreened ionised impurities has a 1/Q dependence, where Q is the change in electronic momentum. When the energy being considered lies at the bottom of the sub-band only small values of q are needed to scatter the electron right around the sub-band and consequently the momentum relaxation rate is large, (and may be singular when $\epsilon=\epsilon_n$).

Sernelius et al report experiments on a GaAs FET in which these predicted effects did not appear. As we discuss in the final chapter this is due to level broadening by the large density of scatterers present.

4.4 Alloy Scattering (two-dimensional systems)

Non-lattice matched quantum well systems are prone to dislocations which appear to relieve the strain. They act as scattering centres. A simple way to avoid them is to match the lattice spacing of the two materials in the structure. The similarity in size between Ga and Al atoms permits such a match between Gallium Arsenide (GaAs) and the $Al_xGa_{1-x}As$ ternary alloy (Adachi (1986)). We consider the scattering process due to the disordered nature of the alloy in a Quantum well. The other mechanisms responsible for limiting the conductivity in these systems are due either to

phonons or surface roughness and impurity scattering all of which can be controlled. Alloy scattering is intrinsic to the materials used. The study of this mechanism is therefore particularly important as it limits the mobility **even in an ideal system.**

Alloy scattering has been well researched in the bulk (Basu et al (1986), Rode and Fedders (1983), Harrison and Hauser (1975), Hall (1959)), but has not received enough attention in the quantum well. Two formulae have recently been proposed (Basu and Nag (1983), G Bastard (1983)). Both of these formulae were relevant to the extreme quantum limit. The formula due to Basu deals with a potential resembling a pill-box whereas the formula due to Bastard was relevant to a more realistic confined spherical potential. In our treatment we adopt the second approach and consider the effect of inter-sub-band scattering due to alloy disorder when more than one sub-band is occupied. Throughout we consider the potential difference between a Gallium atom and an Aluminium atom to be confined to the unit cell, and we suppose that the effective mass envelope function is slowly varying on this length scale.

The first step in the calculation involves determining the wavefunctions for the quantum well, this has been done in the effective mass approximation (see appendix 1) taking into account the varying effective mass in the two materials but not the differing Bloch states at the bottom of each Γ valley. The Γ valley and the L valley of $Al_xGa_{1-x}As$ cross when $x \sim 0.4$ so that only the Γ valley needs to be taken into account when $x = 0.3$. Bulk $Al_xGa_{1-x}As$ has a conduction band minimum above that of GaAs. We treat this conduction band offset energy as the potential which confines the 2-DEG in the quantum well. The band structures are taken to align as shown in Figure 1.2. Okumura (1985) suggested that the conduction band offset, ΔE_c, is equal to 0.62 of the difference in band gap energies of the GaAs and the $Al_xGa_{1-x}As$

and this figure is taken to be independent of the alloy composition.

We work in the virtual crystal approximation (Nordheim (1931), Hall (1959)) and imagine that there is some average potential $U_{Av}(\underline{R})$ and the true potential $U(\underline{R})$ is to be treated as a perturbation about this. We write the true potential $U(\underline{R})$ as

$$U(\underline{R}) = \sum_{\text{Ga atoms}} U_{Ga}(\underline{R}-\underline{\Upsilon}_{Ga}) + \sum_{\text{Al atoms}} U_{Al}(\underline{R}-\underline{\Upsilon}_{Al}) + \sum_{\text{As atoms}} U_{As}(\underline{R}-\underline{\Upsilon}_{As}) \qquad (4.8b)$$

where, it will be remembered that, $\underline{R}=(\underline{r},z)$ is the three-dimensional position vector of an electron, with $\underline{r}=(x,y)$ denoting the projection of $\underline{R}$ onto the plane of the quantum well, $\underline{\Upsilon}_{Ga}$ and $\underline{\Upsilon}_{Al}$ denote position vectors of Ga and Al atoms and $U_i(\underline{R}-\underline{\Upsilon}_i)$ is the potential due to atom i at location $\underline{\Upsilon}_i$. The average potential is given by

$$U_{Av}(\underline{R}) = \sum_{\underline{\Upsilon}}^{\text{cationic}} [(1-x)U_{Ga}(\underline{R}-\underline{\Upsilon}) + xU_{Al}(\underline{R}-\underline{\Upsilon})] + \sum_{\underline{\Upsilon}}^{\text{anionic}} U_{As}(\underline{R}-\underline{\Upsilon}) \qquad (4.9)$$

where the summations are over cationic and anionic sites respectively. The average potential determines the alloy bandstructure. The irregular deviation from $U_{Av}(\underline{R})$ will result in scattering and is given by the difference between formulae (4.8) and (4.9). Within the well, the average potential is the true potential and consequently this contributes nothing to the scattering. We also consider the two confining half-space scattering potentials to be uncorrelated. The total alloy scattering in this symmetric well is then equal to twice the scattering due to one half-space. We can rewrite the potential in one of the alloy half-spaces as (neglecting the anionic sites)

$$U(\underline{R}) = \sum_{\substack{\underline{\Upsilon} \\ \Upsilon_z<0}} C_{\underline{\Upsilon}}\, U_{Ga}(\underline{R}-\underline{\Upsilon}) + (1-C_{\underline{\Upsilon}})U_{Al}(\underline{R}-\underline{\Upsilon}) \tag{4.10}$$

where $C_{\underline{\Upsilon}}$ = 1 if a Ga atom is at $\underline{\Upsilon}$

= 0 if an Al atom is at $\underline{\Upsilon}$

The scattering potential is therefore

$$\Delta U(\underline{R}) = \sum_{\substack{\underline{\Upsilon} \\ \Upsilon_z<0}} (C_{\underline{\Upsilon}}-x)U_{Ga}(\underline{R}-\underline{\Upsilon}) + (x-C_{\underline{\Upsilon}})U_{Al}(\underline{R}-\underline{\Upsilon}) \tag{4.11}$$

where Υ_z is the z component of $\underline{\Upsilon}$ and is negative in the alloy.

Hence

$$\Delta U(\underline{R}) = \sum_{\substack{\underline{\Upsilon} \\ \Upsilon_z<0}} C'_{\underline{\Upsilon}}\, U_{diff}(\underline{R}-\underline{\Upsilon}) \tag{4.12}$$

where

$$C'_{\underline{\Upsilon}} = C_{\underline{\Upsilon}}-x \text{ and } U_{diff}(\underline{R}-\underline{\Upsilon}) \equiv U_{Ga}(\underline{R}-\underline{\Upsilon})-U_{Al}(\underline{R}-\underline{\Upsilon})$$

We can now construct the matrix element M of ΔU. We have

$$M \equiv \langle \zeta_m \underline{k}' | \sum_{\substack{\underline{\Upsilon} \\ \Upsilon_z<0}} C'_{\underline{\Upsilon}}\, U_{diff}(\underline{R}-\underline{\Upsilon}) | \zeta_n \underline{k} \rangle$$

$$= \iint \sum_{\substack{\underline{\Upsilon} \\ \Upsilon_z<0}} \frac{C'_{\underline{\Upsilon}}}{A} U_{diff}(\underline{R}-\underline{\Upsilon})\zeta_n(z)\zeta_m(z)e^{i(\underline{k}-\underline{k}')\cdot\underline{r}}dz\,d^2r \tag{4.13}$$

Let $\underline{R} = \underline{r}+z\underline{k}$ and $\underline{\Upsilon} = \underline{\Upsilon}_2 + \underline{\Upsilon}_z$ where $\underline{\Upsilon}_2$ lies in the (x,y) plane and we perform the co-ordinate transformation $z' = z-\Upsilon_z$ and $\underline{r}' = \underline{r}-\underline{\Upsilon}_2$. Then M reduces to

$$M = \iint \sum_{\substack{\underline{\Upsilon} \\ \Upsilon_z<0}} \frac{C'_{\underline{\Upsilon}}}{A} U_{diff}(\underline{r}',z')\zeta_n(z'+\Upsilon_z)\zeta_m(z'+\Upsilon_z)e^{i(\underline{k}-\underline{k}')\cdot(\underline{r}'+\underline{\Upsilon}_2)} dz'\,d^2r' \tag{4.14}$$

$$- \sum_{\substack{\underline{\tau}_2 \\ \tau_z<0}} \frac{C'_{\underline{\tau}_2+\underline{\tau}_z}}{A} e^{i(\underline{k}-\underline{k}')\cdot\underline{\tau}_2} \iint\!\!\int U_{diff}(\underline{r}',z')\zeta_n(z'+\tau_z)\zeta_m(z'+\tau_z) e^{i(\underline{k}-\underline{k}')\cdot\underline{r}'} dz'd^2r' \tag{4.15}$$

with the assumption that U_{diff} is sharply confined to the unit cell whereas $\zeta_n(z)$ is slowly varying, then we may remove ζ_n and ζ_m from the integral evaluating them at τ_z, to obtain

$$M = -\sum_{\substack{\underline{\tau}_2 \\ \tau_z<0}} \frac{C'_{\underline{\tau}_2+\underline{\tau}_z}}{A} e^{i(\underline{k}-\underline{k}')\cdot\underline{\tau}_2} \zeta_n(\tau_z)\zeta_m(\tau_z) \iint\!\!\int U_{diff}(\underline{r}',z') e^{i(\underline{k}-\underline{k}')\cdot\underline{r}'} dz'd^2r' \tag{4.16}$$

which we rewrite as

$$M = -\sum_{\substack{\underline{\tau}_2 \\ \tau_z<0}} \frac{C'_{\underline{\tau}_2+\underline{\tau}_z}}{A} e^{i\underline{q}\cdot\underline{\tau}_2} \zeta_n(\tau_z)\zeta_m(\tau_z)S(\underline{q}) \tag{4.17}$$

where

$$q = \underline{k}-\underline{k}' \text{ and } S(\underline{q}) = \iint\!\!\int U_{diff}(\underline{r}',z')e^{i\underline{q}\cdot\underline{r}'}dz'd^2r' \tag{4.18}$$

We are concerned with $|M|^2$: we see that

$$|M|^2 = \sum_{\substack{\underline{\tau} \\ \tau_z<0}} \frac{C'_{\underline{\tau}_2+\underline{\tau}_z}}{A} e^{i\underline{q}\cdot\underline{\tau}_2} \zeta_n(\tau_z)\zeta_m(\tau_z) \sum_{\substack{\underline{\tau}' \\ \tau_z'<0}} \frac{C'_{\underline{\tau}_2'+\underline{\tau}_z'}}{A} e^{-i\underline{q}\cdot\underline{\tau}_2'} \zeta_n(\tau_z')\zeta_m(\tau_z') S^2(\underline{q}) \tag{4.19}$$

$$- \sum_{\tau_z<0} \sum_{\tau_z'<0} \zeta_n(\tau_z)\zeta_m(\tau_z)\zeta_n(\tau_z')\zeta_m(\tau_z') \sum_{\underline{N}_2} \sum_{\underline{\tau}_2} \frac{C'_{\underline{\tau}_2+\underline{\tau}_z} C'_{\underline{\tau}_2-\underline{N}_2+\underline{\tau}_z'}}{A^2} e^{i\underline{q}\cdot\underline{N}_2} S^2(\underline{q}) \tag{4.20}$$

Now if the system is uniformly random (see Hall (1959))

$$\sum_{\underline{\Upsilon}_2} {}^{C'}\underline{\Upsilon}_2+\underline{\Upsilon}_z \quad {}^{C'}\underline{\Upsilon}_2-\underline{N}_2+\underline{\Upsilon}_z' = 0 \text{ when } \underline{N}_2\neq 0 \text{ or } \underline{\Upsilon}_z'\neq\underline{\Upsilon}_z \quad (\underline{N}_2=\underline{\Upsilon}_2-\underline{\Upsilon}_2') \tag{4.21}$$

The system is thus self averaging. When $\underline{N}_2=0$ and $\underline{\Upsilon}_z'=\underline{\Upsilon}_z$ we find

$$\sum_{\underline{\Upsilon}_2} \frac{|{}^{C'}\underline{\Upsilon}_2+\underline{\Upsilon}_z|^2}{A} = Nx(1-x) \tag{4.22}$$

where N is the number of cation sites per unit area in any one layer. Thus, finally, we have

$$M^2 = \sum_{\underline{\Upsilon}_z<0} |\zeta_n(\underline{\Upsilon}_z)\zeta_m(\underline{\Upsilon}_z)|^2 \quad \frac{N}{A}\, x(1-x)S^2(\underline{q}) \tag{4.23}$$

and the scattering rate is

$$P(\underline{k},n;\underline{k}',m) = \frac{2\pi}{\hbar}\,|M|^2\delta(\epsilon_n(\underline{k})-\epsilon_m(\underline{k}')) \tag{4.24}$$

To convert the summation in (4.23) to an integral we write a_z for the lattice constant in z direction so that (4.24) becomes

$$P(\underline{k},n;\underline{k}',m) = \frac{2\pi}{\hbar}\int_{-\infty}^{0} \frac{dz}{a_z}\,[\zeta_n(z)\zeta_m(z)]^2S^2(\underline{q})\frac{N}{A}x(1-x)\delta(\epsilon_n(\underline{k})-\epsilon_m(\underline{k}')) \tag{4.25}$$

$n=N/a_z$ is the density of cationic sites per unit volume. Since the

scattering potential is sharp on the atomic scale, S ($\underline{q}$) is independent of $\underline{q}$ for the values of $\underline{q}$ with which we are concerned. If we insert (4.25) into the Siggia and Kwok equations (3.20) the cos θ integral is zero because of the delta function like $\underline{q}$ independence of the scattering potential. The tail of the wavefunction in the alloy possesses the form

$$\zeta_n(z) = A_n e^{-\alpha_n z} \tag{4.26}$$

where the values of α_n and An are given in Figure 4.3. The relaxation time equations again decouple and we find that

$$\frac{1}{\tau_n(\epsilon)} = 2\sum_m \frac{m^* nx(1-x)}{\hbar^3} \frac{[A_n A_m]^2}{2(\alpha_n + \alpha_m)} S^2(0)\theta(\epsilon-\epsilon_m) \tag{4.27}$$

In this result we have introduced an additional factor of 2 to account for the alloy scattering from both sides of the quantum well. This expression is similar to that of Bastard's except that expression (4.27) can be used when more than one sub-band is occupied. The derivation here may be useful in the situation where the alloy is not uniformly random and it could be applied in the treatment of alloy clustering, see equation (4.20). It only remains for us to determine the nature of the scattering potential U_{diff}. The expression S(o) arising in equation (4.27) is simply the volume integral of $U_{diff}(\underline{R})$.

4.4.1 The scattering potential

Several authors have considered the nature of the scattering potential in alloy systems. Mott (1936) suggested that the potential in a metal alloy should be treated as uniform and extending over the cell of the scatterer. More recently authors have been interested in alloy scattering in semiconductor systems (Harrison and Hauser (1975), Rode and Fedders(1983), Fedders and Myles (1983)) and there is some disagreement over the magnitude

of the potential that should be employed. Many authors (Littlejohn (1978), Saxena (1985)) have considered the scattering potential to be strongly related to atomic properties of the elements involved, rather than a function of the material in which the element resides. It has been suggested that U_{diff} should be equal to the difference in (i) band-gaps (Glicksmann (1974)), and (ii) electron affinities (Harrison (1975)), (iii) electronegativities (see Littlejohn (1978)), with no clear agreement as to which should be used. Experiments have been carried out to try to determine U_{diff} by examining alloy samples with varying compositions (Basu (1986), Saxena (1984)). Although the different suggestions are not self-consistent they usually roughly correspond to the values of U_{diff} calculated from experimental data, however they can vary over orders of magnitude (see Littlejohn (1978)). Stringfellow (1979) suggested that the alloy scattering potential should be treated as the energy separation between the direct energy conduction band edges of the unalloyed components. This suggestion is the closest to the truth and we present a justification for this below.

If we consider a superlattice structure (eg GaAs/$Al_xGa_{1-x}As$) it is usual when calculating a miniband structure to model the potential seen by the conduction band electrons with a regular set of Kronig-Penney type barriers. The height of these barriers is taken to be equal to the conduction band offset (Warren (1986)) which can be measured by capacitance-voltage profiling (Okumura (1985)). In the absence of band-bending due to charged impurities or carriers this is an accurate model for even small well widths. We can use this information to treat the randomised alloy system. In this model we consider the conduction band electrons to see the conduction band offset potential as they traverse the unit cell of a scatterer. To approach this problem we consider the form of the matrix element for alloy scattering in the bulk.

We suppose that the perturbation from the periodic virtual crystal approximation to the alloy is small. We write

$$V_{Ga} = \underset{\sim}{U}(\underline{R})+\delta V_{Ga}$$
$$V_{Al} = \underset{\sim}{U}(\underline{R})+\delta V_{Al} \qquad (4.28)$$

where $\underset{\sim}{U}(\underline{R})$ is the average potential given by equation (4.9). Now let us consider the conduction band offset in these two cases.

$$\Delta E_c^{Ga} = \int_\Omega |\psi_o|^2 \delta V_{Ga}(\underline{R}) d^3R \text{ and } \Delta E_c^{Al} = \int_\Omega |\psi_o|^2 \delta V_{Al}(\underline{R}) d^3R \qquad (4.29)$$

where Ω is the total volume of the bulk crystal and ψ_o is the Bloch function at the bottom of the conduction band. The difference is

$$\Delta E_c^{Ga/Al} = \int_\Omega |\psi_o|^2 [\delta V_{Ga}(\underline{R}) - \delta V_{Al}(\underline{R})] = N_c \int_{\Omega_c} |\psi_o|^2 U_{diff}(R) d^3R \qquad (4.30)$$

where $N_c = \frac{\Omega}{\Omega_c}$ is the number of unit cells, Ω_c is the unit cell volume, and $U_{diff}(\underline{R})$ is difference of atomic potentials introduced in equation (4.12) with $\underline{\tau}=0$. Since $U_{diff}(\underline{R})$ is, by hypothesis, confined within the unit cell we may replace Ω_c by Ω in (4.30). Solving for the matrix element which arises in bulk alloy scattering, we find

$$M \equiv \int_\Omega |\psi_o|^2 U_{diff}(\underline{R}) d^3R = \frac{\Delta E_c^{Ga/Al}}{N_c} = \frac{\Delta E_c^{Ga/Al} \Omega_c}{\Omega} \qquad (4.31)$$

This is the result for one scattering centre. If we consider an ensemble of scatterers then the total matrix element squared is

$$|M_{TOT}|^2 = x(1-x) N_c |M_B|^2 = \frac{N_a}{\Omega} x(1-x) |\Delta E_c^{Ga/Al} \Omega_c|^2 \qquad (4.32)$$

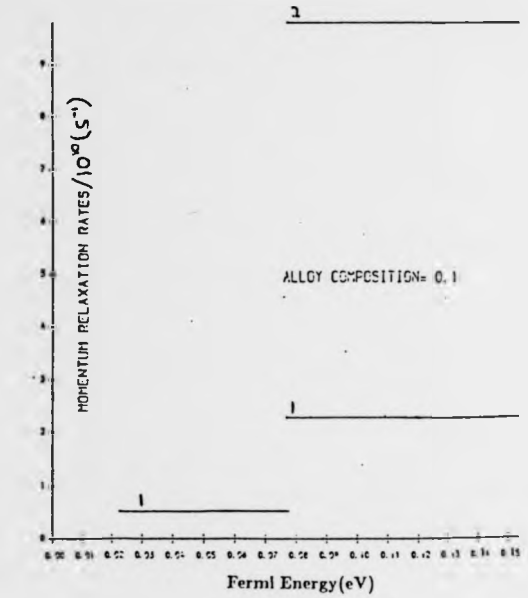

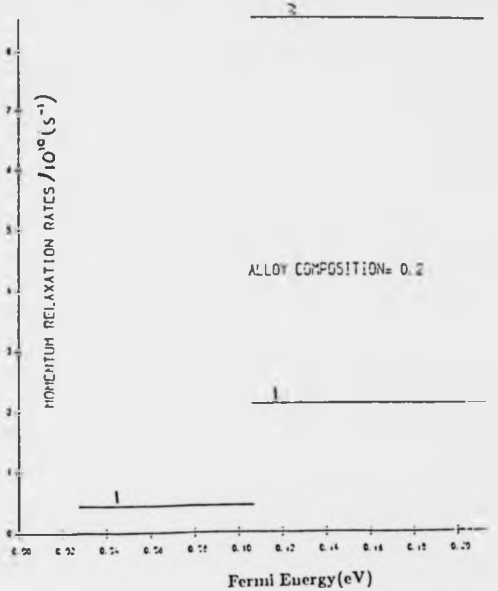

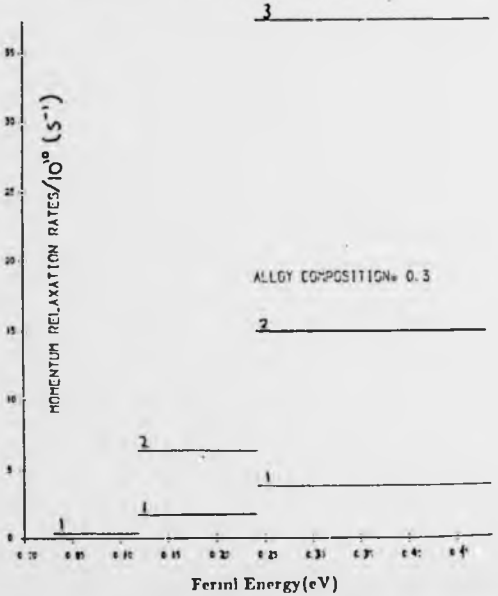

FIG 4.3(b)

Momentum relaxtion rates for Alloy scattering using the conduction band offset as the scattering potential.

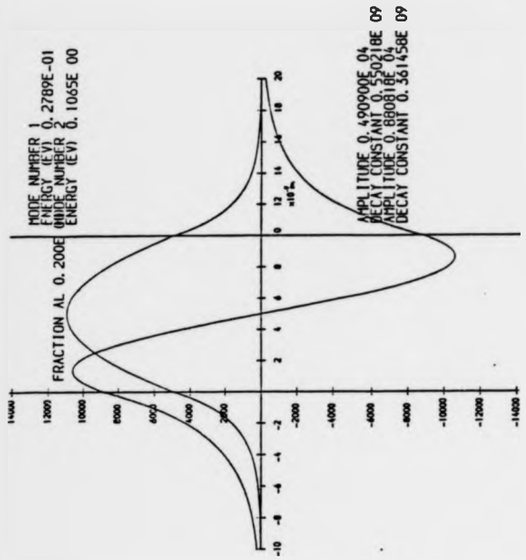

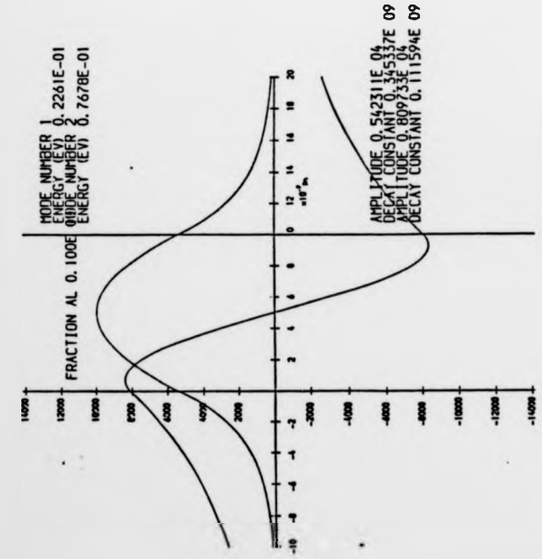

FIG 4.3(a)

Wavefunctions for the GaAs/AlGaAs quantum well. The energy of the modes (eV) and the decay rate of tail (per metre) are indicated.

where Ns is the number of cationic sites per unit volume. With this method we can identify S(o) in equation (4.17) with $\left|\Delta E_c^{Ga/Al}\Omega_c\right|$

We present values of the alloy scattering momentum relaxation rates in Figure 4.3.

CHAPTER 5

SCATTERING FROM EXTENDED DEFECTS

In this chapter we continue to work in the elastic scattering regime using the equations of Siggia and Kwok and we look at the effect of extended defects on the momentum relaxation rates of Quasi-One and Quasi-Two dimensional systems. Throughout we consider the quantum well to be buried in a material which possesses similar acoustic properties, but different electronic properties so that the electrons are confined to the well, whilst the phonons can be considered as three-dimensional.

Extended defects can be due to phonons; they can also arise if the confining material/channel is rough. In 5.1 we consider the electron/acoustic phonon interaction mediated by the deformation potential, in 5.2 we consider the piezoelectric interaction and in 5.2.3 we consider the effect of a rough material interface on a two-dimensional electron gas.

5.1 The Elastic Scattering Approximation for Acoustic Phonons

The linearised scattering rate equation (3.10) may be rewritten as

$$\left[\frac{\partial f_1(\underline{k},n)}{\partial t}\right]_c = \sum_m \int V(\underline{k},n;\underline{k}',m)\left[\frac{1-f_o(\underline{k}',m)}{1-f_o(\underline{k},n)}\right][f_1(\underline{k},n)-f_1(\underline{k}',m)]\frac{A}{4\pi^2}d^2k' \tag{5.1}$$

where we have used the detailed balance relationship and $V(\underline{k},n;\underline{k}',m)$ is the equilibrium transition rate, given by

$$V(\underline{k},n;\underline{k}'m) = f_o(\underline{k},n)[1-f_o(\underline{k}',m)]P(\underline{k},n;\underline{k}',m) \tag{5.2}$$

Consider the large square brackets in 5.1. When the mechanism is perfectly elastic $f_o(\underline{k}',m)=f_o(\underline{k},n)$ the momentum relaxation times which can be defined are independent of the distribution function $f_o(\underline{k},n)$ and the brackets equal 1.

If however the mechanism is quasi-elastic we can still define a set of momentum relaxation times if $f_c(\underline{k}',m)$ and $f_o(\underline{k},n)$ are both much less than 1 or if this is not the case they must be approximately equal to one another, hence

$$|\epsilon(\underline{k},n)-\epsilon(\underline{k}',m)|<<k_BT \qquad (5.3)$$

ie if

$$\hbar\omega_Q<<k_BT$$

We assume that this holds. This not only allows us to use the relaxation time formulae but it also permits us to simplify the scattering rate obtained by using the equipartition limit of the Bose-Einstein distribution, which is the case considered by Ridley (1982). The effect of inelastic scattering will be considered in detail in Chapter 6.

5.2 Two-Dimensional Systems

5.2.1 Deformation Potential Scattering (Acoustic Phonons)

The deformation potential was first considered by Bardeen and Shockley (1951). They noted that the band-gap of a material is related to the separation of its constituent atoms and because a phonon is a lattice distortion this will be responsible for a local change in band-gap. They showed that this effect was proportional to the dilation and in cubic Gallium Arsenide the coefficient of proportionality is a scalar called the deformation potential E_{def}. The additional term on the electronic Hamiltonian is given by

$$Hep = E_{def}\,\underline{\nabla}\cdot\underline{U} \qquad (5.4)$$

Where $\underline{U}$ is the acoustic phonon displacement. $\underline{U}$ can be expressed in second quantised form (Butcher (1973)) as

$$\underline{U} = \sqrt{\frac{\hbar}{2\omega_Q\rho V}}\;\underline{\xi}\;(a_Q^+ e^{-i\underline{Q}\cdot\underline{R}} + a_Q e^{+i\underline{Q}\cdot\underline{R}}) \qquad (5.5)$$

where the phonon has a wavevector $\underline{Q}$ and a frequency $\omega_{\underline{Q}}$, ρ is the density of the medium, V is the total volume of the bulk crystal in which the channel is embedded and $\underline{\xi}$ is the polarisation vector. If we substitute (5.5) into (5.4) and approximate by assuming that perfectly longitudinal and transverse waves exist in the bulk cube we find that

$$H_{ep} = E_{def}\, i \sqrt{\frac{\hbar}{2\omega_Q \rho V}}\, \underline{\xi} \cdot \underline{Q}\, (a_{\underline{Q}} e^{i\underline{Q}\cdot\underline{R}} - a^{\dagger}_{\underline{Q}} e^{i\underline{Q}\cdot\underline{R}}) \qquad (5.6)$$

We now calculate the matrix element between an electronic state $\underline{k}$ in sub-band n with phonon configuration s and a state with momentum $\underline{k}'$ in sub-band m with phonon configuration s'. We look at the contribution from the annihilation operation first, we define

$$H_{ep}^{ann} = E_{def} \sqrt{\frac{\hbar}{2\rho\omega_Q V}}\, \underline{\xi}\cdot\underline{Q}\;\; a_{\underline{i}} e^{i\underline{Q}\cdot\underline{R}} \qquad (5.7)$$

and

$$M^{ann} = \langle s;\underline{k},n|H_{ep}^{ann}|m,\underline{k}';s'\rangle$$

$$= E_{def} i \frac{2}{V} \sqrt{N_Q}\, \sqrt{\frac{\hbar}{2\rho\omega_Q V}}\, \underline{\xi}\cdot\underline{Q} \int_0^L \sin\frac{m\pi z}{L} \sin\frac{n\pi z}{L}\, e^{iq_z z}\, dz$$

$$\times \int e^{i(\underline{k}-\underline{k}')\cdot\underline{r}}\, e^{i\underline{q}\cdot\underline{r}}\, d^2r \qquad (5.8)$$

where N_Q is the equilibrium Bose occupation factor

$$N_Q = \frac{1}{e^{\hbar\omega_{\underline{Q}}/k_B T} - 1} \qquad (5.9)$$

$\underline{q}$ is the component of $\underline{Q}$ in the (x,y) plane and q_z is the projection of $\underline{Q}$ on the z-axis. The integral over $\underline{r}$ results in a two-dimensional momentum conserving Kronecker delta because of the periodic boundary conditions that have been assumed to hold in the plane. The z integral gives rise to the $G_{nm}(q_z)$ function used by Ridley (1982) (see appendix 2).

Defining

$$H^{cre}_{e-p} \equiv -E_{def}\sqrt{\frac{\hbar}{2\rho\omega_Q V}}\,\underline{\xi}\cdot\underline{Q}\;(a^{+}_{\underline{Q}}\,i\,e^{-i\underline{Q}\cdot\underline{R}}) \tag{5.10}$$

we find

$$M^{cre} \equiv \langle s;\underline{k},n|H^{cre}_{e-p}|m,\underline{k}';s'\rangle$$

$$= -E_{def}\,i\sqrt{N_Q+1}\,\sqrt{\frac{\hbar}{2\rho\omega_Q V}}\,\underline{\xi}\cdot\underline{Q}\;G^{*}_{nm}(q_z)\;\delta_{\underline{k}-\underline{k}'+\underline{q}} \tag{5.11}$$

The transition rate can then be expressed as

$$P(\underline{k},n;\underline{k}'m) = \sum_{Q}\frac{2\pi}{\hbar}\left[|M^{cre}|^2\delta(\epsilon_n(\underline{k})-\epsilon_m(\underline{k}')-\hbar\omega_Q)+|M^{ann}|^2\delta(\epsilon_n(\underline{k})-\epsilon_m(\underline{k}')+\hbar\omega_Q)\right] \tag{5.12}$$

We see immediately that only longitudinal phonons contribute to the scattering as $\underline{\xi}\cdot\underline{Q}$ is zero for transverse phonons. We split the summation over $\underline{Q}$ into a summation over $\underline{q}$ and a summation over q_z. The Kronecker deltas in $|M^{cre}|^2$ and $|M^{ann}|^2$ then pick out the terms for which $\underline{q}=\underline{k}'-\underline{k}$ and $\underline{q}=\underline{k}-\underline{k}'$ respectively. We convert the summation over q_z to an integral and introduce a one-dimensional density of states $D/2\pi$, where D is length of the edge of the phonon cube. Hence

$$P(\underline{k},n;\underline{k}',m) = \int dq_z\frac{D}{\hbar}\left[|H^{cre}|^2\delta(\epsilon_n(\underline{k})-\epsilon_m(\underline{k}')-\hbar\omega_Q)+|H^{ann}|^2\delta(\epsilon_n(\underline{k})-\epsilon_m(\underline{k}')+\hbar\omega_Q)\right] \tag{5.13}$$

where H^{cre} and H^{ann} are equal to M^{cre} and M^{ann} with the Kronecker delta removed. When these are squared and substituted into (5.13) only $|\underline{Q}|$ is important and it is understood that $|\underline{q}|=|\underline{k}-\underline{k}'|$. If we apply the equipartition inequality (5.3) and if the phonon energy is much less than the

typical electron energy then we can write

$$P(\underline{k},n;\underline{k}',m) = \int dq_z \frac{D}{\hbar} \times |H_{TOT}|^2 \, \delta(\epsilon_n(\underline{k})-\epsilon_m(\underline{k}')) \tag{5.14}$$

where

$$|H_{TOT}|^2 = \frac{K_B T E^2_{def} |Q|^2}{\omega^2 \rho V} \; G^2_{nm}(q_z) \tag{5.15}$$

We are considering the scattering of electrons around a small fermi circle which will necessarily involve small values of $\underline{q}$. The function $G^2_{nm}(q_z)$ is also insignificant for large q_z . With these observations we may use a linear dispersion relationship for the acoustic phonons with little error, ie

$$\omega_Q = V_L |\underline{Q}| \tag{5.16}$$

where V_L is the longitudinal velocity of sound. Hence we find that

$$P(\underline{k},n;\underline{k}',m) = \frac{K_B T}{\rho V V_L^2} \; D E^2_{def} \int_{-\infty}^{\infty} G^2_{nm}(q_z) \delta(\epsilon_n(\underline{k})-\epsilon_m(\underline{k}')) \, dq_z \tag{5.17}$$

As the function $G^2_{nm}(q_z)$ is sharply peaked we may also extend the range of integration from the zone edge to infinity with little error. Following the treatment of Arora and Awad (1981) 5.17 gives

$$P(\underline{k},n;\underline{k}',m) = \frac{K_B T E^2_{def} D}{\rho V V_L^2} \times \frac{\pi}{L} (2+\delta_{n,m}) \delta(\epsilon_n(\underline{k})-\epsilon_m(\underline{k}')) \tag{5.18}$$

This expression is independent of $\underline{Q}$ and consequently the Siggia and Kwok equations again decouple and we are left with the simple result

$$\frac{1}{\tau_n(\epsilon)} = \sum_m \frac{m^*}{\hbar^3} \; \frac{K_B T E^2_{def}}{\rho V_L^2} \; \frac{(2+\delta_{n,m})}{2L} \; \theta(\epsilon-\epsilon_m) \tag{5.19}$$

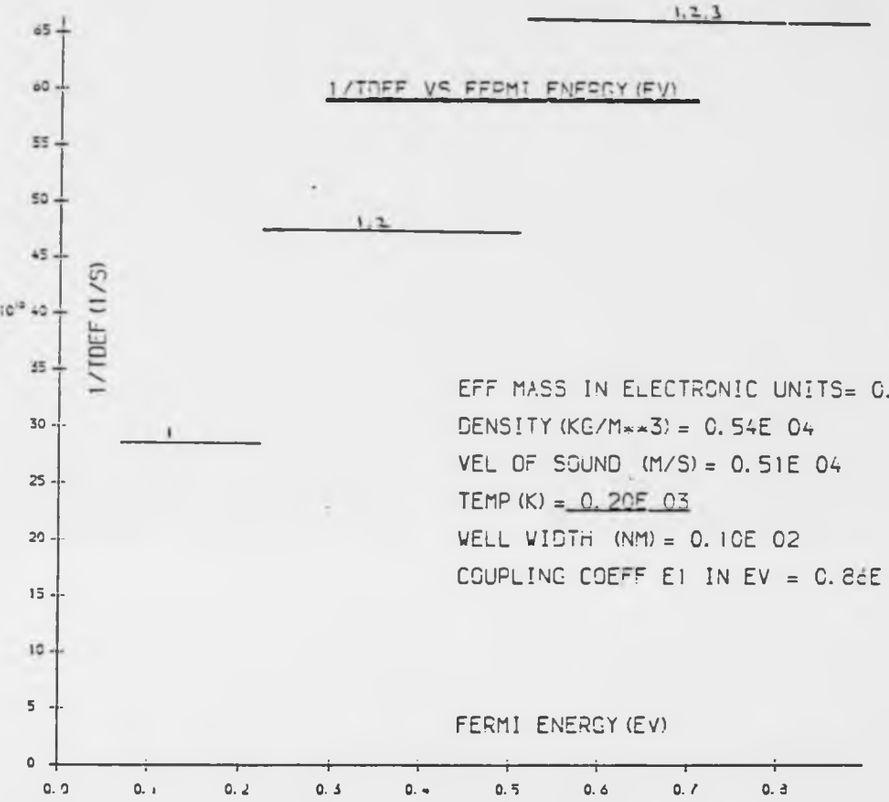

FIG 5.1

Momentum relaxation times for Deformation potential scattering. The material constants were taken from Rode(1975).

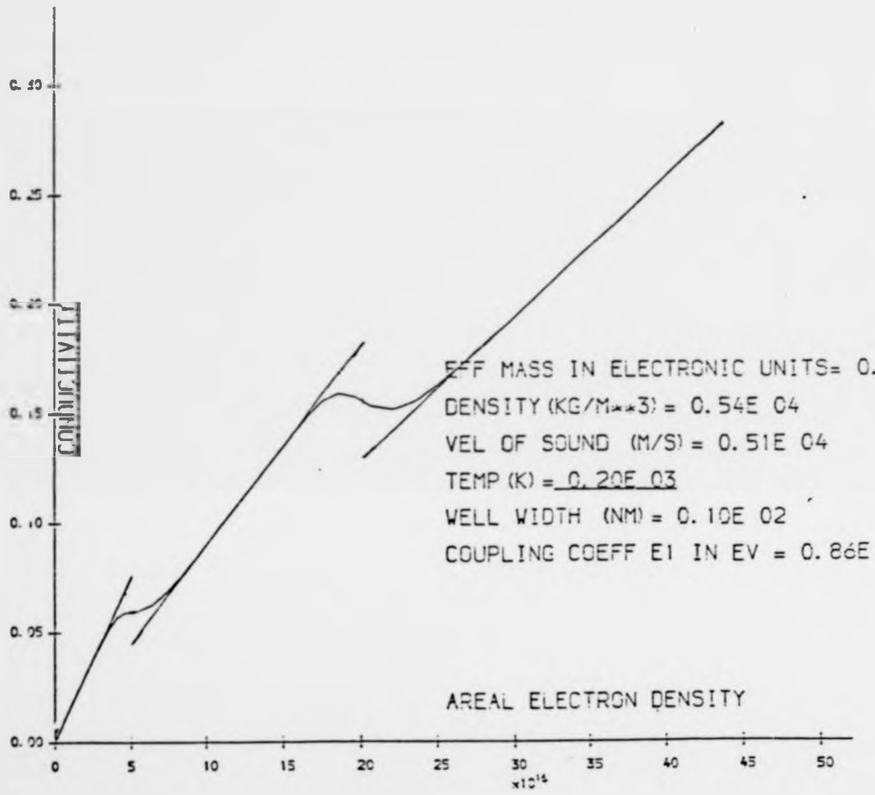

FIG 5.2

The conductivity of a 2-DEG revealing the quantum size effects and the effect of thermal smoothing.

The final formula (5.19) for $\tau_n^{-1}(\epsilon)$ shows a similar staircase structure to the density of state (Ridley (1982)), see Figure 5.1.

5.2.1.1 The Conductivity

We saw that the finite temperature conductivity could be written as (equation 3.33)

$$\sigma(T) = \int \sigma_o(\epsilon) \frac{df_o}{d\epsilon} \, d\epsilon$$

where $\sigma_o(\epsilon)$ is given by

$$\sigma_o = \sum_m \frac{N_m e^2 \tau_m(\epsilon)}{m^*} \theta(\epsilon - \epsilon_m)$$

where N_m was the areal electron density due to sub-band m. The discontinuity in the relaxation times in (5.19) is due to the onset of inter-sub-band scattering giving rise to the sharp quantum size effects in $\sigma_o(\epsilon)$ Figure 5.2 shows σ_o as a function of the total areal electron density and the smooth curve in the same figure shows the effect of finite temperature (200K), which results in the smoothing out of the quantum size effects at the sub-band discontinuities. In between the two sub-band origins, the true conductivity $\sigma(T)$ is matched by σ_o, because σ_o changes linearly over an energy range of $k_B T$. Similar effects have been observed by Stormer (1981) although he associates the smoothing of his quantum size effects with the lifetime broadening of the sub-band energy states, see the final chapter.

5.2.2 Piezoelectric Scattering

The unit cell in GaAs does not possess a centre of symmetry and atoms are partially ionised. When an acoustic phonon disturbs the atomic positions it sets up a dipole moment which couples the phonons to the conduction electrons. We may write the components of the displacement vector D_i as

$$D_i = \sum_j \epsilon_{ij} e_j + \sum_{k,l} e_{ikl} S_{kl} \tag{5.20}$$

where e_j and S_{kl} are components of the electric field and strain tensor respectively, whilst ϵ_{ij} and e_{ikl} are the permittivity and piezoelectric tensors. If we assume that the displacement of the electrons is small compared to that of the ions we may put $D_i=0$ and hence we find that (Seeger (1973), Zook (1964))

$$\sum_j \epsilon_{ij} e_j = -\sum_{k,l} e_{ikl} S_{kl} \tag{5.21}$$

where for cubic symmetry

$$\epsilon_{ij} = \bar{\kappa}\, \epsilon_o \delta_{ij} \tag{5.22}$$

where $\bar{\kappa}$ is the relative permittivity. The strain tensor S_{kl} may be expanded in terms of the phonon displacement (Nye (1967)).

$$S_{kl} = \tfrac{1}{2}\left[\frac{\partial U_k}{\partial x_l} + \frac{\partial U_l}{\partial x_k}\right] \tag{5.23}$$

We notice that S_{kl} is symmetric under the interchange of k and l. In second quantised notation we write,

$$U_l(\underline{Q}) = \sqrt{\frac{\hbar}{2\omega_Q \rho V}}\, \xi_l \left(a_{\underline{Q}}^{+} e^{-i\underline{Q}\cdot\underline{R}} + a_{\underline{Q}} e^{i\underline{Q}\cdot\underline{R}}\right) \tag{5.24}$$

where 1,2 and 3 label the the co-ordinate axes. Hence,

$$S_{12} = \tfrac{1}{2}i \sqrt{\frac{\hbar}{2\omega_Q \rho V}}\, (\xi_2 Q_1 + \xi_1 Q_2)\left[-a_{\underline{Q}}^{+} e^{-i\underline{Q}\cdot\underline{R}} + a_{\underline{Q}} e^{i\underline{Q}\cdot\underline{R}}\right] \tag{5.25}$$

If we consider a quantum well made of GaAs (which possesses the zinc blende structure) then in reduced notation (Nye (1967))

$$e_{14} = e_{25} = e_{36} \tag{5.26}$$

Moreover, if ϕ denotes the scalar potential we have

$$\underline{\nabla}\cdot\underline{\varepsilon} = -\nabla^2\phi$$

Hence from (5.27), (5.21), (5.22), (5.25) and (5.26) we find

$$\phi = -\frac{1}{\underline{k}\epsilon_o}\,\frac{e_{14}e}{Q^2}\sqrt{\frac{\hbar}{2\omega_Q\rho V}}\,i(\xi_1Q_3Q_2 + \xi_2Q_3Q_1 + \xi_3Q_1Q_2)(-a_{\underline{Q}}^{+}e^{-i\underline{Q}\cdot\underline{R}} + a_{\underline{Q}}e^{i\underline{Q}\cdot\underline{R}}) \tag{5.28}$$

When we introduce direction cosines

$$\frac{Q_3}{Q} = \gamma\,,\ \frac{Q_2}{Q} = \beta\,,\ \frac{Q_1}{Q} = \alpha$$

we find from equation (5.28) that

$$H_{e\text{-}p} = -\frac{1}{\underline{k}\epsilon_o}\,e_{14}e\sqrt{\frac{\hbar}{2\omega_Q\rho V}}\;i(\xi_1\beta\gamma + \xi_2\gamma\alpha + \xi_3\alpha\beta)\;\;(-a^{+}_{\underline{Q}}e^{-i\underline{Q}\cdot\underline{R}} + a_{\underline{Q}}e^{i\underline{Q}\cdot\underline{R}}) \tag{5.29}$$

for a longitudinal mode $\xi_1=\alpha$, $\xi_2=\beta$, $\xi_3=\gamma$. Hence

$$H^{1}_{e\text{-}p} = -\frac{i}{\underline{k}\epsilon_o}\,e_{14}e\sqrt{\frac{\hbar}{2\omega_{\underline{Q}}\rho V}}(3\alpha\beta\gamma)(-a^{+}_{\underline{Q}_L}e^{-i\underline{Q}\cdot\underline{R}} + a_{\underline{Q}_L}e^{i\underline{Q}\cdot\underline{R}}) \tag{5.30}$$

and

$$M_1 \equiv \langle s;n,\underline{k}|H'_{e\text{-}p}|\underline{k}',m;s\rangle \tag{5.31}$$

where it should be remembered that $a_{\underline{Q}l}$ and $a_{\underline{Q}l}^{+}$ are the phonon annhialation and creation operators for longitudinal acoustic modes. For transverse modes we can think of $(Q_3Q_2\xi_1+Q_3Q_1\xi_2+Q_1Q_2\xi_3)$ in equation (5.28) as being the

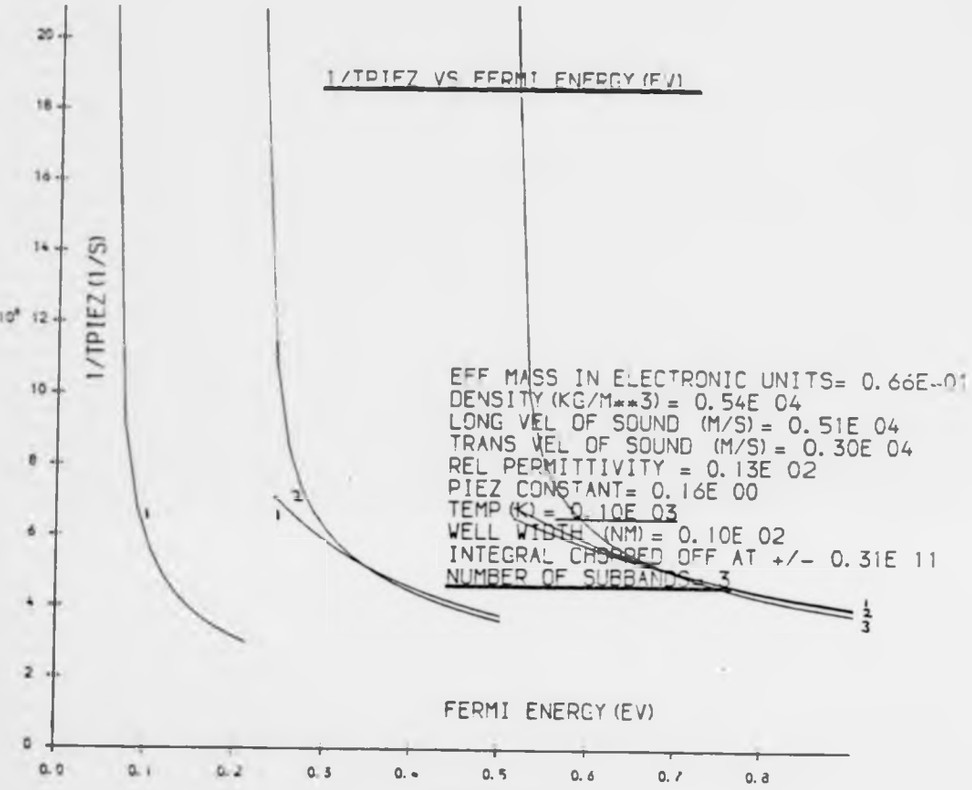

FIG 5.3

Momentum relaxation rates for piezoelectric scattering. The material constants are taken from Zook(1964) and Rode(1975).

dot product of $\underline{\xi}$ with a vector $Q_3Q_2\underline{i}+Q_3Q_1\underline{j}+Q_1Q_2\underline{k}$. The result $(3-\beta\gamma)^2$ in equation (5.30) was obtained by aligning the polarisation with $\underline{Q}$. The contribution due to the transverse modes is found by taking the squared length of the vector $Q_3Q_2\underline{i}+Q_3Q_1\underline{j}+Q_1Q_2\underline{k}$ and subtracting the result $(3-\beta\gamma)^2$. Hence for transverse modes we have

$$|M_t|^2 = (\alpha^2\beta^2+\beta^2\gamma^2+\gamma^2\alpha^2-(3\alpha\beta\gamma)^2) \quad |\langle s;n,\underline{k}| \frac{ee_{14}}{\underline{k}\epsilon_o}\sqrt{\frac{\hbar}{2\omega\rho V}}(a^+_{\underline{Q}t}e^{-i\underline{Q}\cdot\underline{r}}+a_{\underline{Q}t}e^{i\underline{Q}\cdot\underline{r}})|\underline{k}'m;s'\rangle|^2 \tag{5.32}$$

These matrix elements were calculated with one propagation direction in mind. If we average over all possible propagation directions we find (Ridley (1982b)).

$$\langle(3\alpha\beta\gamma)^2\rangle = \frac{3}{35} \quad \text{and} \quad \langle\alpha^2\beta^2+\beta^2\gamma^2+\gamma^2\alpha^2-(3\alpha\beta\gamma)^2\rangle = \frac{4}{35} \tag{5.33}$$

which gives the high temperature result

$$P(\underline{k},n;\underline{k}',m) = \frac{\pi}{\rho A}\left[\frac{e_{14}e}{\underline{k}\epsilon_o}\right]^2 \left[\frac{4}{35}\frac{2k_BT}{\hbar V_t^2}+\frac{3}{35}\frac{2k_BT}{\hbar V_L^2}\right]\times\left(\frac{G^2_{nm}(q_z)}{|Q|^2}\frac{dq_z}{2\pi}\right)\delta(\epsilon_n(\underline{k})-\epsilon_m(\underline{k}')) \tag{5.34}$$

where

$$\underline{Q} = \underline{k}-\underline{k}'+\underline{q}_z$$

and A is the area of the device. By substituting this result into the Siggia and Kwok equations (3.20) we may calculate the relaxation times numerically. Results are given in Figure 5.3. Unlike the deformation potential the piezoelectric relaxation times are different for each sub-band at high temperatures. This is because of the Q dependence of the piezoelectric mechanism which is also responsible for the divergences at the sub-band minima.

The relative importance of the two mechanisms is critically dependent on the carrier density. When the Fermi energy lies at the bottom of a sub-band, the divergence in the piezoelectric scattering momentum relaxation rate and the constant nature of the deformation potential scattering rate implies that the former dominates. However as the Fermi energy is increased the importance of the mechanisms switches. We return to the importance of screening in this problem in the final chapter. However, Figures 5.1 and 5.2 indicate that for realistic carrier densities even ignoring screening the deformation potential will dominate over the piezoelectric scattering mechanism.

5.2.3 Scattering by Monatomic Circular Islands

Joyce (1986) has suggested a model for the state of the GaAs/$Al_xGa_{1-x}As$ interface in a quantum well, arising from the MBE preparation technique. In his model, deduced from electron diffraction measurements, the interface is not smooth but possesses an island structure. The characteristic size of these circular islands depends on whether the GaAs is depositing on a $Al_xGa_{1-x}As$ layer or vice-versa. In the former case the radius of the islands is of the order of 35Å and in the latter 250Å. With no additional information available we suppose that these islands are uncorrelated in position. We look at this problem in a formal way and neglect the atomic structure by representing the islands as thin cylinders of known potential V_o, which will be taken to be small. We assume that our wavefunction can leak out of the well, and the confining potential is taken to be so small that it changes the wavefunction only slightly allowing us to work in the effective mass approximation. To be definite we consider the GaAs/$Al_xGa_{1-x}As$ system and treat the alloy potential in the virtual crystal approximation. Then the scattering potential of each island takes the form

$$V(\underline{r},z) = V_o = \Delta E_c \begin{cases} -h<z<0 \\ |\underline{r}|<r_o \end{cases}$$

$$= 0 \qquad \begin{cases} z>0, z<-h \\ |\underline{r}|>r_o \end{cases} \tag{5.35}$$

where r_o is the radius and h is the height of the cylinder. The matrix element responsible for the scattering is given by

$$M_r = \langle n,\underline{k}|V(\underline{r},z)|\underline{k}',m\rangle$$

$$= \int_o^h dz \int_o^{r_o} r\,dr \int_o^{2\pi} d\theta\, \zeta_n(z)\zeta_m(z) e^{i|\underline{k}-\underline{k}'|r\cos\theta} \frac{V_o}{A} \tag{5.36}$$

where θ is the angle between $|\underline{k}-\underline{k}'|$ and $\underline{r}$. Since the $\zeta n(z)$ are assumed to be slowly varying over the range 0 to -h we can take them outside the integral and evaluate them at 0. Then we have

$$M_r = \frac{V_o}{A} h\zeta_n(0)\zeta_m(0) x \frac{1}{q^2} \int_o^{qr_o} 2\pi J_o(x)x\,dx \tag{5.37}$$

where $q = |\underline{k}-\underline{k}'|$ and we have performed the θ integration. It is a property of Bessel functions that (Abramowitz and Stegun)

$$J_{m-1}(x) = \frac{m}{x} J_m(x) + J'_m(x) \tag{5.38}$$

we can use this property to integrate (5.37) to obtain

$$M_r = \frac{V_o h 2\pi r_o}{A} \zeta_n(0)\zeta_m(0) J_1(qr_o)/q \tag{5.39}$$

Equation (5.39) is the result for a single isolated island in a quantum well. With more than one island present we have to carry out an appropriate average. When many islands are present so that they fit together to form a continuous layer the scattering rate reduces to zero. Consequently, the averaging problem is then the same as that which arises in alloy scattering where a virtual crystal approximation was also used, except that now we have some short-range correlation. By defining an average potential for the layer and assuming that all the islands are of the same radius, r_o, we

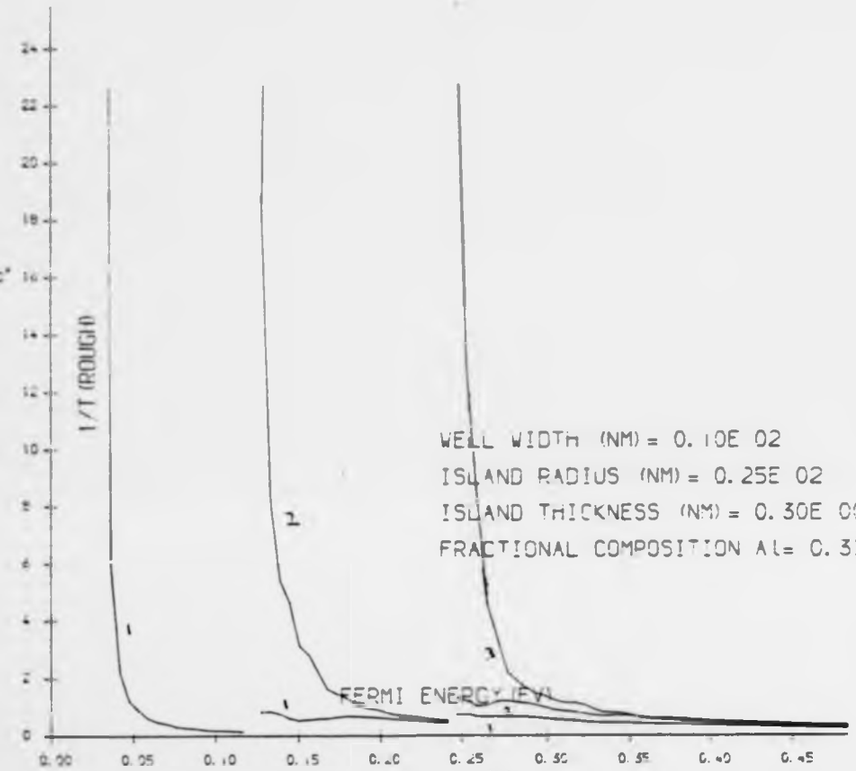
WELL WIDTH (NM) = 0.10E 02
ISLAND RADIUS (NM) = 0.25E 02
ISLAND THICKNESS (NM) = 0.30E 00
FRACTIONAL COMPOSITION Al= 0.30E 00
1/T (ROUGH)
FERMI ENERGY (EV)
1
2
3
24
22
20
18
16
14
12
10
8
6
4
2
0
0.00
0.05
0.10
0.15
0.20
0.25
0.30
0.35
0.40
0.45

(c)

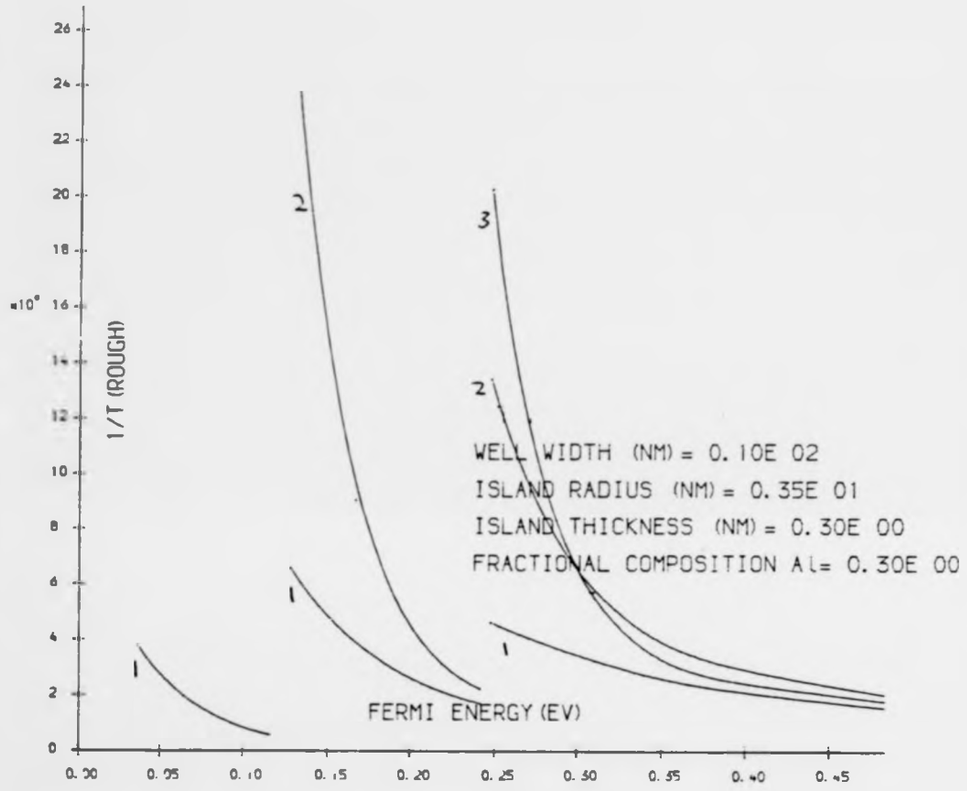
1/T (ROUGH)
x10^6
26
24
22
20
18
16
14
12
10
8
6
4
2
0
0.30
0.35
0.10
0.15
0.20
0.25
0.30
0.35
0.40
0.45
FERMI ENERGY (EV)
WELL WIDTH (NM) = 0.10E 02
ISLAND RADIUS (NM) = 0.35E 01
ISLAND THICKNESS (NM) = 0.30E 00
FRACTIONAL COMPOSITION Al= 0.30E 00
1
2
3

(b)

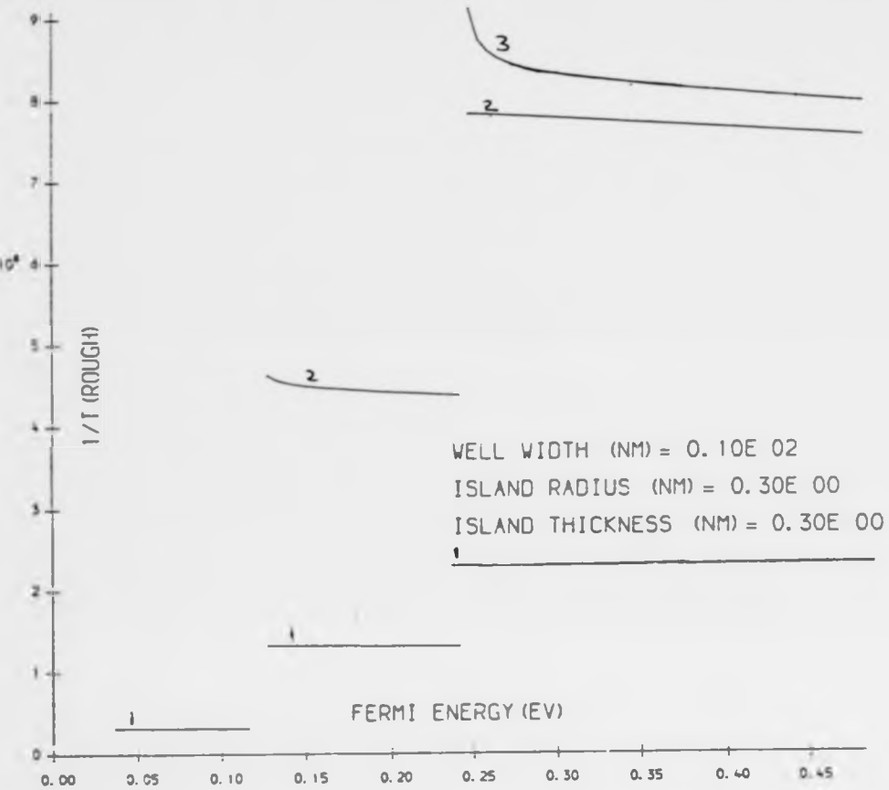

FIG 5.4 (a)

Momentum relaxation rates for surface roughness scattering in a 2-D.E.G. using Joyce's model.

obtain the following approximate expression

$$|M_r|^2 = \frac{Nf(1-f)}{A}\left[\frac{[V_o h 2\pi r_o]\zeta_n(0)\zeta_m(0)\,J_1(qr_o)}{q}\right]^2 \qquad (5.40)$$

where N is the maximum possible number of scatterers per unit area and f is the fraction of the surface covered by the cylinders. This scattering mechanism is elastic and hence the transition rate,

$$P(\underline{k},n;\underline{k}',m) = \frac{2\pi}{\hbar}|M_r|^2\delta(\epsilon_n(\underline{k})-\epsilon_m(\underline{k}')) \qquad (5.41)$$

may be inserted into (3.20) to give the momentum relaxation rates. The magnitude of the relaxation times is principally determined by the value of the N. In all cases we have taken the surface of the quantum well to be 50% covered by the scatterers, the difference between the curves is then mainly due to the size of the islands. The values of r_o were given by Joyce and the value of h was taken as 3Å which is approximately the thickness of one atomic layer. We have plotted the relaxation times for both r = 250Å and r = 35Å in Figure 5.4. For small qr, $J_1(qr_o) \sim qr_o/2$ and the scattering mechanism is q independent. In this case the relaxation time curves have the familiar staircase form, see Figure 5.4a. For larger islands see Figure 5.4c, $J_1(qr_o)$ oscillates and this is reflected in the oscillatory nature of the relaxation times. In reality we would expect there to be some spread in the radius, shape and orientation of these islands and this would smear out the oscillations. For larger islands inter-sub-band scattering is less marked. This is easily explained, there is a minimum value of q, q_{min} needed for an inter-sub-band transition to take place. For larger islands where $r_o \geq 1/k_F$, $J_1(qr_o)/q$ falls off with q, hence when $r_o \geq 1/q_{min}$ inter-sub-band transitions are less probable. The curves then decouple to a large extent. The relaxation times are almost continuous functions of energy and the QSE disappear.

The origin of surface roughness scattering is the same as that of alloy scattering and the two could be described together if the autocorrelation function in equation (4.20) was known exactly. However with the approximations made here we find on referring to Figures 4.3 and 5.4 that the alloy scattering momentum relaxation rates are in general larger for $Al_xGa_{1-x}As$ and this will dominate. It is also worth noting that as x is increased the hidden composition dependence in the quantum-well wavefunction results in smaller alloy scattering relaxation rates even before x=0.3 (see Figure 4.3 for x=0.3). This is primarily due to rapid decay of the wavefunction in the alloy.

5.3 High Temperature Phonon Scattering in Quasi-One-Dimensional Wires

In this section we apply the set of coupled equations (3.31) derived in Chapter 3 to a one-dimensional wire with a rectangular cross-section of dimensions axb. We make the same assumptions as we did for the two-dimensional channel and consider the wire to sit in a three-dimensional cube of volume D^3. We look at scattering due to the piezoelectric and deformation potential mechanisms.

Johnson and Vassell (1984) have looked at this problem. However, they used an expression for a single momentum relaxation rate which neglected the coupling of the one-dimensional Boltzmann equations. Their expression was of the form

$$\frac{1}{\Upsilon(\varepsilon_{n,l}(\underline{k}))} = \frac{2\pi}{\hbar} \sum_{n',l',\underline{k}',\underline{q}} |\langle n',l',\underline{k}'|Vq(x,y,z)|\underline{k},l,n\rangle|^2$$

$$\times (1-k'/k)\delta(\varepsilon_{n',l'}(\underline{k}')-\varepsilon_{n,l}(\underline{k})-\Delta E\underline{q}) \qquad (5.42)$$

We would expect this value of Υ to depend on the choice of n and l and we would also expect it to change discontinuously as another sub-band becomes

occupied, but this feature is absent from their graphs. In general a solution of the linearised Boltzmann equation must be effected by using the coupled relaxation time equations (3.31) which take full account of inter-sub-band scattering. The coupled equations have the form

$$\tau_{nm}(\epsilon_{nm}(k))\sum_{n'm'}\int P(k,n,m;k',n',m')\frac{L}{2\pi}dk' - \sum_{n'm'}\tau_{n'm'}\int\frac{k'}{k}P(k,n,m;k',n',m')\frac{L}{2\pi}dk' = 1$$

with the conductivity given by

$$\sigma_o = \sum_{nm}\frac{N_{n,m}e^2\tau_{nm}}{m^*} \qquad (5.44)$$

In one-dimension only a discrete set of k vectors are involved in the scattering process and these are defined by the endpoints of the Fermi-lines in each occupied sub-band. From now on we work with the notation that $k=|\underline{k}|$ and we introduce the sign of the k's explicitly. The delta-function in the expression for $P(k,n,m;k',n',m')$ means that the integral over $\underline{k}'$ results in two terms one for +k and one for -k. We split the summations up to bring this out. Hence equation (5.43) gives

$$\tau_{nm}\sum_{\substack{n',m'\\ \underline{k}'>0}}\int P(k,n,m;k',n',m')\frac{L}{2\pi}dk' + \tau_{nm}\sum_{\substack{n'm'\\ \underline{k}'<0}}\int P(k,n,m;-k',n',m')\frac{L}{2\pi}dk'$$

$$-\sum_{\substack{n'm'\\ \underline{k}'>0}}\tau_{n'm'}\int\frac{k'}{k}P(k,n,m;k',n',m')\frac{L}{2\pi}dk' + \sum_{\substack{n'm'\\ \underline{k}'<0}}\tau_{n'm'}\int\frac{k'}{k}P(k,n,m;-k',n',m')dk' = 1 \qquad (5.46)$$

where

$$P(k,n,m;k',n',m') = \frac{2\pi}{\hbar}\iint|\langle s',k',n',m'|H_{ep}|m,n,k;s\rangle|^2\frac{A}{4\pi^2}dq_x\,dq_y$$

$$\delta(\epsilon_{n,m}(k)-\epsilon_{n',m'}(k')) \qquad (5.47)$$

and $A=D^2$ the area of a side of the phonon block. Once again we expect the elastic approximation to be useful at high temperatures when equipartition is valid.

5.3.1 Deformation Potential Scattering

For deformation potential scattering and the infinite rectangular well wavefunctions (2.5) we find

$$P(k,n,m;k',n',m') = \frac{k_B T E^2_{def}}{\hbar s^2 \rho D 2\pi} F(a)F(b)\delta(\epsilon_{nm}(k)-\epsilon_{n'm'}(k')) \tag{5.48}$$

where

$$F(a) = \int_0^\infty \left| \int_0^a \frac{2}{a} \sin\frac{n\pi x}{a} e^{iq_x x} \sin\frac{m\pi x}{b} dx \right|^2 dq_x, \; S = V_L \tag{5.49}$$

where the integral over q_x is taken to extend to ∞. The integrations can be performed to give

$$P(k,n,m;k',n',m') = \frac{k_B T E^2_{def}}{\hbar s^2 \rho D 2\pi} \times \frac{\pi^2}{ab}(2+\delta_{n,n'})(2+\delta_{m,m'}) \; \delta(\epsilon_{nm}(k)-\epsilon_{n'm'}(k')) \tag{5.50}$$

which is similar to the result obtained for δ-function scatterers. The coupled equations (5.46) can be rewritten to separate intra from inter-subband scattering, giving

$$\begin{aligned} &\Upsilon_{nm}\Sigma' \int_{k'>0} P(k,n,m;k',n',m') \frac{D}{2\pi} dk' + \Upsilon_{nm}\Sigma' \int_{k'<0} P(k,n,m;-k',n',m') \frac{D}{2\pi} dk' \\ &-\Sigma'\Upsilon_{n'm'} \int_{k'>0} \frac{k'}{k} P(k,n,m;k',n',m') \frac{D}{2\pi} dk' + \Sigma' \Upsilon_{n'm'} \int_{k'<0} \frac{k'}{k} (P(k,n,m;-k',n',m') \frac{D}{2\pi} dk' \\ &+ 2\Upsilon_{nm} \int_{k'<0} P(k,n,m;-k',n,m) \frac{D}{2\pi} dk' = 1 \end{aligned} \tag{5.51}$$

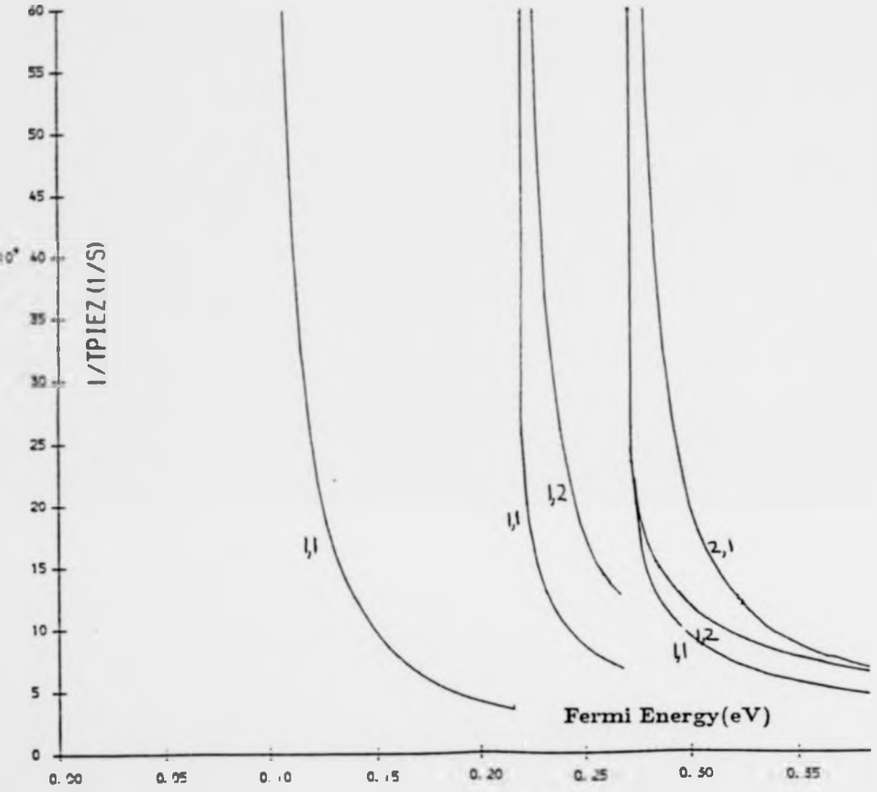

FIG 5.6

Momentum relaxation rates for piezoelectric scattering at high temperatures in a one-dimensional wire(100 K)

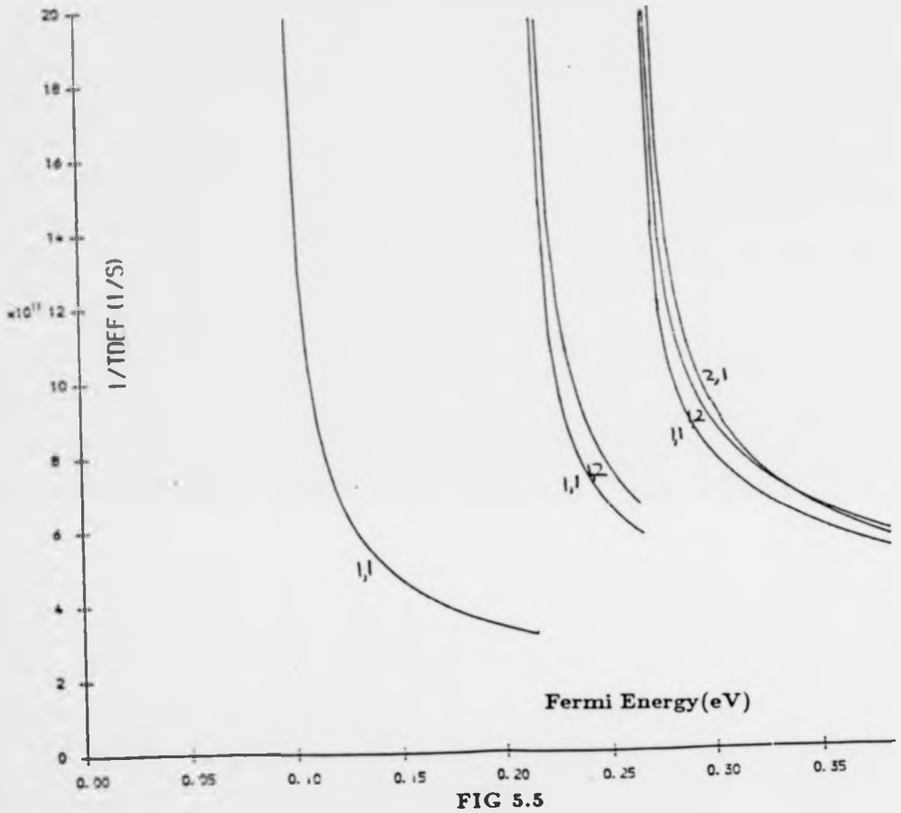

FIG 5.5

Momentum relaxation rates for deformation potential scattering at high temperatures in a one dimensional wire .The wire has a rectangular cross-section (10nm,12nm) and the temperature is 100K.

where

$$\Sigma' = \sum_{\substack{n'm' \\ (n,m)\neq(n',m')}}$$

When we are considering the extreme quantum limit the summations are all zero and we are left with a momentum relaxation rate which is equal to twice the scattering rate.

$$\frac{1}{\tau_{1,1}(\epsilon)} = 2\int_{k'<0} P(k,1,1;-k',1,1)\frac{D}{2\pi}dk'$$

The factor of two arises because the change in momentum is equal to 2k when an electron scatterers across the one-dimensional sub-band. We have solved the algebraic equations (5.51) for the deformation potential and the results are shown in Figure 5.5. The $\tau_{n,m}$ are all different at a particular energy and their shape is dominated by the singular one-dimensional density of states (c.f. the two-dimensional case). When ϵ corresponds to a sub-band energy both intra and inter-sub-band scattering rates are singular and all the momentum relaxation times are zero. One-dimensional systems should therefore exhibit extremely pronounced QSE.

5.3.2 Piezoelectric Scattering

Following the procedure given in section 5.2.2 for piezoelectric scattering in two-dimensional systems we find that the same method gives rise to a scattering rate

$$R_{n,m\rightarrow n',m'}(\epsilon) = \int P(k,n,m;k',n',m')\frac{D}{2\pi}dk'$$

$$= \left[\frac{ee_{14}}{\bar{\kappa}\epsilon_o}\right]^2 \times \frac{m^*k_BT}{32\hbar^3\pi^2\rho} \times \left[\frac{8}{V_t^2}+\frac{6}{V_l^2}\right]\int\frac{1}{35Q^2}\frac{G_n^2(q_x)G_{n'}^2(q_y)dq_xdq_y}{\sqrt{\frac{2m^*\epsilon}{\hbar^2}-\frac{n'^2\pi^2}{a^2}+\frac{m'^2\pi^2}{b^2}}} \qquad (5.52)$$

where $Q^2=[k-k']^2+q_x^2+q_y^2$ and $G_{mn}^2(q_x)$ is the function given by Ridley (see appendix 2). The relaxation time equations have been solved and the results are shown in Figure 5.6. The curves are again singular at the sub-band origins.

When the energy is well away from the sub-band bottom the momentum relaxation rates are small because the value q needed to effect scattering across a sub-band is large and this is prohibited by the $1/Q^2$ dependence of the scattering rate. The deformation potential on the other hand was Q independent at high temperatures and consequently we would expect this to be the dominant mechanism in one-dimensional systems at high temperatures and large Fermi energies.

CHAPTER 6

INELASTIC SCATTERING

6.1 Introduction

We mentioned in Chapter 5 that the elastic scattering approximation is only valid for acoustic phonons when the characteristic energies involved in the scattering are much less than the thermal excitation energies. Here we consider what happens when this criterion is no longer valid and we develop an approximate scheme for solving the problem. In 6.2 we consider the effect of inelasticity on the momentum relaxation rates of two-dimensional systems. In three-dimensional metallic systems these considerations lead to a conductivity which varies as T^{-5} at very low temperatures (Butcher (1973)). We investigate this Bloch-Gruneisen law in two-dimensional and one-dimensional systems.

We start by reconsidering the phonon absorption and emission processes. We imagine an electron to start at energy ε and to finish at energy $\varepsilon+\Delta(\underline{Q})$ after absorbing a phonon of energy $\Delta(\underline{Q})$. The scattering rate due to phonon absorption is proportional to the Bose factor

$$N_Q = \frac{1}{e^{\beta\Delta(\underline{Q})}-1} \qquad (6.1)$$

At low temperatures the probability of such a transition is small and consequently the momentum relaxation rate due to this route is also low. On the other hand, we may consider the phonon emission process which is proportional to (N_Q+1). At very low temperatures this factor is equal to 1. If we were to place our faith in the elastic scattering approximation and the equations of Siggia and Kwok we might expect there to be a finite contribution to the DC resistance of the 2-DEG due to acoustic phonon emission even at absolute zero. This argument is clearly wrong, if we were

to continuously emit phonons, N_Q would grow, the temperature would rise and the steady-state would be destroyed.

The solution of this dilemma involves rejecting the elastic scattering approximation. The equations of Siggia and Kwok (3.20) are independent of the electronic statistics and this is what is causing the problem. In order to proceeed we must first reject the relaxation time approximation which is exact for elastic mechanisms and develop a variational principle for quasi-two-dimensional systems. An effective relaxation time will be reintroduced later in the application of the variational principle.

6.2 Inelastic Scattering in Two-Dimensional Systems

The variational form of the three-dimensional Boltzmann equation was first introduced by Kohler (1948) and was used by Sondheimer and Howarth (1953) in their treatment of polar optic phonon scattering in bulk semiconductors. This approach is particularly useful because the iterative approach (Rode (1970)) requires extensive use of a computer, whereas the amount of work involved in a variational calculation is under the control of the user. When linearised the Boltzmann equation may be written in the form

$$Z^n = C\psi_n(\underline{k}) \tag{6.2}$$

where

$$Z^n = \frac{-e}{\hbar} E \frac{\partial f_o}{\partial k}(\underline{k}), \quad f_1^n(\underline{k}) = -\chi_n(\underline{k}) \frac{df_o}{d\epsilon} \tag{6.3}$$

and

$$C\psi_n(\underline{k}) = -\left[\frac{\partial f_1^n(\underline{k})}{\partial t}\right]_{coll}$$

$$= -\beta \sum_m \int f_o(\epsilon_n(\underline{k}))[1-f_o(\epsilon_m(\underline{k}'))]P(\underline{k},n;\underline{k}',m)\ (\psi_m(\underline{k}')-\psi_n(\underline{k}))\frac{A}{4\pi^2}d^2k' \tag{6.4}$$

we shall call C the collision operator. The low-field conductivity of the 2-DEG is given by

$$\sigma_o = \frac{-e}{2\pi^2} \sum_n \int f^n(\underline{k}) V_x^n(\underline{k}) d^2k \tag{6.5}$$

where $V_x^n(\underline{k})$ is the x component of the electron velocity in sub-band n and the summation is over all sub-bands. In first order equation (6.5) reduces to

$$\sigma = \frac{-e^2}{2\pi^2 (E_x)^2} \sum_n \int z^n \psi_n(\underline{k}) d^2k \tag{6.6}$$

Alternatively, we can use the Boltzmann equation (6.2) and write

$$\sigma = \frac{-e^2}{2\pi^2 (E_x)^2} \sum_n \int \psi_n(\underline{k}) C\psi_n(\underline{k}) d^2K \tag{6.7}$$

To develop the variational method we first need to look at the symmetry properties of the operator C.

6.2.1 Symmetry Properties of the Collision Operator

Using the equilibrium electron transfer rate (5.2), consider the expression

$$\begin{aligned} E &= \sum_n \int g(\underline{k},n) Ch(\underline{k},n) d^2k \\ &= \beta \sum_n \int d^2k \sum_m \int g(\underline{k},n) V(\underline{k},n;\underline{k}',m) [h(\underline{k}',m) - h(\underline{k},n)] \frac{A}{4\pi^2} d^2k' \\ &= \beta \sum_n \int d^2k \sum_m \int g(\underline{k}',m) V(\underline{k}',m;\underline{k},n) [h(\underline{k},n) - h(\underline{k}',m)] \frac{A}{4\pi^2} d^2k' \end{aligned} \tag{6.8}$$

In the second line we have used equation (6.4). In the third line we have interchanged $\underline{k}$ and $\underline{k}'$.

If we add the last two expressions and divide by two we find

$$E = -\frac{\beta}{2}\sum_n \int d^2k \sum_m \int [g(\underline{k},n)-g(\underline{k}',m)]V(\underline{k}',m;\underline{k},n)[h(\underline{k},n)-h(\underline{k}',m)]\frac{A}{4\pi^2}d^2k' \dagger$$

$$- \sum_n \int h(\underline{k},n)Cg(\underline{k},n)d^2k \qquad (6.9)$$

Hence C is symmetrical. Inserting equation (6.9) into (6.7) we find that

$$\sigma = \frac{\beta}{2}\frac{e^2}{2\pi^2(E_x)^2}\sum_n \int d^2k \sum_m \int f_o(\epsilon_n(k))[1-f_o(\epsilon_m(k'))]P(\underline{k},n;\underline{k}',m)$$

$$x\ [\psi_m(\underline{k}')-\psi_n(\underline{k})]^2 x \frac{A}{4\pi^2}d^2k' \qquad (6.10)$$

which, we note, is positive definite.

6.2.2 A Variational Principle

Using the result (6.9) and the expressions (6.6) and (6.7) we can write down an expression for the conductivity which has an extremum in ψ_n space when the Boltzmann equation is satisfied:

$$\sigma = \frac{-e^2}{\pi^2(E_x)^2}\left[\sum_n \int Z^n\psi_n(\underline{k})d^2k - \frac{1}{2}\sum_n \int \psi_n(\underline{k})C\psi_n(\underline{k})d^2k\right] \qquad (6.11)$$

To prove that (6.11) is stationary we consider a trial function $\phi_n(\underline{k})$ which is expressed as the true solution $\psi_n(\underline{k})$ plus a small deviation $\delta\psi_n(\underline{k})$ and we look at the first order deviation $\delta\sigma$ from the true conductivity σ_T obtained from $\psi_n(\underline{k})$. Hence

† The interchange of g and h leaves the equality intact.

$$\delta\sigma+\sigma_T = \frac{-e^2}{\pi^2(E_x)^2}\left[\sum_n \int z^n\psi_n(\underline{k})d^2k + \sum_n \int z^n\delta\psi_n(\underline{k})d^2k\right.$$

$$\left. - \sum_n \int \delta\psi_n(\underline{k})C\psi_n(\underline{k})d^2k - \tfrac{1}{2}\sum_n \int \psi_n(\underline{k})C\psi_n(\underline{k})d^2k \right]$$

Hence

$$\delta\sigma = \frac{-e^2}{\pi^2(E_x{}^2)} \sum_n \int \delta\psi_n(k)[z^n - C\psi_n]d^2k = 0 \qquad (6.12)$$

when the Boltzmann equation is satisfied. We can use this variational principle to obtain a best estimate of the conductivity for a given functional form $\emptyset_n(\underline{k})$. Sondheimer and Howarth (1953) expanded their single band trial function in terms of a complete set of functions of energy. In principle an exact value for the Boltzmann conductivity may be obtained by using this approach, however it is necessary to truncate the series expansion at some point. We use the simplest expansion, a constant, which may depend on Fermi level positioning but not on energy. The aim is to see how the relaxation time expression which is exact for elastic scattering is modified as the temperature is lowered. Thus we use the ansatz

$$\emptyset_n = V_x{}^n E_x \tau_n \qquad (6.13)$$

where τ_n is a constant independent of energy for a given value of ϵ_F, the Fermi Energy.

6.2.3 Deformation Potential Scattering at Low Temperatures

We consider the physical configuration discussed in Chapter 5, where we used the elastic scattering approximation to obtain Ridley's scattering rate

formula for deformation potential scattering. We noted that this approach was valid if the typical values of phonon energy $\Delta(Q)$ arising in the integrals were much less than the thermal energy. The deformation mechanism has no Q dependence and a typical value of Q may be taken as $2k_F$. The maximum value for k in a single sub-band in the square well approximation is $2\pi/L$. The elastic scattering approximation will be valid if

$$\hbar V_L \times \frac{4\pi}{L} \ll k_B T$$

$$\text{ie if } T \gg \frac{\hbar 4\pi}{k_B} \frac{V_L}{L}$$

where L is the width. For a 40Å well the temperature must be greater than about 100k, at temperatures lower than this the effects of inelasticity will be important.

The transition probability due to the absorption of acoustic phonons through the deformation potential is given by

$$P_{abs}(\underline{k},n;\underline{k}',m) = \int_{-\infty}^{+\infty} \frac{D}{2\pi} \frac{\pi E^2_{def}}{\rho V V_L} N_Q G^2_{nm}(q_z) |Q| \delta(\epsilon_n(\underline{k}) - \epsilon_m(\underline{k}') + \Delta(Q)) dq_z \tag{6.14}$$

where $\Delta(Q)$ is the energy of a phonon with wavevector $\underline{Q}$. Let θ and θ' denote the angles between $\underline{k}$ and $\underline{k}'$ and the x-axis and replace $\epsilon_n(\underline{k})$ by ϵ and $\epsilon_n(\underline{k}')$ by ϵ'; then equation (6.11) yields

$$\sigma = \frac{e^2\beta}{4\pi^2} \sum\sum_{nm} \int_0^{2\pi} d\theta \int_o^{\infty} d\epsilon' \frac{m^*}{\hbar^2} \int_{-\infty}^{+\infty} dq_z \frac{V}{8\pi^3} \int_0^{2\pi} d\theta' \Big[f_o(\epsilon' - \Delta(Q))[1 - f_o(\epsilon')]$$

$$\times F_{abs}(n,m;q_z,Q)(V_x^n \gamma_m - V_x^m \gamma_n)^2 \Big] \times \frac{m^*}{\hbar^2} \tag{6.15}$$

where $Q=|\underline{Q}|$ and Fabs (n,m,q_z,Q) is defined as

$$F_{abs}(n,m;q_z,Q) = \frac{\pi E^2 def}{\rho V_L} N_{\underline{Q}} \; G^2_{nm}(q_z)Q \tag{6.16}$$

The only rapidly varying function of energy in (6.15) is then $f_o(\epsilon'-\Delta(Q))(1-f_o\epsilon)$ which peaks at ϵ_F. We integrate this and treat the other functions as constants, evaluating them at ϵ_F. Now

$$\int_o^\infty f_o(\epsilon-\Delta(Q))(1-f_o(\epsilon))d\epsilon = \frac{\Delta(Q)}{1-\exp(-\beta\Delta(Q))} \tag{6.17}$$

so that

$$\sigma = \frac{\beta e^2}{4\pi^2} \sum\sum_{nm} \int_o^{2\pi} d\theta' \int_o^{2\pi} d\theta \int_{-\infty}^{+\infty} \frac{V}{8\pi^3} \, dq_z \frac{m^*}{\hbar^2} \frac{\Delta(Q)}{1-\exp(-\beta\Delta(Q))} F(n,m;q_z,Q)$$

$$\times \; (k_F{}^m\cos\theta'\tau_m - k_F{}^n\cos\theta\tau_n)^2 \tag{6.18}$$

where k_F^m is the Fermi radius in sub-band m.

The alternative expression for the conductivity (6.6) gives

$$\sigma = \sum_n \frac{N_n e^2 \tau_n}{m^*} \tag{6.19}$$

When we construct the variational form (6.11), the variational equation $\frac{\partial\sigma}{\partial\tau_r}=0$ reduces to

$$1 = \frac{\beta m^*}{\hbar^2}\tau_r \sum_n \int_o^{2\pi} d\alpha \int_{-\infty}^{+\infty} \frac{V}{8\pi^3} \, dq_z G_{abs}(r,n;q_z,Q)$$

$$- \frac{\beta m^*}{\hbar^2} \sum_n \tau_n \int_o^{2\pi} d\alpha \int_{-\infty}^{+\infty} \frac{V}{8\pi^3} \, dq_z \frac{k_F{}^n}{k_F{}^r} \cos\alpha G_{abs}(r,n;q_z,Q) \tag{6.20}$$

1/TDEF VS FERMI ENERGY(EV)

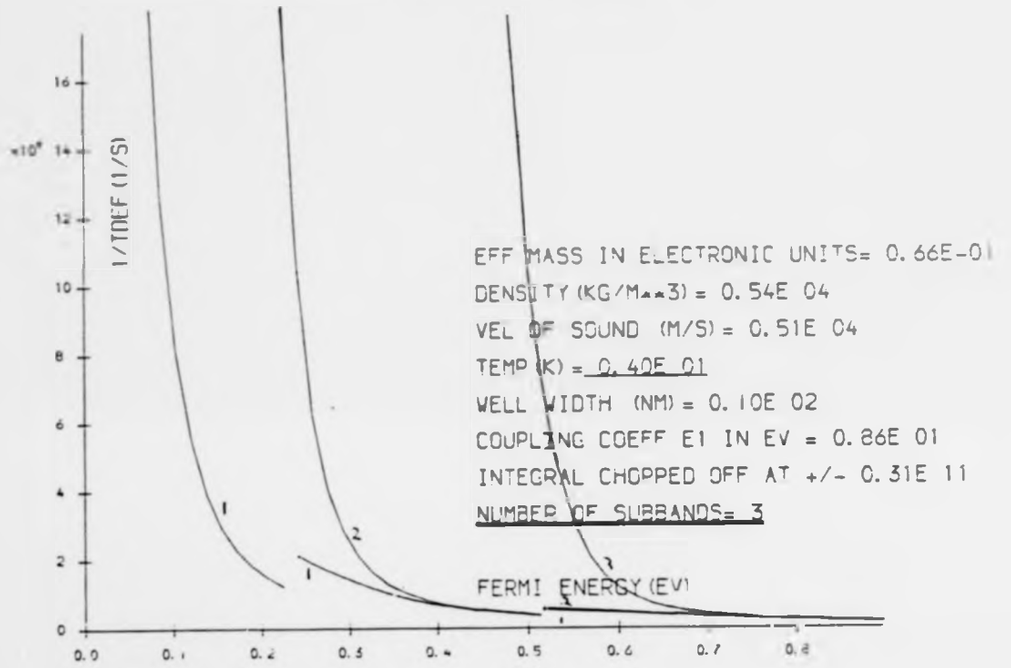

EFF MASS IN ELECTRONIC UNITS= 0.66E-01
DENSITY (KG/M**3) = 0.54E 04
VEL OF SOUND (M/S) = 0.51E 04
TEMP (K) = 0.40E 01
WELL WIDTH (NM) = 0.10E 02
COUPLING COEFF E1 IN EV = 0.86E 01
INTEGRAL CHOPPED OFF AT +/- 0.31E 11
NUMBER OF SUBBANDS= 3

(c)

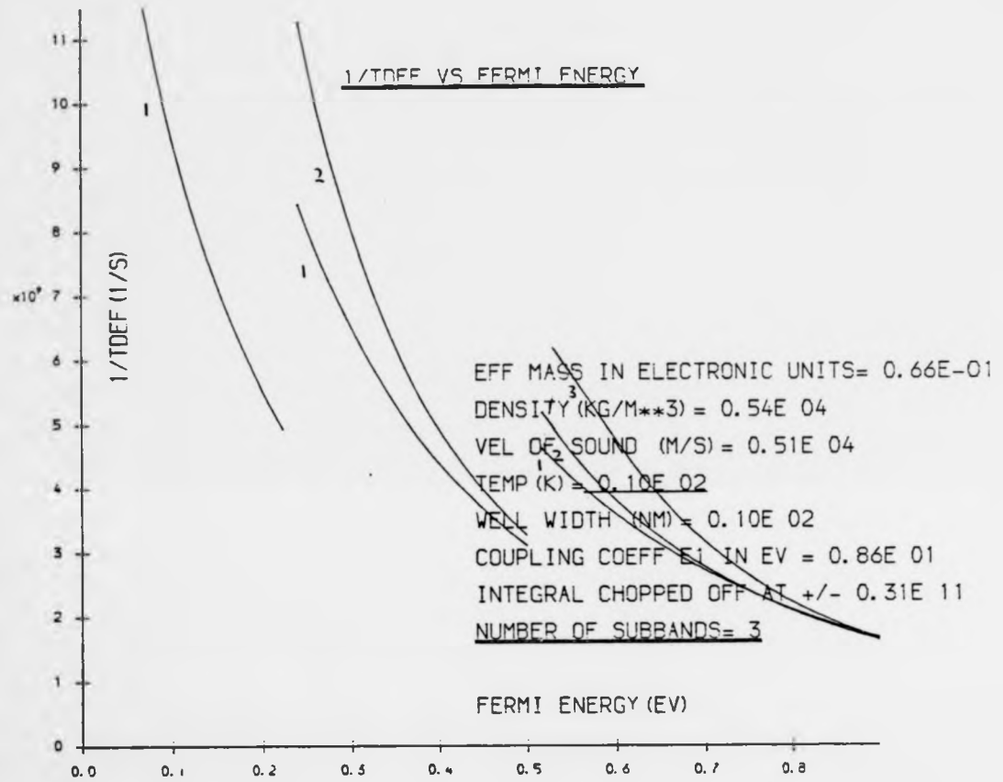
1/TDEF VS FERMI ENERGY
1/TDEF (1/S)
x10⁷
11
10
9
8
7
6
5
4
3
2
1
0
1
2
1
2
3
EFF MASS IN ELECTRONIC UNITS= 0.66E-01
DENSITY (KG/M**3) = 0.54E 04
VEL OF SOUND (M/S) = 0.51E 04
TEMP (K) = 0.10E 02
WELL WIDTH (NM) = 0.10E 02
COUPLING COEFF E1 IN EV = 0.86E 01
INTEGRAL CHOPPED OFF AT +/- 0.31E 11
NUMBER OF SUBBANDS= 3
FERMI ENERGY (EV)
0.0
0.1
0.2
0.3
0.4
0.5
0.6
0.7
0.8

(b)

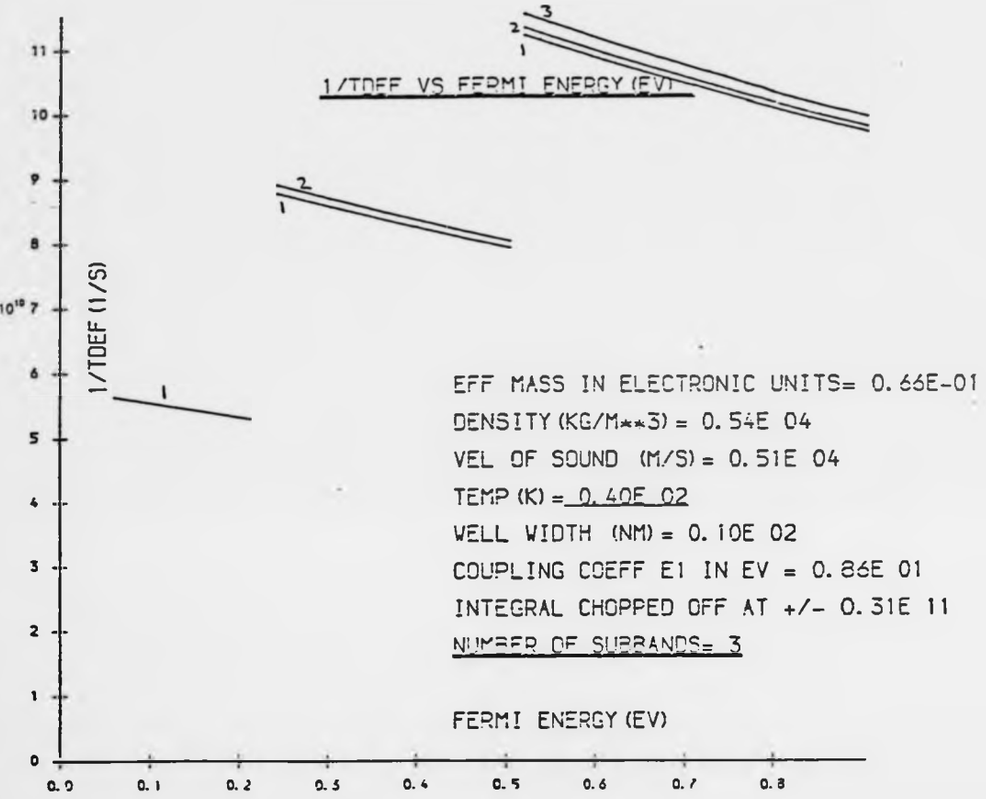

FIG 6.1 (a)

Momentum relaxation rates for deformation potential scattering at low temperatures, revealing the effects of inelasticity.

where

$$G_{abs}(r,n;q_z,Q) = \frac{\Delta(Q)}{1-\exp(-\beta\Delta(Q))} F_{abs}(r,n;q_z,Q) \tag{6.21}$$

and we have used the identity

$$F_{abs}(r,n;q_z,Q) = F_{abs}(n,r;q_z,Q) \tag{6.22}$$

The inclusion of the emission process is straightforward because of detailed balance which implies

$$\sum_n \int \psi_n(k) C_{abs} \psi_n(k) d^2k = \sum_n \int \psi_n(k) C_{em} \psi_n(k) d^2k \tag{6.23}$$

with C_{abs} and C_{em} denoting the collision operators involving absorption and emission processes respectively. Hence we only need to double each of the integrals in (6.20) to include both processes. The coupled equations (6.20) have been solved numerically for a range of temperatures (see Figures 6.1(a),(b) and (c). We note that even at 40K the inelasticity is evident and at lower temperatures there are significant deviations away from Ridley's scattering rate result (see equation (5.19)). In the high temperature limit β tends to zero and the Siggia and Kwok equations (3.20) are recovered from (6.20). In this regime the elastic scattering limit is a good approximation, equipartition holds and $F(n,r;q,Q)$ is independent of Q. The second integral in (6.21) is identically zero and Ridley's scattering rate formula is exact. As the temperature is lowered both the equipartition limit and the elastic scattering approximation are invalid.

6.2.3.1 Discussion of the Deformation Potential Relaxation Time Curves

Figure 6.2 shows a transition between $\underline{k}$ and $\underline{k}'$ in the lowest sub-band by the

FIG 6.2

Momentum relaxation by small angle acoustic phonon scattering at low temperatures. At very low temperatures the sub-bands are decoupled.

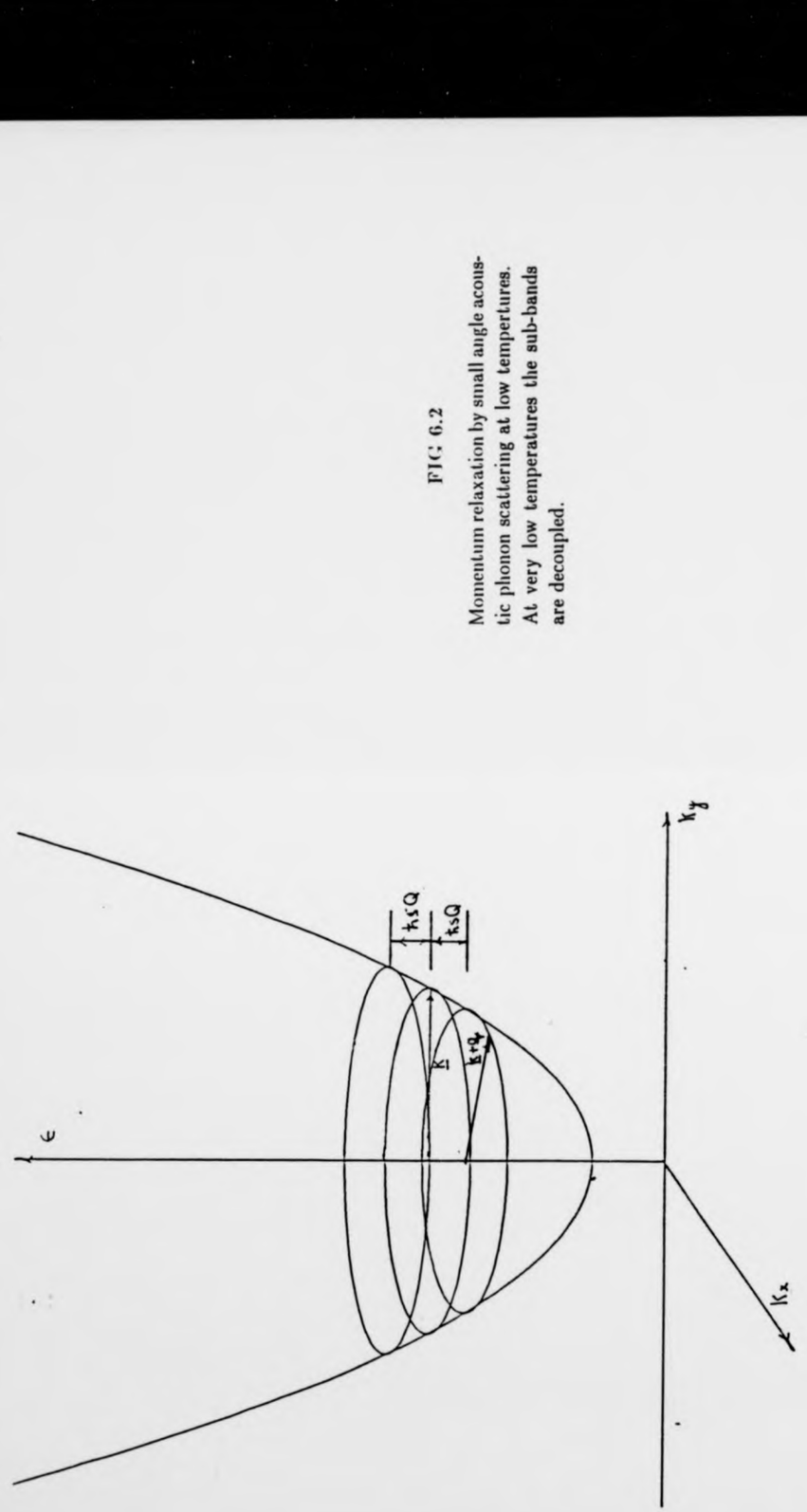

emission of an acoustic phonon. The electron changes its momentum state and at the same time loses energy to the phonon. At low temperatures the Fermi sea will have a sharp boundary curve and consequently momentum changes which involve the emission of a phonon with energy much greater than $k_B T$ are blocked by the Pauli principle. Hence only small angle scattering is allowed at low temperatures. There is also a minimum phonon wavevector required for an inter-sub-band transition and a corresponding minimum phonon energy. So at very low temperatures, when the phonon occupancy is small, inter-sub-band transitions due to phonon absorption are improbable and transitions due to phonon emission are unlikely. This suggests an approximate sub-band decoupling scheme at low temperatures with the momentum relaxing by small angle intra-sub-band scattering. This effect is seen in the relaxation time curves Figure 6.1. At high temperatures a large change in the relaxation time occurs when another sub-band is becoming occupied. At lower temperatures the electrons in one sub-band see less of the states in the other sub-bands and the relaxation time discontinuities are less marked. At very low temperatures the QSE are frozen out completely.

6.2.3.2 Limiting Temperature Dependence in 2-DEG's due to Three-Dimensional Phonons

Three-dimensional metallic systems have a phonon-scattering limited resistivity which is proportional to T^5 at low temperatures (see Ziman (1960)). We may now consider the limiting temperature dependence in a 2-DEG. At low temperatures we know that inter-sub-band transitions are not permitted and only small angle intra-sub-band transitions are allowed. Hence, from (6.20)

$$\frac{1}{\tau_n} = \frac{\beta m^*}{\hbar^2} \int_0^{2\pi} d\alpha \int_{-\infty}^{+\infty} \frac{V}{8\pi^3} \frac{\hbar V_L Q}{1-\exp(\beta \hbar V_L Q)} (1-\cos\alpha) F(n,n;q_z,Q) dq_z \qquad (6.24)$$

where

$$Q = (4k_F^2 \sin^2(\tfrac{1}{2}\alpha) + q_z^2)^{\frac{1}{2}} \tag{6.25}$$

We insert the full expression for $F(n,n,q_z,Q)$ equation (6.16) to obtain

$$\frac{1}{\tau_n} = \frac{\beta m^*}{\hbar^2} \int_0^{2\pi} d\alpha \int_{-\infty}^{+\infty} \frac{dq_z}{8\pi^3} \frac{\hbar V_L Q}{1-\exp(-\beta\hbar V_L Q)} (1-\cos\alpha) \frac{\pi E^2_{def} Q}{\rho V_L} \times \frac{1}{\exp(\beta\hbar V_L Q)-1} G^2_{nn}(q_z) \tag{6.26}$$

Now, for small angles, $q = 2k_F \sin(\tfrac{1}{2}\alpha) \sim k_F \alpha$ and as q_z is taken to be small we know

$$G_{n,n}(q_z) = 1 \qquad q_z \to 0 \tag{6.27}$$

we change the integral variable α to q so that (6.26) yields

$$\frac{1}{\tau_n} = \frac{\beta m^*}{\hbar^2} \int_0^{\infty} \frac{dq}{2\pi k_F} \int_{-\infty}^{\infty} dq_z \frac{\hbar V_L Q^2}{\sinh^2(\beta\hbar V_L Q/2)} \frac{q^2}{2k_F^2} \frac{\pi E^2_{def}}{\rho V_L} \tag{6.28}$$

Finally by introducing polar co-ordinates in the (q, q_z) plane, we find that the angular integration is elementary and yields

$$\frac{1}{\tau_n} = \frac{\beta m^*}{\hbar^2} \frac{\hbar V_L}{k_F^3 \rho} \frac{E^2_{def}}{32} \left[\frac{2}{\beta\hbar V_L}\right]^6 \int_0^{\infty} \frac{x^5}{4\sinh^2(x)} dx \tag{6.29}$$

where $x = \beta\hbar V_L Q/2$. We see by inspection that τ_n^{-1} is proportional to T^5. Vinter (1986) has suggested that the electronic mobility should vary as T^{-1} at low temperatures. This is true at moderately low temperatures when Ridley's scattering-rate formula is approximately valid (Ridley (1982)) and the Fermi surface is fairly sharp. It fails at very low temperatures and the T^{-5} law holds.

6.2.4 Piezoelectric Scattering at Low Temperatures

We can now examine low temperature piezoelectric scattering in 2-DEGs. The full inelastic transition rate takes the form

$$P(\underline{k},n;\underline{k}',m) = \frac{2\pi}{\hbar}\left[\frac{e_{14}e}{k\epsilon_o}\right]^2\frac{\hbar}{2\rho V}\sum\left[\frac{4}{35}\frac{N_{Qt}}{V_t}\delta(\epsilon_n(\underline{k})-\epsilon_m(\underline{k}')+\Delta_t(Q_t))\right.$$
$$+\frac{4}{35}\frac{(N_{Qt}+1)}{V_t}\delta(\epsilon_n(\underline{k})-\epsilon_m(\underline{k}')-\Delta_t(Q_t))$$
$$+\frac{3}{35}\frac{N_{Ql}}{V_l}\delta(\epsilon_n(\underline{k})-\epsilon_m(\underline{k}')+\Delta_l(Q_l))$$
$$\left.+\frac{3}{35}\frac{(N_{Ql}+1)}{V_l}\delta(\epsilon_n(\underline{k})-\epsilon_m(\underline{k}')-\Delta_l(Q_l))\right]$$
$$\times\frac{G^2_{nm}(q_z)}{Q}\frac{L}{2\pi}dq_z \qquad (6.30)$$

This can be included in the equations (6.20), again we find that the absorption and emission processes contribute equally to the conductivity. The equations now take a similar form to the ones for deformation potential scattering, but now we replace

$$\frac{\Delta\ (Q\ )}{1-\exp(\beta\Delta\ (Q\ ))}\times F_{abs}\ (r,n;q_z,Q)$$

by two terms, one for the longitudinal phonons and one for transverse phonons

$$\frac{\Delta_t(Q_t)}{1-\exp(-\beta\Delta_t(Q_t))}\times F^t_{abs}\ (r,n;q_z,Q)\frac{4}{35}+\frac{\Delta_l(Q_l)}{1-\exp(-\beta\Delta_l(Q_l))}F^l_{abs}\ (r,n;q_z,Q)\frac{3}{35}$$

where

$$F^{t/l}_{abs} = \frac{\pi}{\rho}\left[\frac{e_{14}e}{k\epsilon_o}\right]^2\frac{N_Q{}^{t/l}}{V_{t/l}}\frac{G^2_{r,n}(q_z)}{|Q|} \qquad (6.31)$$

where $N_Q{}^{t/l}$ is the Bose factor, and $V_{t/l}$ the velocity of the transverse/longitudinal modes. These equations have been used to calculate

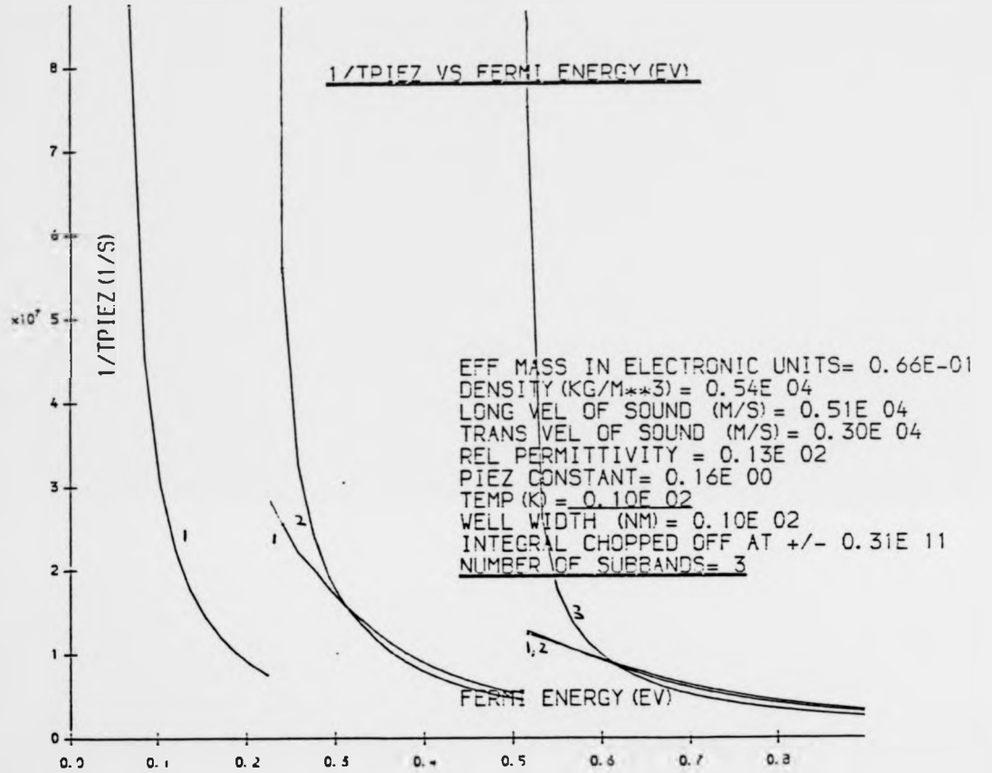
1/TPIEZ VS FERMI ENERGY (EV)
EFF MASS IN ELECTRONIC UNITS= 0.66E-01
DENSITY (KG/M**3) = 0.54E 04
LONG VEL OF SOUND (M/S) = 0.51E 04
TRANS VEL OF SOUND (M/S) = 0.30E 04
REL PERMITTIVITY = 0.13E 02
PIEZ CONSTANT= 0.16E 00
TEMP (K) = 0.10E 02
WELL WIDTH (NM) = 0.10E 02
INTEGRAL CHOPPED OFF AT +/- 0.31E 11
NUMBER OF SUBBANDS= 3
1/TPIEZ (1/S)
x10⁷
FERMI ENERGY (EV)
1
2
3
1,2
0
1
2
3
4
5
6
7
8
0.0
0.1
0.2
0.3
0.4
0.5
0.6
0.7
0.8

(b)

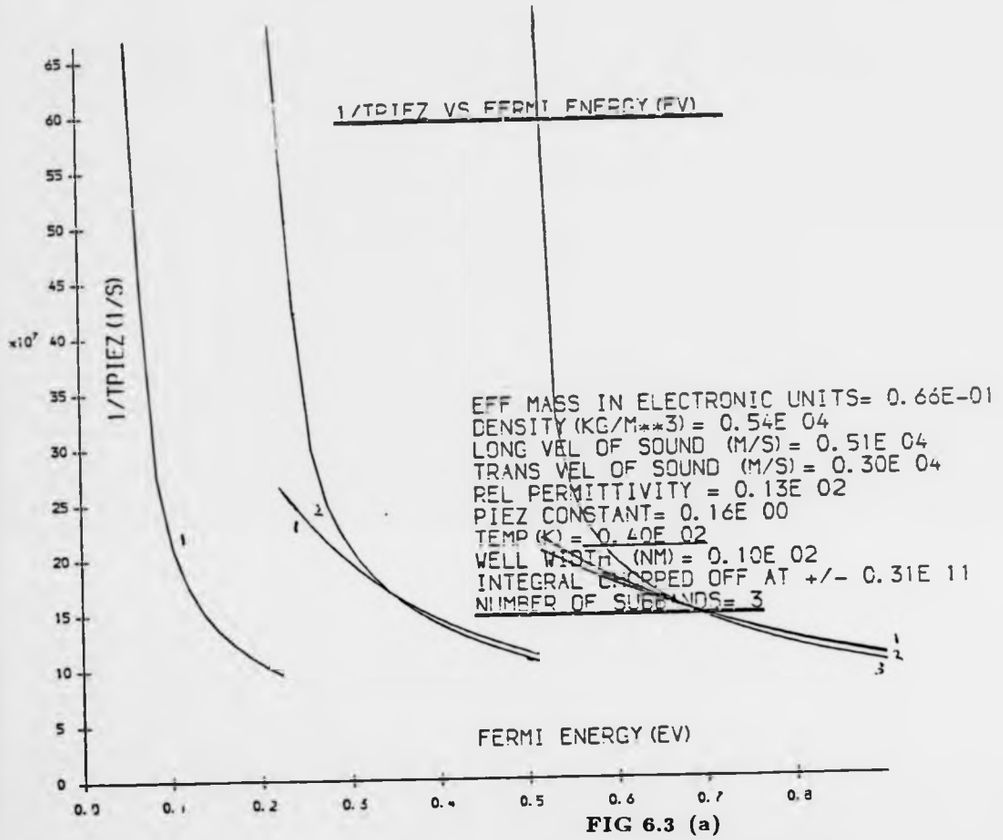

FIG 6.3 (a)

Momentum relaxation rates for piezoelectric scattering at low temperatures in a 2-D.E.G. . The elastic approximation is approximately valid here because of the Q dependance of the mechanism.

the results shown in Figure 6.3 which are for T=40,10K. The qualitative behavior is similar to that found in section 6.2.3 for deformation potential scattering, but we see on referring to Figure 5.3 , for high temperature piezoelectric scattering that a large amount of sub-band decoupling is already present because of the $1/Q^2$ dependence of the mechanism and the finite q necessary for the transition. We note that the deformation potential dominates over the piezoelectric mechanism even at low temperatures, even before screening is included.

6.2.5 Low Temperature Conduction in One-Dimensional Wires

We now address the inelasticity problem in one-dimensional systems. In the elastic approximation electrons have to scatter across the sub-band to relax momentum, this may involve acoustic phonons which have energies large compared to $k_B T$ and consequently we can expect the effects of inelasticity to be important. If this were the only way of relaxing momentum we would expect the conductivity to increase rapidly when $k_B T < 2\hbar v_L k_F$. To study this problem we modify the approach of sections (6.2.1-6.2.4). Thus, we write the linearised one-dimensional Boltzmann equations (3.27) in the form

$$z^{nm} = C\phi^{nm} , \tag{6.33}$$

where

$$f_1^{nm}(k) = -\phi^{nm}(k)\frac{df_0}{d\epsilon}$$

$$C\phi^{nm} \equiv \left[\frac{\partial f_1^{nm}}{\partial t}\right]_c = \beta\Sigma_{n'm'} \int f_0(\epsilon_{nm}(k))\left[1-f_0(\epsilon_{n'm'}(k'))\right] P(k,n,m;k',n',m') \times [\phi^{n'm'}(k')-\phi^{nm}(k)] \frac{L}{2\pi} dk' \tag{6.34}$$

and

$$z^{nm} \equiv -EV^{nm}\frac{df_o}{d\epsilon} \tag{6.35}$$

The collision operator here again possesses the symmetry property

$$\sum_{nm}\int h(k,n,m)Cg(k,n,m)dk = \sum_{nm}\int g(k,n,m)Ch(k,n,m)dk \tag{6.36}$$

and the one-dimensional conductivity takes the form

$$\sigma_o = \frac{-e^2}{\pi E^2}\sum_{nm}\int \phi^{nm}C\phi^{nm}dk \tag{6.37}$$

which can be rewritten in the familiar form

$$\sigma_o = \frac{\beta e^2}{2\pi E^2}\sum_{n'm'n'm}\iint f_o(\epsilon_{nm}(k))[1-f_o(\epsilon_{n'm'}(k'))]P(k,n,m;k',n',m') \times [\phi^{n'm'}(k')-\phi^{nm}(k)]^2\frac{L}{2\pi}dk'dk \tag{6.38}$$

The expression

$$\sigma_o = \frac{-2e^2}{\pi E^2}\sum_{nm}\int z^{nm}\phi^{nm}dk + \frac{e^2}{\pi E^2}\sum_{nm}\int \phi^{nm}C\phi^{nm}dk \tag{6.39}$$

has a minimum in ϕ^{nm} space when the one-dimensional Boltzmann equation is satisfied. We shall use this result to look at conduction at moderately low

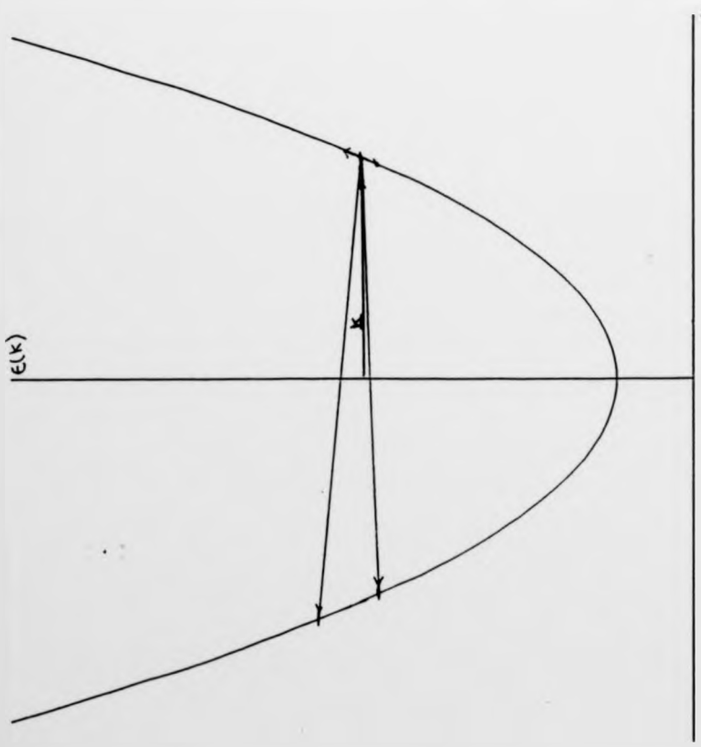

FIG 6.4

Quasi-elastic scattering in a 1-D.E.G., the two states on the same side of the sub-band are normally ignored and contribute nothing to momentum relaxation in the elastic scattering limit. It is necessary to consider them at very low temperatures as transitions across the sub-band are highly improbable.

($k_BT \sim 2\hbar v_L k_F$) and very low temperatures ($k_BT \ll 2\hbar v_L k_F$).

6.2.6 Transport in One-Dimension at Moderately Low Temperatures

Consider Figure 6.4, this shows the four classes of scattering process that an electron can be involved in, in one-dimension . Two of these processes change the electrons momentum by a large amount. The other two leave the electron on the same side of the sub-band and hardly change its momentum at all. In this section we consider the across sub-band transitions to be the important ones. When $k_BT \ll 2\hbar v_L k_F$ these transitions will be prohibited and the other two need to be considered in detail, this is done in section 6.2.7. We inspect the expression

$$K \equiv \sum_{nm} \int \phi^{nm} C \phi^{nm} dk \tag{6.40}$$

and convert the integrals over k to integrals over energy. Thus, we have from (6.38), (6.37) and (2.7)

$$K = -\beta/2 \sum_{nm} \int \frac{d\epsilon}{\hbar} \mathcal{J}a(\epsilon,n,m) \sum_{n'm'} \int \frac{d\epsilon'}{\hbar} \mathcal{J}a(\epsilon',n',m')$$

$$\times V(\epsilon,n,m;\epsilon',n',m')[\phi(\epsilon',n',m')-\phi(\epsilon,n,m)]^2 \frac{L}{2\pi} \tag{6.41}$$

where

$$\mathcal{J}a(\epsilon,n,m) = \sqrt{\frac{m^*}{2\left[\epsilon - \frac{\hbar^2 n^2 \pi^2}{2m^* a^2} - \frac{\hbar^2 m^2 \pi^2}{2m^* b^2}\right]}} \tag{6.42}$$

$V(\epsilon,n,m',\epsilon',n'm)$ is the equilibrium transition rate with the energies substituted for the k's. We introduce the ansatz

$$\phi^{nm} = -v^{nm}\xi^{nm} \tag{6.43}$$

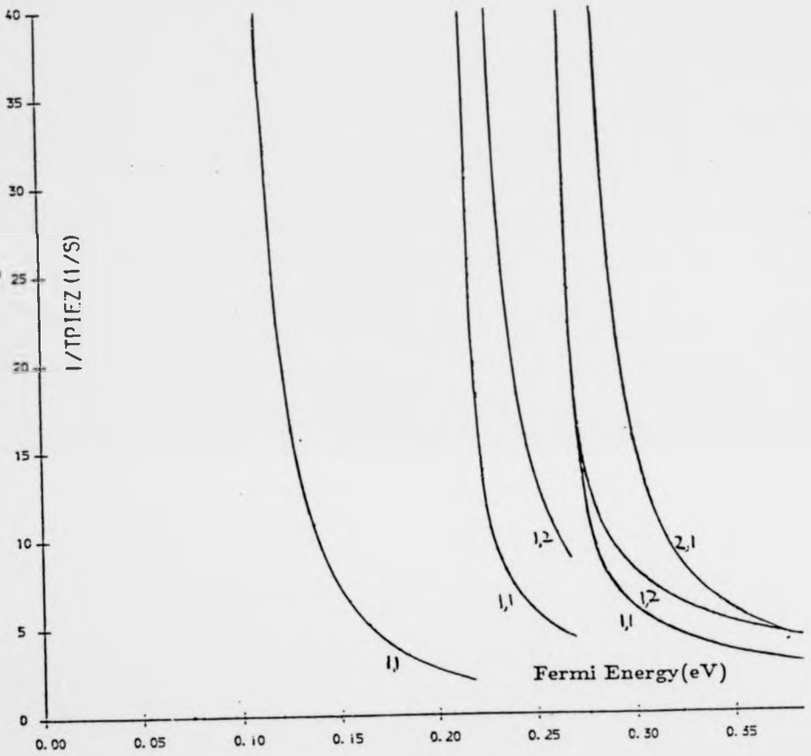
40
35
30
x10⁶ 25
20
15
10
5
0
1/TPIEZ (1/S)
1,1
1,2
2,1
1,2
1,1
1,1
Fermi Energy(eV)
0.00
0.05
0.10
0.15
0.20
0.25
0.30
0.35

FIG 6.6 (b)

T=10K

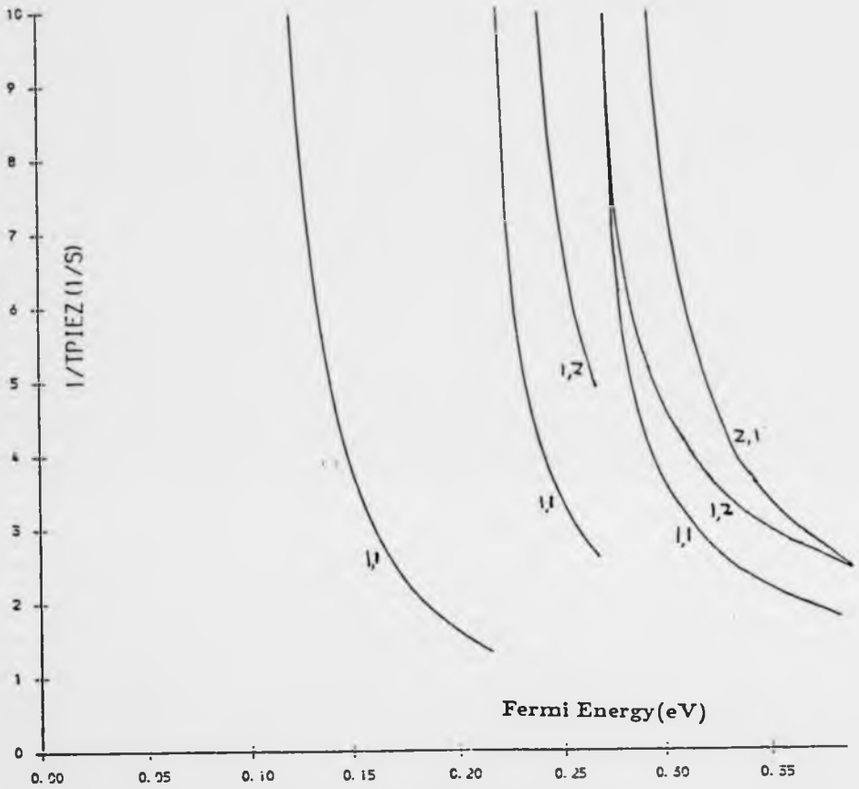

FIG 6.6 (a)

Momentum relaxation rates for piezoelectric scattering in a 1-D.E.G. at moderately low temperatures. T=40K cross-section=(10nm,12nm).

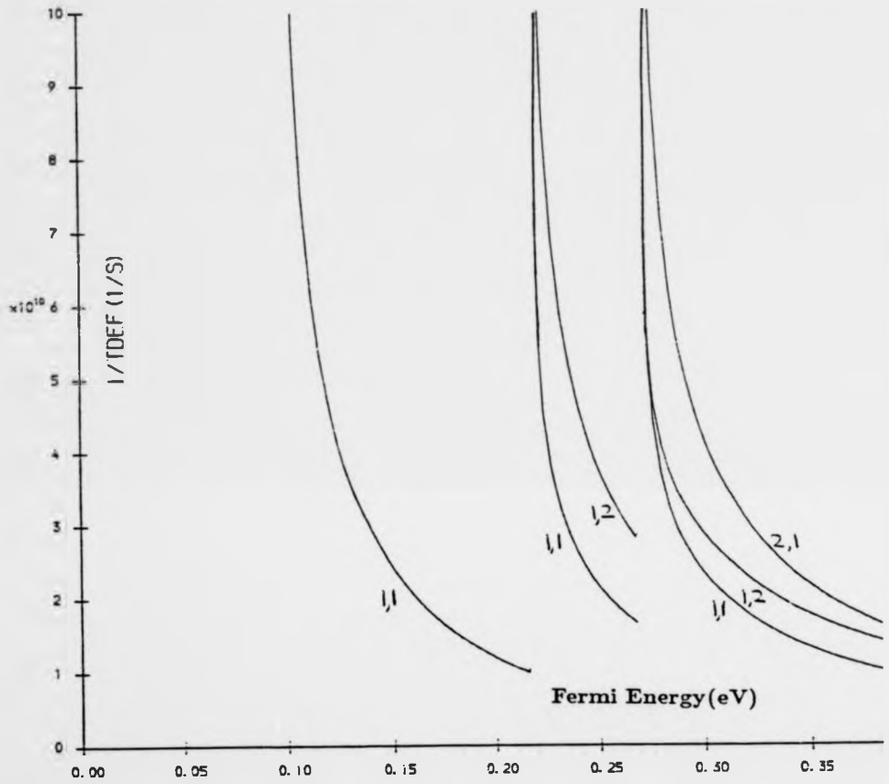
10
9
8
7
×10^10 6
5
4
3
2
1
0
1/TDEF (1/S)
1,1
1,1
1,2
1,1
1,2
2,1
Fermi Energy(eV)
0.00
0.05
0.10
0.15
0.20
0.25
0.30
0.35

FIG 6.5 (b)T=10K

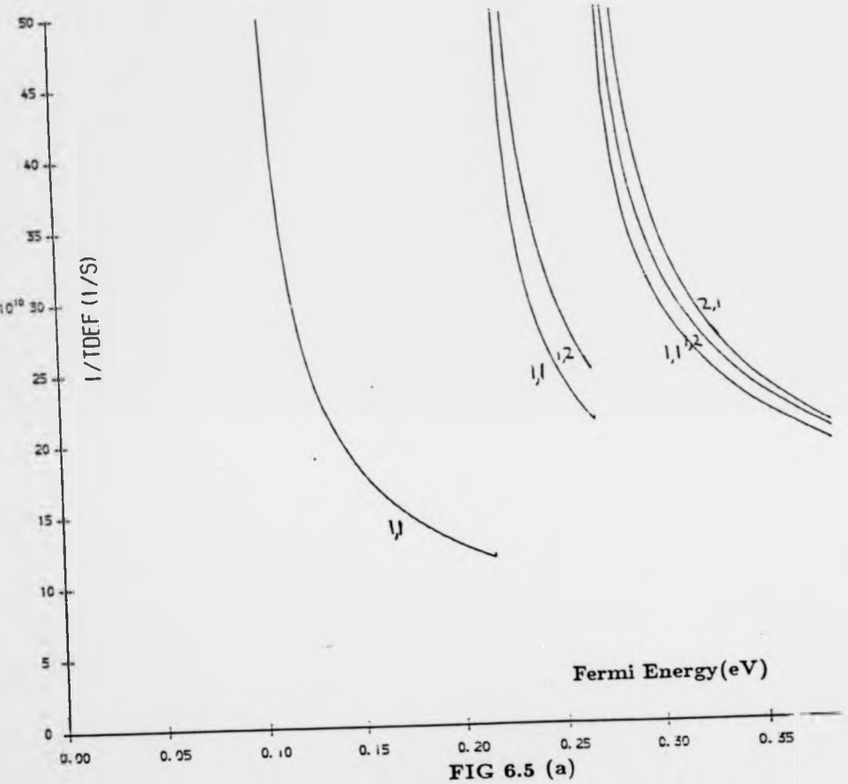

FIG 6.5 (a)

Momentum relaxation rates for deformation potential scattering in a 1-D.E.G. at moderately low temperatures. T=40K cross-section= (10nm,12nm).

where again γ^{nm} is taken to be independent of the electron energy for a particular value of the chemical potential, but dependent on the sub-band number, we find that

$$\bar{K} = \frac{-\beta E^2}{2} \sum_Q \sum_{nm} \sum_{n'm'} \int \frac{d\epsilon}{\hbar} \left]a(\epsilon,n,m) f_o(\epsilon)[1-f_o(\epsilon-\Delta(Q))]\right.$$

$$\times W(k,k',Q,n,m;n',m')[-V^{n'm'}(\epsilon-\Delta(Q))\gamma^{n'm'} + V^{nm}(\epsilon)\gamma^{nm}\left]^2\right.$$

$$\times \frac{L}{2\pi} \frac{1}{\hbar} \left]a(\epsilon-\Delta(Q),n,m)\right. \qquad (6.44)$$

where $W(k,k',Q,n,m;n',m')$ is the expression arising from a Fermi Gold Rule calculation. The only rapidly varying function is $f_o(\epsilon)[1-f_o(\epsilon-\Delta(Q))]$ and we treat the rest of the integrand as constants evaluated at the Fermi level. For the intermediate temperature range we make the assumption that $V^{nm}(\epsilon_F) \sim V^{nm}(\epsilon_F-\Delta(Q))$. With this assumption, the only contribution to $\bar{k}$ from intra-sub-band scattering comes from the scattering of electrons across a sub-band. The expression (6.37) for the conductivity is then given by

$$\sigma_o = \frac{e^2\bar{k}}{\pi E^2} \qquad (6.45)$$

The alternative expression

$$\sigma_o = \frac{-e^2}{\pi} \sum_{nm} \int \phi^{nm} z^{nm} dk \qquad (6.46)$$

reduces to

$$\sigma_o = \sum_{nm} \frac{e^2 \tau_{nm}}{m^*} \times \frac{2k_y^{nm}}{\pi} \qquad (6.47)$$

where k_F^{nm} is the length of the Fermi line in each occupied sub-band. We now proceed as in section 6.2.2 constructing the variational form (6.39) and writing down the variation equation $\frac{\partial \sigma}{\partial \tau_{rp}} = 0$. After some manipulation we find that the coupled equations take the expected form

$$\tau_{rp} \sum_{n'm'} \iint \frac{\beta\Delta}{1-e^{-\beta\Delta}} W(k_F, k_F, Q, r, p; n', m') \frac{V}{8\pi^3} \, dq_x dq_y$$

$$- \sum_{n'm'} \tau_{n'm'} \iint \frac{\beta\Delta}{1-e^{-\beta\Delta}} W(k_F, k_F, Q, r, p; n', m') \frac{k_F^{n'm'}}{k^{rp}} \frac{V}{8\pi^3} dq_z dq_y = 1 \qquad (6.48)$$

With the aid of these equations we have calculated the relaxation times τ_{nm} for both the deformation and piezoelectric mechanisms for a range of low temperatures, see Figures 6.5 and 6.6, in which W is multiplied by two to allow for phonon emission.

6.2.7 Phonon Scattering at Very Low Temperatures in 1-DEG's

We now consider the situation where the temperature is very low and $k_B T \ll 2\hbar v k_F$. In this case only low momentum phonon modes are excited and scattering across the one-dimensional sub-bands or between sub-bands is highly improbable. The most probable transitions are between $\underline{k}$ states in the same sub-band on the same side of the sub-band (see Figure 6.4). We drop the assumption that $V(\epsilon_F) \sim V(\epsilon_F - \Delta(Q))$, and we look at expressions (6.44) and (6.45) in the case where only one sub-band is occupied. In this case

$$\sigma_o = \frac{\beta e^2}{2\pi}\iint \frac{\Delta}{1-e^{-\beta\Delta}}\ \frac{1}{m^*}\frac{1}{k_F^2}[-V(\epsilon-\Delta(Q))+V(\epsilon)]^2\quad \frac{V}{8\pi^3}$$

$$x\ W(k_F,k_F',Q,1,1;1,1)dq_x dq_y \tag{6.49}$$

To make progress with the evaluation of σ_o we consider the requirements of energy and momentum conservation. For scattering from a state $\underline{k}$ to a state $\underline{k}'$ by phonon absorption, energy conservation gives

$$\frac{\hbar^2k^2}{2m^*} + \Delta(Q) = \frac{\hbar^2k'^2}{2m^*}$$

Hence

$$\hbar V_L\ Q = \Delta(Q) = \frac{\hbar^2}{2m^*}(k+k')(k'-k) = \frac{\hbar^2}{2m^*}(k+k')q_x \tag{6.50}$$

where we have made use of momentum conservation along the length of the wire. For a transition between $\underline{k}$ states on the same side of the sub-band $k\sim k'\sim k_F$ and hence we find that

$$q_x = \frac{V_L Q}{V_F} = Q\cos\psi \tag{6.51}$$

where v_F is the fermi velocity and hence we conclude

$$\cos\psi \sim V_L/V_F$$

Only phonons propagating on or close to this angle can scatter electrons in the wire. We can now rewrite the expression for the conductivity as

$$\sigma_{xx} = \frac{\beta e^2}{2\pi}\iint dq_z dq_y \frac{V}{8\pi^3}\ \mathrm{In}(\beta,Q,V_L)\frac{\pi E^2_{def}}{\rho V_L}\ Q\ \frac{m^*}{2\epsilon_F}\left[\frac{q_x}{2m^*}\right]^2 \Upsilon_2 \tag{6.52}$$

where

$$\text{In}\,(\beta,Q,V_L) = \frac{\beta\hbar V_L Q}{\left[1-e^{-\beta\hbar V_L Q}\right]\left[e^{\beta\hbar V_L Q}-1\right]} \tag{6.53}$$

and we have inserted the expression for $W(k_F,k_F',Q)$ used the results that $G_n^2(q_y)=1$ and $\Delta(Q)=\hbar v_L Q$. We convert to circular polar co-ordinates $q_y \to 0$ in y space and use result (6.51)

$$\sigma_{xx} = \frac{e^2}{2\pi}\int_0^{\infty}\frac{Q^2 dQ\sin^2\psi}{8\pi^3}\int_0^{2\pi} d\theta\,\text{In}(\beta,Q,V_L)\,\frac{\pi E^2 def}{\rho V_L}\,Q^2\,\frac{m^*}{2\epsilon_F}\,\frac{\cos^2\psi\tau^2}{(2m^*)^2} \tag{6.54}$$

Finally we make the substitution $x=\hbar V_L Q$ and perform the θ integral to obtain

$$\sigma_{xx} = \frac{e^2}{2\pi}\int\frac{x^2}{(\beta\hbar V_L)^5}\,\frac{1}{4\pi^2}\,\frac{x}{[1-e^{-x}]}\,\frac{1}{[e^x-1]}\,\frac{x^2\cos^2\psi\sin^2\psi}{(2m^*)^2}\,\frac{m^*\tau^2}{2\epsilon_F}\,\frac{\pi E^2_{def}}{\rho V_L}\,dx \tag{6.55}$$

When the alternative expression for the conductivity (6.47) and (6.55) are combined in the variational form (6.39) and operated on by $\partial/\partial\tau$ they give an expression for τ which varies as β^5 and hence the resistivity again obeys a Bloch-Gruneisen T^5 law. The angle ψ may only be defined for reasonable densities. At low densities the assumption that only the transitions on the same side of the sub-band are important breaks down and a more elaborate theory would be needed.

Conclusions

We have seen that the elastic approximation breaks down for acoustic phonon

mechanisms at low temperatures in both two-dimensional and one-dimensional systems. At very low temperatures we have a resistivity which obeys a Bloch-Gruneisen type T^5 law. Energy and momentum conservation along with inelasticity considerations in one-dimension predict that at very low temperatures only three-dimensional phonons propagating on or close to an angle of $\cos^{-1}(V_L/V_F)$ to the axis of the wire may interact strongly with the electrons. This analysis assumes that $V_L<V_F$ which is unlikely to be violated in most experimental situations. The inelasticity also has the effect of decoupling the sub-bands in two-dimensions at low temperatures and freezing out any Quantum Size Effects. In one-dimensional systems the singularity in the density of states means that total decoupling of the Boltzmann equations is not possible when the Fermi energy is aligned at a sub-band origin. At any other position the decoupling concept is accurate provided a sufficiently low temperature is chosen.

CHAPTER 7

POLAR OPTIC PHONON SCATTERING IN QUASI ONE-DIMENSIONAL WELLS

We saw in Chapter 3 that we were able to define a characteristic relaxation time for both elastic and quasi-elastic mechanisms. In both cases this has a simple interpretation as the time which enters into the conductivity expression

$$\sigma_o(\varepsilon) = \sum_{\text{sub-bands}} \frac{Ne^2\tau}{m^*}$$

In this section we look at a scattering mechanism which changes the electron energy by a large amount when compared to a typical Fermi Energy: polar optic phonon scattering. This scattering mechanism is strongly inelastic and in GaAs, for example, an electron will change its energy state by 35meV (Fletcher and Butcher (1972)). The Boltzmann equation has been used to treat optical phonon scattering in bulk materials (Rode (1970), Fletcher and Butcher (1972)) and in inversion layers (Vinter (1984)). All of these authors use an iterative approach although Sondheimer and Howarth (1953) have obtained approximate solutions in three-dimensions using a variational approach. The aim of this chapter is to discover an effective relaxation time for one-dimensional systems. We adopt the iterative approach, because this generates the exact electron distribution function whereas the variational method generates a good estimate for the Boltzmann conductivity but not necessarily a good value for f_1. It is only in the limit of low temperatures (where the optical phonon scattering mechanism is unimportant) that we expect the two approaches to give the same relaxation time.

Polar-optic phonon scattering has been considered in one-dimensional wires using a relaxation time formalism (Ridley (1983)). This approach was

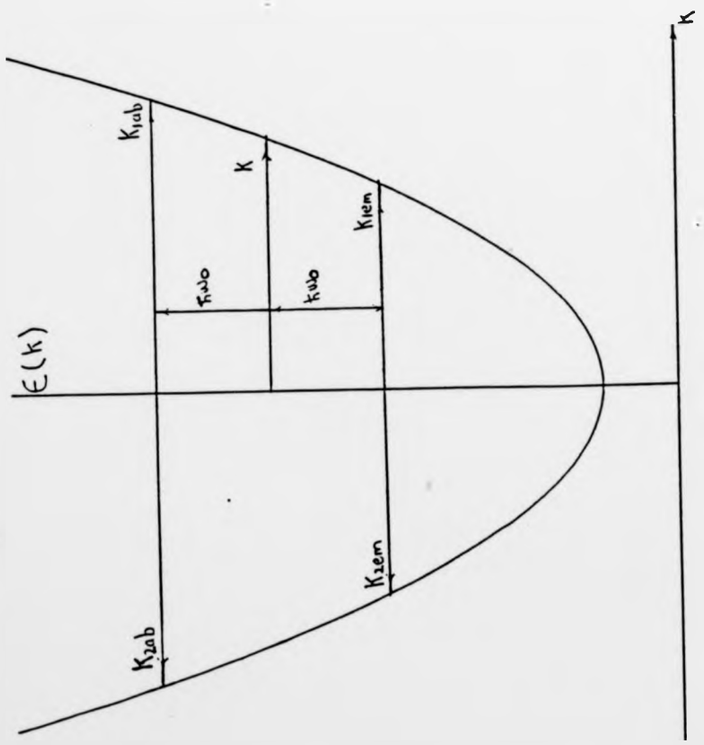

FIG 7.1
Possible states for polar optic phonon scattering in a one-dimensional wire

expected to give a good first estimate of the importance of the mechanism. However it suggested that for some well sizes and electron energies the momentum relaxation time may be negative and as the conductivity is usually related to this time we would expect the system to have some unusual properties! We show that the effects of the electron statistics (ignored in Ridley's model) are important and we calculate an effective relaxation time which is positive. In section 7.1 we present the arguments giving rise to the negative relaxation time and introduce the effect of the electron statistics in a simple way. In 7.2 we calculate the perturbed part of the distribution function and derive an effective relaxation time relevant to transport measurments.

7.1 Polar Optic Phonon Scattering and the Approach to Equilibrium

To explain the negative time we consider an electron lying low down in a one-dimensional sub-band with an energy less than that of a polar optic phonon, see Figure 7.1. Then a L.O. phonon cannot be emitted. A phonon absorption process can take the electron to one of two positions in the sub-band marked 1 and 2. Now the polar optic phonon transition rate has a $1/Q^2$ dependence. Hence, scattering to position 1 is therefore more probable than scattering to position 2, indicating that the electron momentum will be increased on average so that the momentum relaxation time is negative.

To consider this problem further, we use the Boltzmann equation and we look at the behaviour of the electrons in a one-dimensional wire starting with a particular momentum. Throughout we consider the phonons to be monoenergetic with energy $\hbar\omega_0$ and we consider the sub-bands to be separated by many optical phonon energies. In this regime we may confine our attention to the lowest sub-band permitting a simple discussion of Ridley's result.

When the electron energy is greater than $\hbar\omega_o$, the emission process is allowed and there are another two states associated with this as shown in Figure 7.1.

We consider a homogeneous system which is in thermodynamic equilibrium. The occupation of the states is described by the Fermi-Dirac distribution function

$$f_o'(\epsilon) = \frac{1}{\exp(\beta(\epsilon-\mu')) + 1} \tag{7.1}$$

where μ' is the chemical potential and ϵ is the energy of the electron.

At time t=0 we inject a small packet of electrons with momentum k close to k_o. The system will eventually redistribute this additional momentum so that thermal equilibrium is again reached with the new distribution function,

$$f_o = \frac{1}{\exp(\beta(\epsilon-\mu)) + 1} \sim f_o'(\epsilon) - \delta\epsilon_F \frac{df_o(\epsilon_F)}{d\epsilon} \tag{7.2}$$

where $\mu=\mu'+\delta\epsilon_F$ is the new value of the chemical potential corresponding to the new electron density

$$n_o = \frac{1}{\pi}\int f_o(\epsilon)dk \tag{7.3}$$

In the absence of applied fields

$$\frac{\partial f}{\partial t}(k,t) = \left[\frac{\partial f}{\partial t}(k,t)\right]_{coll} \tag{7.4}$$

$$= -\int dk'\, V(k,k') \left[\frac{f_1(k',t)}{f_o(\epsilon')[1-f_o(\epsilon')]} - \frac{f_1(k,t)}{f_o(\epsilon)[1-f_o(\epsilon)]}\right] \tag{7.5}$$

In this equation

$$V(k,k') = f_o(\epsilon)[1-f_o(\epsilon')]P(k,k') \tag{7.6}$$

where $P(k,k')$ is the intra-band transition rate and $V(k,k')$ is the equilibrium transition rate (see Chapter 5).

The average momentum of the system is

$$\bar{k}(t) = \frac{\int f(k,t)kdk}{\int fdk} \tag{7.7}$$

In the present case

$$\underset{1}{f(k,o)} = \delta\epsilon_F \frac{df_o(\epsilon_F)}{d\epsilon} + \pi n_o \lambda \delta(k-k_o) \tag{7.8}$$

where λ is the fractional change in electron density due to the injection of the electrons. We substitute (7.8) into (7.7) and remember that f_o is an even function of $\underline{k}$. Hence

$$\bar{k}(o) = \lambda k_o \tag{7.9}$$

Our main interest lies in the momentum relaxation rate at time t=0. Now using (7.8), (7.7) and (7.5) we see that

$$\left[\frac{d\bar{k}(t)}{dt}\right]_{t=0} = \frac{1}{\pi n_o}\int dkk \left[\frac{\partial f_1}{\partial t}(k,o)\right]_{coll}$$

$$= \int dkk \int dk' V(k,k')[B(k')-B(k)] \tag{7.10}$$

where

$$B(k') = \frac{\lambda\delta(k'-k_o) + \frac{\delta\epsilon_F}{\pi n_o}\frac{df_o}{d\epsilon}(\epsilon')}{f_o(\epsilon')[1-f_o(\epsilon')]} \tag{7.11}$$

Hence

$$\left[\frac{d\bar{k}(t)}{dt}\right]_{t=0} = -\lambda k_o \int \frac{dkV(k_o,k)}{f_o(\epsilon)[1-f_o(\epsilon)]} \left[1-\frac{k}{k_o}\right] \tag{7.12}$$

Since the terms involving $\delta\epsilon_F$ cancel out. Hence we may write

$$\frac{d\bar{k}(o)}{dt} \Big/ \bar{k}(o) = -1/\tau_{mom} \tag{7.13}$$

where

$$1/\tau_{mom} = \int dkP(k_o,k) \quad \frac{1-f_o(\epsilon(k))}{1-f_o(\epsilon(k_o))} \left[1-\frac{k}{k_o}\right] \tag{7.14}$$

This quantity may be negative.

For non-degenerate statistics $f_o \ll 1$ and expression (7.14) is identical to the conventional formula for the momentum relaxation time (Ridley (1982)). However the initial relaxation rate does not determine the conductivity of the system to which we now turn attention.

7.2 Steady State Transport

In the absence of screening the polar optic phonon gives rise to a potential given by (Butcher (1986))

$$U(\underline{R}) = -i\left[\frac{\hbar\omega_o}{2V\epsilon_o}\left[\frac{1}{\kappa_\infty}-\frac{1}{\kappa_o}\right]\right]^{1/2}\sum_{\underline{Q}}\frac{a_{\underline{Q}}e^{i\underline{Q}\cdot\underline{R}}}{Q} - \frac{a^+_{\underline{Q}}e^{-i\underline{Q}\cdot\underline{R}}}{Q} \tag{7.15}$$

Where κ_∞ and κ_o are the high and low frequency relative dielectric constants, whilst $a^+_{\underline{Q}}$ and $a_{\underline{Q}}$ are phonon creation and annhialation operators respectively (as in Chapter 5). We work with the hypothetical model in which there is only one sub-band whose wavefunction is given by

$$\psi(k) = L^{-1/2}\zeta(x)\zeta(y)e^{ikz} \tag{7.16}$$

where

$$\zeta(u) = \left[\frac{2}{a}\right]^{\frac{1}{2}} \sin \frac{\pi u}{a} \tag{7.17}$$

We consider the matrix element (taking the annhialation operator first)

$$M^{ann} \equiv \langle \zeta(x)\zeta(y)k' | -e\, U^{ann}(R) | k\zeta(y)\zeta(x) \rangle$$

$$-\sqrt{\frac{N}{Q}}\, ie \left[\frac{\hbar\omega_o}{2V\epsilon_o}\left[\frac{1}{K_\infty} - \frac{1}{K_o}\right]\right]^{1/2} G(q_x)G(q_y) \tag{7.18}$$

where

$$N = \frac{1}{e^{\hbar\omega_o/k_B T} - 1} \quad \text{and} \quad Q^2 = ((k-k')^2 + q_x^2 + q_y^2) \tag{7.19}$$

Squaring and integrating over q_x and q_y we find

$$M^{ann^2}_{TOT} = Ne^2 \frac{\hbar\omega_o}{2\epsilon_o}\left[\frac{1}{K_\infty} - \frac{1}{K_o}\right] \iint \frac{G^2(q_x)G^2(q_y)}{|k-k'|^2+q_x^2+q_y^2} \frac{1}{L} \frac{dq_x dq_y}{4\pi^2} \tag{7.20}$$

The matrix element for the creation operator takes a similar form except that N is replaced by N+1. The q_x integration can be performed analytically (see appendix 3) and hence the scattering probability, due to absorption/emission is found to be

$$P^{abs}_{en}(k,k') = F^{abs}_{em} \int_{-\infty}^{+\infty} \left[\frac{2\pi(1-\exp(-ba))}{b^3a^2\left[\left[\frac{ba}{2\pi}\right]^2 + 1\right]^2} + \frac{2\pi}{b^2a} + \frac{\pi}{a\left[\left[\frac{2\pi}{a}\right]^2 + b^2\right]}\right] G^2(q_y)dq_y \tag{7.21}$$

MOMENTUM RELAXATION RATES FOR A 1-DEG

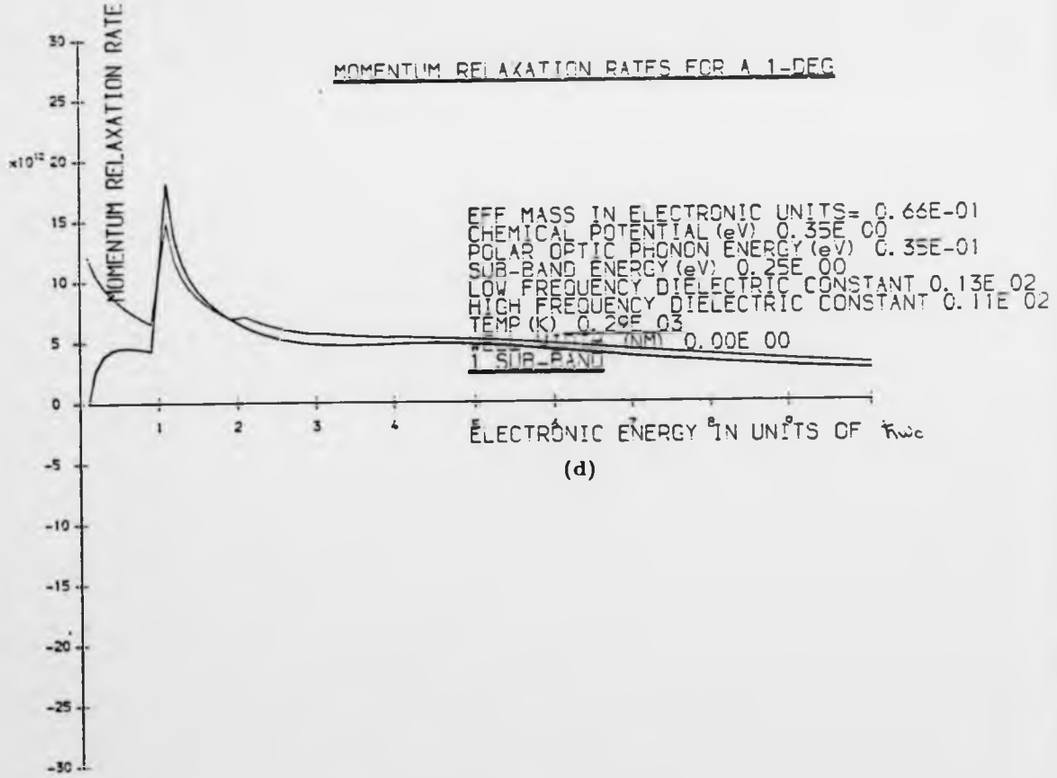

(d)

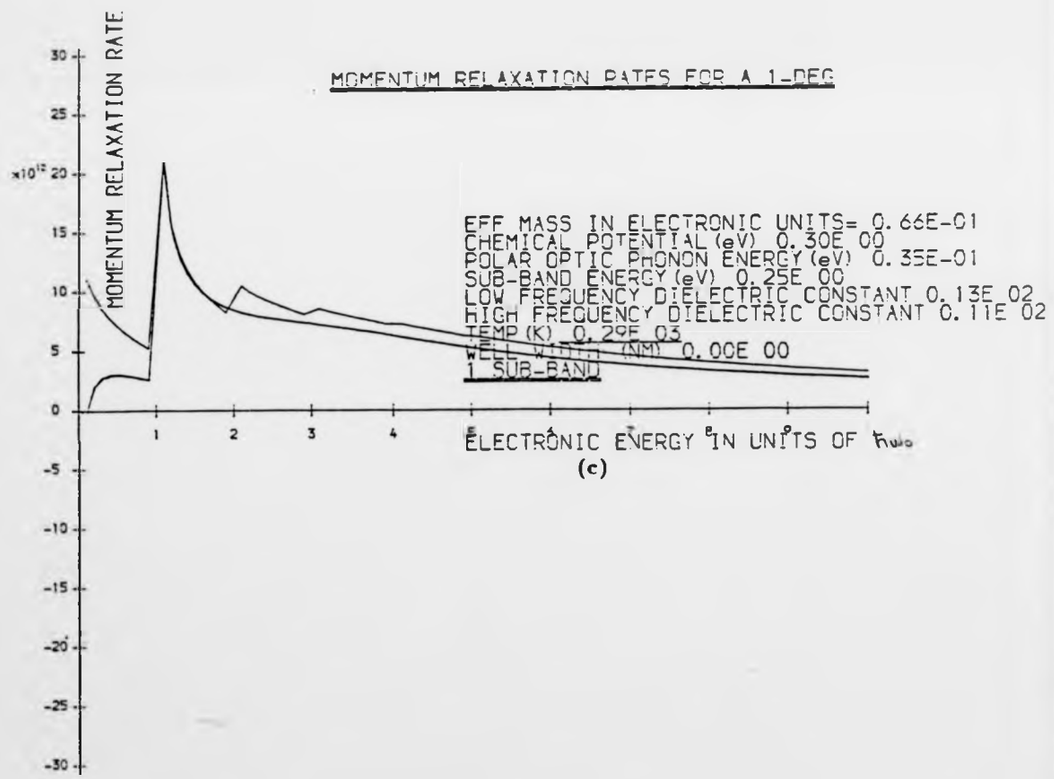
MOMENTUM RELAXATION RATE
×10¹² 30
25
20
15
10
5
0
-5
-10
-15
-20
-25
-30
1
2
3
4
MOMENTUM RELAXATION RATES FOR A 1-DEG
EFF MASS IN ELECTRONIC UNITS= 0.66E-01
CHEMICAL POTENTIAL(eV) 0.30E 00
POLAR OPTIC PHONON ENERGY(eV) 0.35E-01
SUB-BAND ENERGY(eV) 0.25E 00
LOW FREQUENCY DIELECTRIC CONSTANT 0.13E 02
HIGH FREQUENCY DIELECTRIC CONSTANT 0.11E 02
TEMP(K) 0.29E 03
WELL WIDTH (NM) 0.00E 00
1 SUB-BAND
ELECTRONIC ENERGY IN UNITS OF ħω₀

(c)

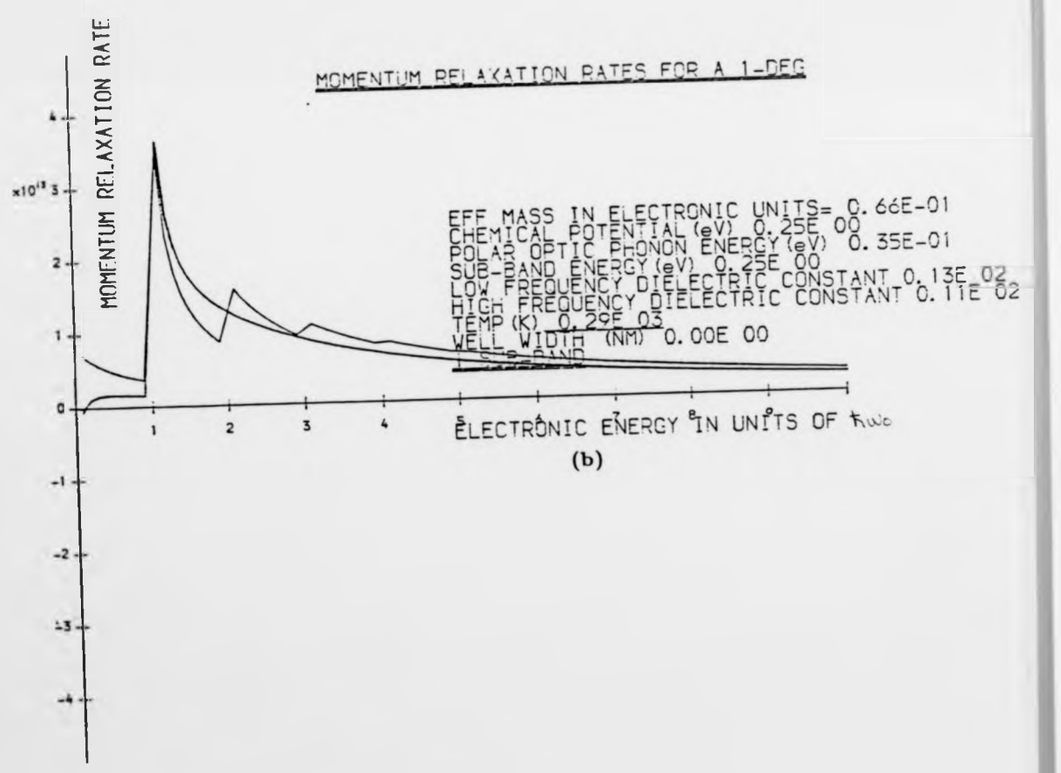
MOMENTUM RELAXATION RATE
×10¹³ s⁻¹
4
3
2
1
0
-1
-2
-3
-4
1
2
3
4
ELECTRONIC ENERGY IN UNITS OF KT
EFF MASS IN ELECTRONIC UNITS= 0.66E-01
CHEMICAL POTENTIAL (eV) 0.25E 00
POLAR OPTIC PHONON ENERGY (eV) 0.35E-01
SUB-BAND ENERGY (eV) 0.25E 00
LOW FREQUENCY DIELECTRIC CONSTANT 0.13E 02
HIGH FREQUENCY DIELECTRIC CONSTANT 0.11E 02
TEMP (K) 0.29E 03
WELL WIDTH (NM) 0.00E 00

(b)

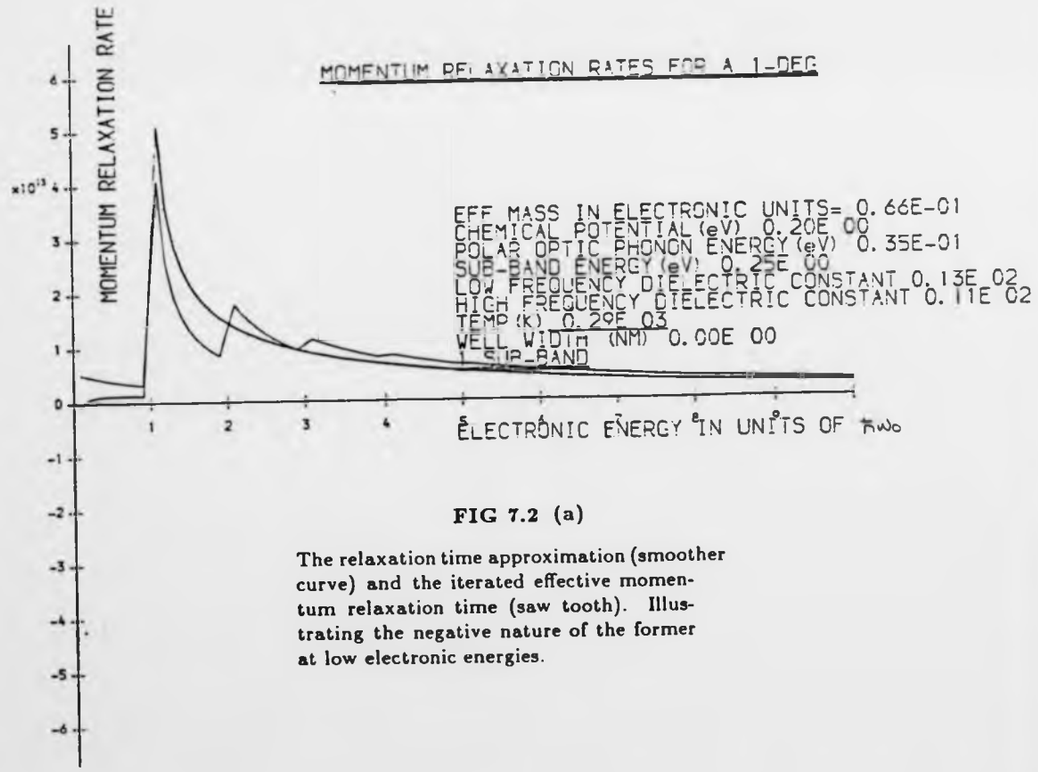

FIG 7.2 (a)

The relaxation time approximation (smoother curve) and the iterated effective momentum relaxation time (saw tooth). Illustrating the negative nature of the former at low electronic energies.

where

$$F^{abs}_{em} = \pi(N+\tfrac{1}{2}\mp\tfrac{1}{2})\frac{e^2\omega_o}{\varepsilon_o}\left[\frac{1}{K_\infty}-\frac{1}{K_o}\right]\delta(\varepsilon(k)-\varepsilon(k')\pm\hbar\omega_o)$$

$$a = A^{\frac{1}{2}},\quad b = ((k-k')^2+q_y^2)^{\frac{1}{2}}$$

The expression for P^{abs}_{em} was evaluated numerically and was substituted into equation (7.14) to give the relaxation time approximation (see Figure 7.2).

7.2.1 The Iterative Solution of the Steady State Boltzmann Equation

In the steady state, the linearised one-dimensional Boltzmann equation reads

$$\frac{-e}{\hbar}E\frac{\partial f_o}{\partial k} = \left[\frac{\partial f_1}{\partial t}\right]_{coll} \qquad (7.22)$$

and the right hand side is given by (7.5) and (7.6). These equations can be rearranged to give

$$f_1(k) = \frac{z(k',k)+\frac{e}{\hbar}E\frac{\partial f_o}{\partial k}}{Y(k',k)} \qquad (7.23)$$

where

$$z(k',k) = \int[f_1(k')[1-f_o(k)]P(k',k)+f_o(k)f_1(k')P(k,k')]\frac{L}{2\pi}dk'$$

and

$$Y(k',k) = \int[[1-f_o(k)]P(k,k')+f_o(k')P(k',k)]\frac{L}{2\pi}dk' \qquad (7.24)$$

where P(k,k') is given by (7.21). Equation (7.23) can be iterated until convergence to obtain an accurate value of $f_1(k)$. With this method the electron statistics are treated exactly.

The terms involving P(k',k) describe the scattering of electrons into state k whereas P(k,k') are the outscattering terms. To evaluate the integrals in (7.24) it is useful to keep this distinction in mind. For example, the first term in Z(k',k) is an inscattering process. We can go from k_{1ab} to k by the

emission of a polar optic phonon, hence

$$\int \frac{L}{2\pi} dk' \, f_1(k')[1-f_o(k)]P^{em}(k',k) = M(\epsilon,\hbar\omega_o)\, N^{em}(k)$$

where

$$M(\epsilon,\hbar\omega_o) = f_1(\epsilon+\hbar\omega_o)[1-f_o(\epsilon)]\,\frac{L}{2\pi}\,\frac{1}{\hbar}\sqrt{\frac{m^*}{2(\epsilon+\hbar\omega_o)}} \tag{7.25}$$

and

$$N^{em}(k) = W^{em}_{k_{1ab}\to k} - W^{em}_{k_{2ab}\to k}$$

where $W^{em}_{k_{1ab}\to k}$ is the transition rate with the energy conserving delta function removed and k_{1ab} and k_{2ab} are given by the two roots of

$$\frac{\hbar^2 k'^2}{2m^*} = \hbar\omega_o + \frac{\hbar^2 k^2}{2m^*} \tag{7.26}$$

We can make a transition from k_{lem} to k by phonon absorption if $\epsilon > \hbar\omega_o$ and we find

$$\int f_1(k')[1-f_o(k)]P^{ab}(k',k)\,\frac{L}{2\pi}\,dk' = M(\epsilon,-\hbar\omega_o)\, N^{ab}(k)\,\theta(\epsilon-\hbar\omega_o) \tag{7.27}$$

The other terms in (7.24) can be treated in the same way. We find that most of the terms on the right hand side of (7.24) involve $f_1(\epsilon+\hbar\omega_o)$ and $f_1(\epsilon-\hbar\omega_o)$ and we see that each part of the distribution function is coupled to the next. Using numerically determined values for P(k',k) we iterated this equation to find $f_1(k)$. We found that convergence was usually reached after about 10 iterations. To compare the results with those of the previous section for the initial momentum relaxation time we follow Fletcher and Butcher (1972) and introduce an effective relaxation time τ_{eff} defined by

$$\frac{-f_1(k)}{\tau_{eff}(\epsilon(k))} = \frac{-e}{\hbar} E \frac{\partial f_o(k)}{\partial k} \tag{7.28}$$

We have plotted τ_{eff} as a function of energy for a range of chemical potentials at room temperature (300k) (see Figure 7.2). The discontinuities at integral numbers of $\hbar\omega_o$ are well understood. The discontinuity at $\epsilon=\hbar\omega_o$ is due to the onset of the emission process. The other discontinuities are due to the coupling of the distribution function at ϵ to the distribution function at $\epsilon+\hbar\omega_o$, and $\epsilon-\hbar\omega_o$ by the inelasticity of the process. Nevertheless, in the high temperature and large electronic energy regime the iterative procedure duplicates the momentum relaxation time given in equation (7.14). It is interesting to note that the relaxation time equation (7.14) is non-zero as $k\rightarrow 0$, even though we may expect an equal amount of forward and backward scattering at this point (Ridley (1985)). On evaluating the expression (7.14) in the limit $k\rightarrow 0$ we find

$$\frac{1}{\tau_{mom}} = 2W(k\rightarrow k_{+ab})\,\frac{(1-f_o(\epsilon(k_{+ab})))}{(1-f_o(\epsilon(k_o)))}\,\frac{m^*}{\hbar^2 k_{+ab}} \qquad (7.29)$$

which is positive and non-zero. So we expect the relaxation time (7.14) to be negative over some energy range but positive at the origin. The details of the change from positive τ to negative near the origin are not shown in the Figures simply because of the large amount of computer time required. The value of τ calculated from (7.29) will be small on the scale used in the graphs and hence we find the curve approximately goes through the origin.

7.3 Discussion

In section 7.2 we gave an interpretation of the relaxation time formula for one-dimensional systems in the presence of polar mode scattering. It is strictly valid when the electrons obey Boltzmann statistics and it describes the initial behaviour of the average wavenumber k(t) following the injection of a small number of electrons with wavenumber k_o. The negative values which arise at low energies mean that initially k(t) increases above k_o. Ultimately, however, k(t) must reach a peak and then decay to zero

because the electrons eventually achieve a new equilibrium distribution function with the chemical potential shifted to be consistent with the number of electrons after injection. Both before injection and a long time after injection the mean wavenumber vanishes because equilibrium distribution functions depend only on the electron energy which is an even function of k.

It would be possible to calculate k(t) by numerical solution of equation (7.5) subject to the boundary condition (7.8). However, the general features of the behaviour of k(t) are clear from the physical arguments given here and detailed calculations are premature in the absence of time resolved experimental data.

CHAPTER 8

CONCLUSION AND DISCUSSION

Our aim in the work described in this thesis has been to study the effects of a range of scattering mechanisms on the conductivity of two-dimensional and one-dimensional electron gases in the Boltzmann regime. We have extended earlier work in the field by emphasising the effects of inter-sub-band coupling and electron statistics. In Chapter 3 we saw that it was necessary to define a characteristic scattering time for each sub-band that is occupied by electrons. Some authors have used only one relaxation time (Johnson (1984), Ridley (1982)). However, we have seen (by using the equations of Siggia and Kwok for two-dimensional systems and by developing our own for one-dimension) that the single relaxation time approximation is only correct in the extreme quantum limit when only one sub-band is occupied. We have shown in Chapter 6 that the Siggia and Kwok equations form a useful framework for quasi-elastic mechanisms at temperatures when the thermal energy $k_B T$ is greater than the characteristic change in electron energy. At lower temperatures (about 100 K for typical well dimensions) we modified these equations to take account of the electron statistics because some states are full and not all transitions are allowed. The relaxation times derived in this way show why the quantum size effects predicted by Siggia and Kwok are frozen out for inelastic scattering mechanisms at very low temperatures. The sub-band decoupling effect associated with this is particularly apparent in the deformation potential curves in two dimensions. The relaxation times for piezoelectric scattering do not show any drastic change in shape as the temperature is lowered because there is already some decoupling due to the Q dependence of the scattering potential. It is also interesting to note that the singular one-dimensional density of states has an effect on the sub-band coupling even at very low temperatures. However, we would expect this to be removed by the lifetime broadening of the sub-

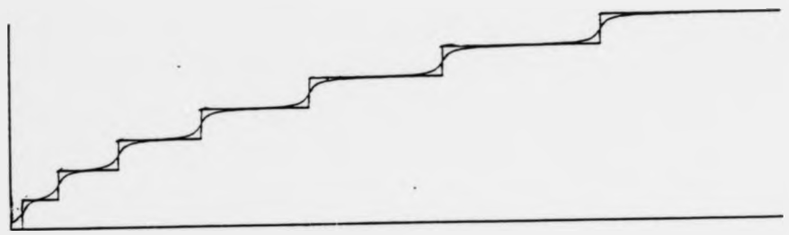

FIG 8.1

The "ideal" and lifetime broadened density of states.

band states, as we discuss in the next section.

The aim of this chapter is to discuss how the theory we have developed is deficient and to suggest possible methods of improvement. In 8.1 we look at the Boltzmann equation and consider the effect of the uncertainty principle on the transport times. In 8.2 we consider how realistic potential wells may affect the relaxation times which were derived from our simple sinusoidal wavefunctions. In 8.3 we discuss the problem of screening the various interactions with a dielectric function relevant to 2-DEG's. In 8.4 we reconsider alloy scattering theory and look at a first principles calculation for the scattering strength s(o).

8.1 Lifetime Broadening

In this section we ask how accurately does the Boltzmann conductivity relate to the true conductivity. Sernelius and Bergrenn (1985) suggest that the Boltzmann equation is inadequate in that it fails to duplicate experimental results. Cantrell and Butcher (1985) explain this in terms of the finite lifetime of the electron states. We give a simple explanation of their argument in terms of the Boltzmann equation and the Heisenberg uncertainty principle. To be definite we concentrate on the two-dimensional case.

The Boltzmann equation treats the time evolution of the distribution function $f(\underline{k},n,\underline{r}\ t)$ for a set of extended states. The density of states calculated from these is step-like and gives rise to the quantum size effects. These effects have been observed by some authors, Stormer et al (1982), and not by others Bergrenn et al (1985). This is because the finite scattering limited lifetime of the electron smooths out the sharp staircase density of states by introducing an uncertainty in the electron energy, the form of this is shown schematically in Figure 8.1. Inter-sub-band scattering will now be switched on more slowly when the electron energy

is raised and the abrupt quantum size effects will be smoothed out to some extent. Stormer (1982) observed this smoothing and he was able to attribute it to an energy uncertainty of $\hbar/\tau$ where τ was a characteristic lifetime of the carriers. To explain this with the Boltzmann equation we make the assumption that it is only the modification to the density of states which is important and scattering probabilities can still be evaluated accurately with unperturbed plane waves.

In the absence of scattering we can write the density of states in two-dimensions as

$$D^{2D}(\epsilon) = \sum_n \frac{m^*}{\pi\hbar^2}\,\theta(\epsilon-\epsilon_n) \tag{8.1}$$

$$= \int_{-\infty}^{\epsilon} d\epsilon' \sum_n \frac{m^*}{\pi\hbar^2}\,\delta(\epsilon'-\epsilon_n) \tag{8.2}$$

In the presence of scatterers the δ functions are broadened out to produce an area preserving line shape which is usually approximated by a Lorentzian, so that the new density of states is given by

$$D^{2D}_{scat}(\epsilon) = \frac{m^*}{\pi\hbar^2}\sum_n \int_{-\infty}^{\epsilon} d\epsilon' \,\frac{\Gamma_n}{[(\epsilon'-\epsilon_n)^2+\Gamma_n^2]\pi} \tag{8.3}$$

where Γ_n is related through the uncertainty principle to an energy or order $\hbar/$ scattering rate for sub-band n. The integral in (8.3) can be performed to give

$$D^{2D}_{scat}(\epsilon) = \frac{m^*}{\pi\hbar^2}\sum_n \frac{1}{\pi}\left[\frac{\pi}{2} + \tan^{-1}\,\frac{\epsilon-\epsilon_n}{\Gamma_n}\right] \equiv \sum_n D^n_{scat}(\epsilon) \tag{8.4}$$

For low values of Γ_n when $\epsilon-\epsilon_n >> \Gamma_n$ the expression reduces to the expression given by (8.2). We now modify the Siggia and Kwok equations by replacing the density of states term which arises in the summations over k states by the new broadened density of states. With this method we can allow the steps to switch on more slowly altering the relaxation times, hence the Siggia and Kwok equations become

$$\frac{1}{\tau_n} - \tau_n \sum_m \int P(k,n;k',m) D^m_{scat}(\epsilon) d\epsilon \frac{d\theta}{2\pi}$$

$$- \sum_m \tau_m \int \frac{k'}{k} \cos\theta \; P(k,n;k',m) \; D^m_{scat}(\epsilon) d\epsilon \frac{d\theta}{2\pi} \qquad (8.5)$$

For delta function scatterers the second integral reduces to zero and the relaxation times decouple to leave

$$\frac{1}{\tau_n} - \sum_m \int P(n,m) \left[\frac{1}{2} + \frac{1}{\pi} \tan^{-1} \frac{\epsilon-\epsilon_m}{\Gamma_m}\right] d\epsilon \frac{d\theta}{2\pi} \frac{m^*}{\pi\hbar^2} \qquad (8.6)$$

For delta function scatterers $P(k,n;k',m)$ is $\underline{k}$ independent and we have written this as $P(n,m)$. In this case the momentum relaxation rate is identically equal to $2\Gamma m/\hbar$ and hence we have

$$\frac{2\Gamma_n}{\hbar} \sim \sum_m \int P(n,m) \left[\frac{1}{2} + \frac{1}{\pi} \tan^{-1} \frac{\epsilon-\epsilon_m}{\Gamma_m}\right] \frac{m^*}{\pi\hbar^2} d\epsilon \qquad (8.7)$$

which may be solved iteratively.

The argument presented here is simple, Cantrell and Butcher (1985) show in a rigorous approach that for delta function scatterers $\tau_n = \hbar/2\Gamma_n$. Unfortunately their method is unable to treat realistic scattering mechanisms. The correspondence between (8.7) and their equations indicates

that equation (8.5) may be a best first guess for a solution to the transport problem with level broadening for realistic mechanisms.

The density of the scatterers reduces as the temperature is lowered and so will the level broadening. So, at very low temperatures in pure systems the QSE should be observable and due to static impurity scattering (see Stormer et al (1982)). Sernelius failed to see these features because their sub-band energies were very close together, due to their large well width. Their systems were severely disordered with the reciprocal of its mean free path (ie the uncertainty in $\underline{k}$)$\sim\frac{k}{2}$. Consequently both level broadening and thermal smoothing could be held responsible for removing the quantum size effects here.

At present an exact solution for the transport problem including lifetime broadening and realistic scattering mechanisms is intractable and the Boltzmann approach adopted here should serve as a useful tool in relatively pure systems. However, even these results are in need of some modification because they will be screened by the electrons in the 2-DEG.

8.2 Screening in 2-DEG's

The lack of three-dimensional translational invariance, and the resulting sub-band structure, complicate the screening of impurities in 2-DEG's and 1-DEG's. We have omitted this screening effect from our calculations. Screening in 2-DEG's is considered by Ando et al (1982) who examined a strictly two-dimensional system in the Thomas-Fermi approximation. They treat the charge sheet as having infinitesmal thickness and write the induced charge in the form

$$\rho_{ind}(\underline{r}) = -e[N_s(\bar{\phi})-N_s(0)]\delta(z) \qquad (8.8)$$

Here: $N_s(\bar{\phi})$ is the areal electron density due to the application of a potential $\bar{\phi}=\phi(\underline{r},o)$ the value of the electrostatic potential at the 2-DEG

layer. The screened potential ϕ must satisfy Poisson's equation

$$\underline{\nabla}\cdot(k\underline{\nabla}\phi) = \frac{-\rho}{\epsilon_o} \tag{8.9}$$

where $\rho = \rho_{ext} + \rho_{ind}$, with ρ_{ext} denoting the external charge due to the impurities. In the Thomas-Fermi approximation we consider the potential $\bar{\phi}$ to change the energy levels in the quantum well by an amount $-e\bar{\phi}$ and the separation of the Fermi energy ϵ_F from the bottom of the conduction band by $e\bar{\phi}$. The potential is assumed to be weak and we linearise the expression for ρ_{ind} to give

$$\rho_{ind}(\underline{r}) = -e\bar{\phi}(\underline{r})\frac{dN_s}{d\phi}\delta(z)$$

$$= -e^2\bar{\phi}(\underline{r})\frac{dN_s}{d\epsilon_F}\delta(z) \tag{8.10}$$

Poisson's equation then becomes (Ando (1982))

$$\underline{\nabla}\cdot(k\underline{\nabla}\phi) - 2\bar{k}\bar{q}_s\bar{\phi}(\underline{r})\delta(z) = -\rho_{ext}/\epsilon_o \tag{8.11}$$

where

$$\bar{k} = \frac{K_{sc} + k_{ins}}{2}$$

with

$$\bar{q}_s = \frac{-e^2}{\bar{k}\epsilon_o}\frac{dN_s}{d\epsilon_F} \tag{8.12}$$

To solve (8.10) Ando used a Bessel function expansion for the potential

$$\phi(\underline{r},z) = \int_0^\infty qA_q(z)J_o(qr)dq \tag{8.13}$$

The value of the coefficient Aq(0) is given by

$$\bar{A}_q(0) = \frac{ze}{\bar{k}}\frac{e^{qz_o}}{q+\bar{q}_s} \tag{8.14}$$

For large r the average potential falls off as r^3

$$\phi(r) \sim \frac{ze(1+\bar{q}_s z_o)}{\bar{k}\,\bar{q}_s^{\,2} r^3} \tag{8.15}$$

which is not so strongly screened as the Yukawa potential found for screened impurities in three-dimensional systems.

Unfortunately, this approach is only useful for treating the single sub-band case. The most interesting features which arise in quantum well transport are due to the switching on of new states when a new sub-band becomes occupied (Ogrin et al (1966)). Sernelius et al (1985) address this problem using perturbation theory. They consider a GaAs FET and equate the induced charge with an expression derived from first order perturbation theory to obtain

$$\rho_{ind}(\underline{R}) = 2e^2 \sum_{\substack{n,\underline{k} \\ m,\underline{k}'}} \frac{f_o(\underline{k},n)\left[1-f_o(\underline{k}',m)\right]}{\epsilon_n(\underline{k})-\epsilon_m(\underline{k}')} \langle \underline{k},n|V_i|\underline{k}',m\rangle \psi_{n,\underline{k}}\psi^{*}_{m,\underline{k}'}(\underline{R}) + \text{c.c.} \tag{8.16}$$

where V_i is the impurity potential and c.c. stands for the complex conjugate. If we Fourier expand the induced charge density and the perturbing potential V_i, we find that

$$\rho_{ind}(\underline{R}) = V^{-1}\sum_{\underline{q},q_z} \rho_{ind}(\underline{q},q_z)\exp(iq_z z+i\underline{q}\cdot\underline{r})$$

and

$$\rho_{ind}(\underline{Q}) = e^2\sum_{nm} \Pi_o(n,m;\underline{q})\langle n|\exp(iq_z z)|m\rangle \tag{8.17}$$

$$\times \frac{1}{L_z}\sum_{p_z} \langle m|\exp(ip_z z)|n\rangle V_i(p_z,q) \tag{8.18}$$

where L_z is the macroscopic width of the system in the z-direction. The quantity $\langle n|\exp(ip_z z))|m\rangle$ is the equivalent to Ridley's (1982) $G_{nm}(p_z)$ for an arbitrary confining potential and

$$\Pi_o(n,m,\underline{q}) = \frac{2}{A}\sum_{\underline{k}} \frac{f_o(\underline{k},n) - f_o(\underline{k}+\underline{q},m)}{\epsilon_n(\underline{k}) - \epsilon_m(\underline{k}+\underline{q})} \tag{8.19}$$

Poisson's equation again relates the induced potential to the induced charge, hence

$$\nabla^2 \phi_{ind} = \frac{-\rho_{ind}}{k\epsilon_o} \tag{8.20}$$

giving

$$-Q^2 \phi_{ind}(\underline{Q}) = \frac{-e^2}{k\epsilon_o}\sum_{nm} \Pi_o(n,m;q)\langle n|\exp(-iq_z z)|m\rangle$$

$$\times \frac{1}{L_z}\sum_{p_z} \langle m|\exp(ip_z z)|n\rangle Vi(p_z,\underline{q}) \tag{8.21}$$

for the Fourier transform of $Q_{ind}(\underline{R})$. To make our argument self-consistent we must include this induced potential as part of the perturbation. Hence following Sernelius, we have

$$V_i(Q) = V_o(Q) + \nu(Q)\sum_{nm} \Pi_o(n,m;\underline{q})\langle n|\exp(-iq_z z)|m\rangle$$

$$\times \frac{1}{L_z}\sum_{p_z} \langle m|\exp(ip_z z)|n\rangle\, V_i(p_z,\underline{q}) \tag{8.22}$$

The true impurity potential is made up of the potential from the bare impurity plus a contribution to the potential from the screening electrons which move in response to the screened impurity potential. In equation (8.22)

$$\nu(\underline{Q}) = \frac{e^2}{k\epsilon_o Q^2} \tag{8.23}$$

The inversion of the three-dimensional equivalent of (8.22) results in the Lindhard dielectric function. The inversion of (8.22) however results in a

matrix equation

$$V_{q_z}(\underline{q}) = \epsilon^{-1}(\underline{q})\, Vo_{q_z}(\underline{q})$$

where

$$\epsilon(\underline{q})_{q_z,p_z} = \delta q_z,p_z - v(\underline{Q})\frac{1}{L_z}\sum_{n,m}\Pi_o(n,m;\underline{q})$$

$$x\ \langle n|\exp(-q_z z))m\rangle\langle m|\exp(ip_z z)|n\rangle \qquad (8.24)$$

In principle we could have included the screening in our calculations but the computational effort involved is excessive, Sernelius includes the influence of the five lowest sub-bands to calculate the screening of the impurity potential before calculating the conductivity of the lowest sub-band. In the absence of refined experimental data, these considerations appear to be premature. The extension of Sernelius' screening theory to one-dimensional systems is straightforward although we consider the implementation to involve substantial computational effort. We find that

$$\rho_{ind}(q_x,q_y,q_z) = e^2\sum_{\substack{n,n'\\m,m'}}\Pi_o(n,n',m,m';q_z)\langle n|\exp(-iq_x x))n'\rangle$$

$$x\ \langle m|\exp(-iq_y y)|m'\rangle$$

$$x\,\frac{1}{A}\sum_{p_z,p_y}\langle m'|\exp(ip_x x)|m\rangle\langle n'|\exp(ip_y y)|n\rangle\ V_i(p_x,p_y,p_z)$$

leading to

$$\epsilon(q_z)\ q_z,p_x;q_y,p_y = \delta(q_x,p_x),(q_y,p_y) - \nu(\underline{Q})\frac{1}{A}\sum_{\substack{n'n'\\m,m'}}\Pi_o(n,n';m,m',q_z)$$

$$x\ \langle n|\exp(-iq_x x)|n'\rangle\langle m|\exp(-iq_y y)|m'\rangle$$

$$x\ \langle n'|\exp(ip_x x)|n\rangle\langle m'|\exp(ip_y y)|m\rangle \qquad (8.25)$$

We shall return to the screening problem in our discusssion of alloy scattering, section 8.4.

8.3 Realistic Potential Wells

The sinusoidal wavefunctions used throughout our calculations are extremely useful in simplifying quantum well calculations, this is why we use them. Of course, in doing so we ignore complicated many body effects (Ando (1982)). The quantum well is usually embedded in a material with a different dielectric constant and we really should include the coulomb interaction with image charges. If we consider the presence of only one material interface and two electrons we obtain an expression for the electrostatic potential given by the standard result (Jackson (1962)).

$$V(\underline{r}-\underline{r}';z,z') = \frac{e^2}{k_{sc}\epsilon_o}[(\underline{r}-\underline{r}')^2 + (z-z')^2]^{-\frac{1}{2}}$$

$$+ \frac{e^2(k_{sc}-k_{ins})}{k_{sc}(k_{sc}+k_{ins})\epsilon_o}\ [(\underline{r}-\underline{r}')^2 + (z+z')^2]^{-\frac{1}{2}} \qquad (8.26)$$

With two snarp interfaces arranged parallel to one another the problem becomes more complicated with multiple image charges and the evaluation of some kind of Madelung sum is necessary before the potential is obtained. The potential in the well must also be solved for self-consistently, taking full account of the quantum nature of the well and the Poisson equation. In performing these calculations it is usual to work in the Hartree approximation and to use the one electron Schroedinger equation and a self-consistent potential, which is usually expressed as the sum of the potential due to electrons, the donors and the image potentials. Self-consistent solutions have been attempted, Vinter (1982), Stern (1972). These results compare well with Ando (1982) and with the results of variational calculations (Fang and Howard (1966)), indicating that the use of elementary wavefunctions may be justified.

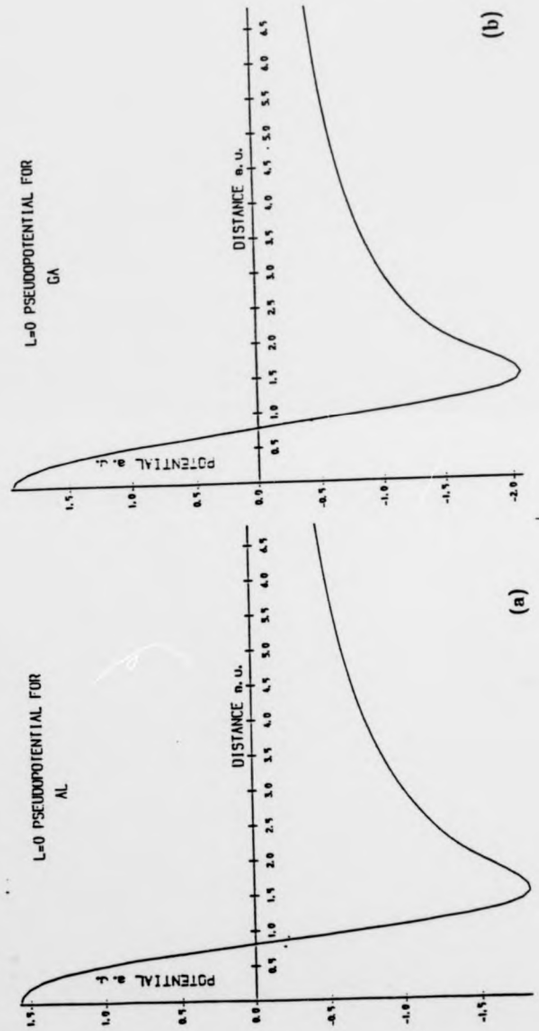

FIG 8.2

The l=0 pseudopotentials for Gallium and Aluminium, and the pseudopotential difference (after Bachelot(1982)).

Here we have adopted the philosophy that, while the effects predicted from our over-simplified wavefunctions will not be correct in detail, they serve as a useful basis for preliminary calculations and give a good indication of what can be expected in realisable experimental situations. The precise details of the wavefunctions will change the magnitudes of the relaxation times and quantum size effects but we expect the shape of the curves to remain substantially unchanged.

8.4 Alloy Scattering

In 4.4 we considered alloy scattering in GaAs/$Al_xGa_{1-x}As$ quantum wells and we noted that there was still controversy in the literature over the nature of the scattering potential. We suggested that the conduction band offset was responsible for the scattering (fortunately this is known for GaAs/$Al_xGa_{1-x}As$) and we went on to show that this should be expressible in terms of suitably screened atomic pseudopotentials, in this section we probe this statement further.

The basic theory of pseudopotentials is presented in appendix 4, and model potentials are plotted in Figures 8.2(a),(b) and (c). In transport theory we usually treat the electron wavefunctions as being plane waves and consequently when we are looking at the scattering of electrons by lattice imperfections it is natural to think of the pseudopotential as the element responsible for the scattering (Harrison (1965)). As pseudopotentials are available for all the elements (Heine and Abarenkov (1964), Bachelot, Hamann and Schluter (1982)), whilst data for the conduction band offsets are available only in special cases, it is natural to attempt a pseudopotential approach. This would allow us to evaluate the barrier heights for a large range of quantum wells and it would allow us to calculate the alloy scattering in each case. In this section we outline an attempt to do this.

Alloy scattering has been examined in metals with the pseudopotential method (Harrison (1965)). He obtained a relaxation time suitable for a three-dimensional system given by

$$\frac{1}{\tau} = \frac{Vk_F m^*}{2\pi\hbar^3} \int |\langle \underline{k}+\underline{Q}|W|\underline{k}\rangle|^2 (1-\cos\theta)\sin\theta d\theta \qquad (8.27)$$

where W is the difference between the pseudopotentials of the individual atoms involved. He treated a range of binary alloys, but the agreement of experiment was not very good, the experimental resistivity sometimes differing by as much as five times from the theoretical values. We should note at this point that no data was presented for the Gallium/Aluminium alloy.

In Harrison's case he treats impurities which are not always isoelectronic (for example Zn/Al) and the pseudopotential difference contains a large coulombic tail which was screened with the Lindhard metallic dielectric function. In our case the impurities are isoelectronic, consequently any pseudopotential difference is due to the difference between the small scale atomic cores. The other major difference is in the size of the Fermi wavevectors. In Harrison's case these are large and the Fourier transform which arises in (8.27) cannot be approximated to a potential strength. The essence of our calculation is simple: we are concerned with the scattering strength s(o) (see chapter 4). Hence we only have to take the pseudopotential differences, integrate them over space and divide them by q=0 component of a suitable dielectric screening function. This has been done for Ga/Al. For the Animalu-Heine (1965) pseudopotentials we find that

$$s(o) = \int V(\underline{R})d^3R = 1.41\times10^{-29} eVm^3 \qquad (8.28)$$

and for the Hamann pseudopotentials we find that

$$s(o) = 2.78\times10^{-29}eVm^3 \qquad (8.29)$$

When screened s(0) should be comparable with conduction band offset if the theory is correct. If we take Okumura's (1985) model and assume linear interpolation we find

$$\Delta E_c(GaAs/AlAs) = 831meV \qquad (8.30)$$

The volume of the scattering potential must be taken as the size of the elemental GaAs unit, which is

$$V_c = 4.52\times10^{-29}m^3$$

Hence the scattering strength in this model is

$$s(o) = \Delta E_c V_c = 3.75\times10^{-29}eVm^3$$

which lies above the values of s(0) calculated from the unscreened pseudopotential approach. Fedders (1984) has carried out an independent tight-binding calculation for the effect of the alloy scattering potential. By correlating his result with our approach we find that the potential strength used in his calculation is

$$s(o) = 1.62\times10^{-29}eVm^3$$

However, the tight-binding method is an involved calculation while the conduction band offset method only relies on experimental C-V profiling. The pseudopotential approach has none of these drawbacks, but to assess its usefulness we must consider the screening problem.

It seems that without screening we are close to an acceptable answer, (recent experimental work by Saxena (1985) has suggested a value of $3.52\times10^{-29}eVm$ for the scattering strength). However, the screening of the pseudopotential is non-trivial. The first step is to associate the

screening in the pseudopotential model with the screening encountered in the true semiconductor. The next step is to consider the scale of the scattering pseudopotential. This is plotted in Figure 8.2(c) and is sharply confined to the unit cell and this will be screened by the valence band electrons which must be considered to be distributed inhomogeneously on this length scale. The real problem is then to evaluate the screened potential and to consider how the conduction electrons are scattered off this. Baldereschi and Hopfield (1970) encountered a similar problem when they considered the binding of electrons to isoelectronic impurities, producing shallow states within the band-gap. Experimental data suggests that an electron can be bound to such an impurity only if its electronegativity is larger than that of the host atom which it replaces. They consider the unscreened binding potential to be due to the difference of the pseudopotential and they screen this with a dielectric function which was adapted from Penn's (1962) empirical ideas. Penn's static dielectric function is of the form

$$\epsilon(o) = 1 + \left[\frac{\hbar\omega_p}{E_g}\right]^2 \qquad (8.31)$$

where ω_p is the plasma frequency due to a uniform electron gas with a density given by the average valence electron density. E_g was fitted by setting $\epsilon(o)$ equal to its observed value. Penn's full expression then gave the $\underline{Q}$ dependence of $\epsilon(\underline{Q})$. Baldereschi (1972) proposed a model for the sharp impurity potential. The average electron density in (8.31) has very little meaning on the scale of the pseudopotential differences under consideration here. Baldereschi suggests that it is more reasonable to work in terms of a local average electron density, whilst still retaining the value of E_g he modified ω_p. With this adjustment he was able to predict with some degree of accuracy whether the impurity would bind an electron.

Our problem is similar, the matrix element arising in our scattering rates is the $\underline{Q}=0$ component of the $l=0$ pseudopotential. Whereas the full screened potential in the inhomogeneous medium involves the use of a dielectric matrix Baldereschi (1979, 1978), Adler (1962) in which all $\underline{Q}$ components must be taken into account. In three-dimensions the screened potential $\phi(\underline{Q}+\underline{G})$ is related to the unscreened potential $\phi_o(\underline{Q}+\underline{G})$ by the dielectric matrix, through the relation

$$\phi(\underline{Q}+\underline{G}) = \sum_{\underline{G}'} \epsilon^{-1}(\underline{Q}+\underline{G},\underline{Q}+\underline{G}')\phi_o(\underline{Q}+\underline{G}') \tag{8.32}$$

where $\underline{Q}$ is inside the Brillouin zone and $\underline{G}$ and $\underline{G}'$ are reciprocal lattice vectors. Before we proceed we consider the meaning of ϵ^{-1} and examine some of its properties.

If we let $F(\underline{R}-\underline{R}',\underline{R}')$ denote the screened potential at $\underline{R}$ produced by a delta-function bare potential at $\underline{R}'$. Then with $\underline{R}-\underline{R}'$ fixed, $F(\underline{R}-\underline{R}',\underline{R}')$ is periodic in $\underline{R}'$. Hence we may write

$$F(\underline{R}-\underline{R}',\underline{R}) = \sum_{\underline{G}'} f_{\underline{G}'}(\underline{R}-\underline{R}')e^{i\underline{G}'\cdot\underline{R}'} \tag{8.33}$$

and $F_{G'}(\underline{R}-\underline{R}')$ may be Fourier expanded to give

$$f_{G'}(\underline{R}-\underline{R}') = \int \frac{dQ}{(2\pi)^3} e^{i\underline{Q}\cdot(\underline{R}-\underline{R}')} \tilde{f}_{\underline{G}'}(\underline{Q}) \tag{8.34}$$

we substitute (8.34) into (8.33) to obtain

$$F(\underline{R}-\underline{R}',\underline{R}') = \sum_{\underline{G}'}\int \frac{dQ'}{(2\pi)^3} \hat{f}_{\underline{G}'}(\underline{Q}')e^{i\underline{Q}'\cdot\underline{R}}e^{i(\underline{G}'-\underline{G}')\cdot\underline{R}'} \tag{8.35}$$

we consider the screened potential produced by a plane-wave of the form

$$e^{i(\underline{Q}+\underline{G}')\cdot\underline{R}} = \int d\underline{R}' \delta(\underline{R}-\underline{R}')e^{i(\underline{Q}+\underline{G}')\cdot\underline{R}'} \tag{8.36}$$

Now $F(\underline{R}-\underline{R}',\underline{R}')$ describes the response due to a delta-function, as the system is linear we find.

$$\phi(R) = \int dR' F(\underline{R}-\underline{R}',\underline{R}') e^{i(\underline{Q}+\underline{G}')\cdot\underline{R}'} \tag{8.37}$$

which from (8.34) gives

$$\begin{aligned}\phi(\underline{R}) = &\int dR' F(\underline{R}-\underline{R}',\underline{R}') e^{i(\underline{Q}+\underline{G}')\cdot\underline{R}'} \\ &- \sum_{\underline{G}''} \int \frac{dQ'}{(2\pi)^3} \tilde{f}_{\underline{G}'}(\underline{Q}') e^{i\underline{Q}'\cdot\underline{R}} \int dR' e^{i(\underline{G}''-\underline{Q}'+\underline{Q}+\underline{G})\cdot\underline{R}'} \\ &- \sum_{\underline{G}''} \int dQ' \; \hat{f}_{\underline{G}-}(\underline{Q}') e^{i\underline{Q}'\cdot\underline{R}} \, \delta(\underline{Q}'-\underline{Q}-\underline{G}-\underline{G}'') \\ &- \sum_{\underline{G}''} \tilde{\tilde{f}}_{\underline{G}''}(\underline{Q}+\underline{G}+\underline{G}'') e^{i(\underline{Q}+\underline{G}+\underline{G}'')\cdot\underline{R}} \\ &- \sum_{\underline{G}'''} \epsilon^{-1}(\underline{Q}+\underline{G},\underline{Q}+\underline{G}''') e^{i(\underline{Q}+\underline{G}''')\cdot\underline{R}}\end{aligned}$$

where we have made the identification (8.38)

$$\epsilon^{-1}(\underline{Q}+\underline{G},\underline{Q}+\underline{G}'') = \hat{f}_{\underline{G}''-\underline{G}}(\underline{Q}+\underline{G}'') \tag{8.39}$$

We are concerned with the volume integral of the potential which to a first approximation we say is a delta function situated at the Gallium site, ie

$$\int d^3R F(\underline{R}-\underline{R}',\underline{R}') = \sum_{\underline{G}'} \int dQ' \; \tilde{f}_{\underline{G}'}(\underline{Q}') e^{i(\underline{G}'-\underline{Q}')\cdot\underline{R}'} \, \delta(\underline{Q}') \tag{8.40}$$

where we have used (8.35). Hence

$$\int d^3R F(\underline{R}-\underline{R}',\underline{R}') = \sum_{\underline{G}'} \tilde{f}_{\underline{G}'}(o) e^{i\underline{G}'\cdot\underline{R}'} \tag{8.41}$$

From (8.39) with $\underline{G}''-\underline{G}=\underline{G}'$

$$\int d^3RF(\underline{R}-\underline{R}',\underline{R}') - \sum_{\underline{G}'} \tilde{f}_{\underline{G}'}(o)e^{i\underline{G}'\cdot\underline{R}'} = \sum_{\underline{G}'} \epsilon^{-1}(-\underline{G}',0)e^{i\underline{G}'\cdot\underline{R}'} \qquad (8.42)$$

where we have taken the $\underline{Q}\rightarrow 0$ limit.

Baldereschi (1979) presents values for $|\underline{Q}+\underline{G}|\epsilon^{-1}(\underline{Q}+\underline{G},\underline{Q})/|\underline{Q}|$ for $\underline{Q}\rightarrow 0$. The $\underline{G}=0$ element is the reciprocal of the macroscopic dielectric constant and all the other elements are finite for $\underline{G}\neq 0$ hence $\epsilon^{-1}_{\underline{Q}\rightarrow 0}(\underline{Q}+\underline{G},\underline{Q})$ is equal to the inverse macroscopic dielectric constant when $\underline{G}=0$ and zero for $\underline{G}\neq 0$. The summation in (8.42) is then equal to ϵ_o^{-1} and the $\underline{Q}=0$ component of the delta function potential is to be screened with the large scale macroscopic dielectric constant even though the potential is such a microscopic scattering centre. This result is contrary to that obtained by Baldereschi using the local Penn method and has been confirmed by Tosatti (1985) leaving us with a dilemma. If we are to screen the scattering strength obtained we will decrease its value by a factor of about 13 (12·91 is the dielectric constant relevant to GaAs (Rode (1975)). Such a reduction will give resistivities in GaAs/$Al_xGa_{1-x}As$ quantum wells which are about two orders of magnitude down on experimentally determined resistivities and band offsets. Clearly there is a problem with this approach, and we must re-examine the steps that have been taken.

The pseudopotential method has been used by Walter and Cohen (1971) to determine the band structure in GaAs. The basic method involves inputting the atomic positions and pseudopotentials. The charge density, wavefunctions and eigenvalues in the system are then determined self-consistently. We could envisage doing this for the $Al_xGa_{1-x}As$ system in the virtual crystal approximation (see Andreoni and Car (1980)). The difference in pseudopotentials must then be responsible for the scattering.

We must now ask whether it is viable to change our pseudopotential difference by a factor of 10 and still have a sensible form for the pseudopotentials of both of our elements. To examine this question we look at the Animalu-Heine pseudopotentials. If we were to change the value of A_o for the two elements so that the resistivity matched experimental data we would have to alter them so much that they would break out of the periodic trend which is evident in these tables and this is clearly unsatisfactory. At least for the Animalu potentials the values of A_o (see appendix 4) were calculated at the Fermi energies of the elements and consequently it may be inappropriate to apply them here. The Bachelot pseudopotentials however were devised for maximum transferability and the authors claim that they can be used to "accurately reproduce the results of all electron calculations for the self-consistent electronic structure of atoms, molecules and solids". The accuracy of these calculations is impressive for some atoms, for instance they reproduce the band energies of silicon with errors in the range of 0.05eV (Bachelot et al). For the more exotic elements (for example Nb and CsAu) the errors are in the range of 0.1-0.2eV (Bachelot et al) although it is not clear in which part of the bandstructure. If the GaAs and AlAs band-structures both had an accuracy on the limit of this range then a 0.4eV shift in the band-gap would still be half the amount necessary to give the correct magnitude for the resistivity.

Our conclusion is that the attractiveness of atomic pseudopotentials for alloy scattering calculations is illusory. It appears that they are not known with sufficient accuracy in the core region (see also Andreoni and Car (1980)) and the theory of inhomogeneous screening of tightly confined potentials is not sufficiently well developed to yield reliable results for a property as sensitive as s(0). It is preferable to proceed semi-empirically by using measured band offsets as has been done in Chapter 4 where the results are closer to what one would expect from resistivity

measurements. Andreoni and Car (1980) also noticed a problem with the screened Ga/Al pseudopotential difference. They note that the results of several authors range over at least one order of magnitude; confirming our beliefs.

APPENDIX 1

EFFECTIVE MASS THEORY

The potential in a bulk semiconductor is strongly dependent on position but is periodic. The wavefunctions satisfy the time-independent Schroedinger equation and Bloch's Theorem is valid. The eigenvalues are a function of a continuous variable $\underline{k}$ and a band index n. Once the bandstructure has been calculated for a given material it is natural to ask how the system behaves when impurities are present or when an external field is applied. Luttinger and Kohn (1955) considered this problem in a rigorous fashion and put effective mass theory which had been used for many years (Frohlich (1937)) on a firm footing. They proved that once the bandstructure of a pure crystal was known it is a simple matter to calculate the response of the electrons in the crystal to slowly varying potentials without referring to the details of the unperturbed wavefunctions. We give an account of the theory in simplified and less rigorous terms. Following the approach of Smith et al (1967). In the absence of impurities or external potentials we may write the eigenvalues for a periodic three-dimensional system as

$$\psi_{n,\underline{k}} = U_{n,\underline{k}}(\underline{R})e^{i\underline{k}\cdot\underline{R}} \qquad 1$$

where n is a band-index and $\underline{k}$ is a wavevector. The $U_{n,\underline{k}}(\underline{R})$ are determined from the Schroedinger equation.

$$H_o\psi_{n,\underline{k}} = \varepsilon_n(\underline{k})\psi_{n,\underline{k}} \qquad 2$$

where H_o is the unperturbed Hamiltonian for the semiconductor and $\varepsilon_n(\underline{k})$ are the energy eigenvalues giving the bandstructure. If the perturbation applied to the crystal is small so that transitions between bands can be neglected, then the motion of an electron in a band can be described in terms of a wavepacket constructed from the basis states in that band. Hence

$$\psi_n(\underline{R},t) = \sum_{\underline{k}} a(k,t)\psi_{n,\underline{k}}(\underline{R}) \qquad 3$$

The new Hamiltonian for the system may be written as

$H = H_o + V(\underline{R})$

where $V(\underline{R})$ is the slowly varying perturbing potential. We apply the operator H to the wavefunction in (3)

$$H\psi(\underline{R},t) = \sum_{\underline{k}} a(\underline{k},t)\left[H_o+V(\underline{R})\right]\psi_{n,\underline{k}}(\underline{R}) = \sum_{\underline{k}} a(k,t)\left[\epsilon_n(k)+V(\underline{R})\right]\psi_{n,k}(R) \qquad 5$$

To proceed we use the periodic nature of $\epsilon_n(\underline{k})$ and we Fourier expand it in terms of lattice translation vectors. Hence,

$$\epsilon_n(\underline{k}) = \sum_{\iota} \epsilon_{n\iota}\exp(i\underline{k}\cdot\underline{R}_\iota)$$

and

$$\epsilon_n(-i\underline{\nabla}) = \sum_{\iota} \epsilon_{n1}\exp(\underline{R}_\iota\cdot\underline{\nabla})$$

if we operate with $\epsilon_n(-i\nabla)$ on $\psi_{n,\underline{k}}(\underline{R})$ we obtain

$$\begin{aligned}\epsilon_n(-i\underline{\nabla})\psi_{n,\underline{k}}(\underline{R}) &= \sum \epsilon_{n,1}\psi_{n,\underline{k}}(\underline{R}+\underline{R}_\iota)\\ &= \sum \epsilon_{n,1}\exp(i\underline{k}\cdot\underline{R}_\iota)\psi_{n,\underline{k}}(\underline{R})\\ &= \epsilon_n(\underline{k})\psi_{n,\underline{k}}(\underline{R})\end{aligned}$$

we substitute this result into (5) to obtain

$$H\psi(\underline{R},t) = \left[\epsilon_n(-i\underline{\nabla}) + V(\underline{R})\right]\psi = i\hbar\frac{\partial\psi}{\partial t} \qquad 6$$

where we have taken $\epsilon_n(-i\underline{\nabla})$ outside the summation. To use this equation we must take the full details of the bandstructure and the ψ that is obtained will be the full wavepacket (3) representation, which may have

rapid oscillations in $\underline{R}$ space. The usual effective mass equation describes the envelope behaviour of the wavefunction. To develop this we suppose that the coefficient $a(\underline{k},t)$ is large only for $\underline{k}$ near $\underline{k}_o$, the wavevector marking the bottom of the band. The periodic part of the Bloch function is usually a relatively weak function of $\underline{k}$. If $\underline{k}$ is near $\underline{k}_o$ then

$$\psi_{n,\underline{k}}(\underline{R}) = \exp(i\underline{k}\cdot\underline{R})U_{n,\underline{k}}(\underline{R}) \sim \exp(i\underline{k}\cdot\underline{R})U_{n,\underline{k}_o}(\underline{R})$$

$$= \exp\left[i(\underline{k}-\underline{k}_o)\cdot\underline{R}\right]\psi_{n,k_o}(\underline{R}) \qquad 7$$

we can re-express the wavefunction as

$$\psi = F(\underline{R},t)\psi_{n,\underline{k}_o}(R) \qquad 8$$

where

$$F(\underline{R},t) = \sum_{\underline{k}} a(\underline{k},t)\exp\left[i(\underline{k}-\underline{k}_o)\cdot\underline{R}\right]$$

It can be shown that

$$\epsilon_n(-i\underline{\nabla})\psi = \psi_{n,\underline{k}_o}(\underline{R})\epsilon_n(\underline{k}_o-i\underline{\nabla})F(\underline{R},t)$$

which allows us to rewrite the effective mass equation (6) in the form

$$\left[\epsilon_n(\underline{k}_o-i\underline{\nabla}) + V(\underline{R})\right] F(\underline{R},t) = i\hbar\frac{\partial F}{\partial t} \qquad 9$$

where $F(\underline{R},t)$ is the envelope function. If we apply (9) to an arbitrary potential and find that $F(\underline{R},t)$ does not vary appreciably with distance then we can take it that ∇F is a small quantity and the assumption that $a(\underline{k},t)$ is large only near $\underline{k}$ is a valid one. The wavefunction for the system is then described accurately by expression (8). So long as the function $F(\underline{R},t)$ is a slowly varying function of $\underline{R}$ the potential can vary rapidly and the effective mass representation is still valid.

The effective mass equation allows us to leave out the details of the atomic

potential and model the motion of an electron by a free particle of mass m*. This quantity may vary with the direction of motion and in general an effective mass tensor is needed, but in GaAs where the conduction band minimum is spherical and parabolic only a scalar is needed, as is assumed in this thesis.

Wavefunctions in a Quantum Well

Suppose that $V(\underline{R})$ in equation (9) is a function of z only, taking the form of a square well with V=0 inside and $V=\Delta E_c$ outside. Then the effective mass equation (9) has steady state solutions of the type

$$\Psi(\underline{R},t) = e^{-iEt/\hbar} e^{i\underline{k}\cdot\underline{R}} \zeta(z)$$

where $\zeta(z)$ and the relation between E and $\underline{k}$ remains to be determined. The equations for $\zeta(z)$ can be written immediately both inside and outside the well. There are sinusoidal solutions inside which must be properly matched to damped solutions outside the well. The quantitites which must be matched up at the edges of the well are $\psi(z)$ and $(m^*)^{-1}\frac{d\psi}{dz}$ Collins (1985)) and this has been neglected by some authors, Marsh (1984). In the case of interest to us m* changes from 0.067m inside to 0.075m outside the well. This small change complicates the solution of the eigenvalue problem. We have taken it into account in our calculations of the sub-band energies and wavefunctions when $\underline{k}=0$ (see Figure 4.3). When $\underline{k}\neq 0$ we have simplified the problem by assuming that m* has the value m* appropriate to $Al_xGa_{1-x}As$ everywhere (Palmer (1982)). We write $\zeta_n(z)$ for the wavefunction in sub-band n and ϵ_n for its minimum energy. With this approximation the energy in sub-band n is

$$\epsilon_n(\underline{k}) = \epsilon_n + \frac{\hbar^2 k^2}{2m_a^*}$$

APPENDIX 2

$$|G(q_z,n,m)|^2 = \left|\frac{2}{L}\int_0^L e^{iq_z z} \sin\frac{n\pi z}{L} \sin\frac{m\pi z}{L}\, dz\right|^2$$

$$\text{let } k_z = \frac{n\pi}{L}, \quad k_z' = \frac{m\pi}{L}$$

$$= \frac{1}{4}\left[\left[\frac{\sin[q_z-(k_z'-k_z)]L/2}{[q_z-(k_z'-k_z)]L/2}\right]^2 + \left[\frac{\sin[q_z+(k_z'-k_z)]L/2}{[q_z+(k_z'-k_z)]L/2}\right]^2\right.$$

$$+ \left[\frac{\sin[q_z-(k_z'+k_z)]L/2}{[q_z-(k_z'+k_z)]L/2}\right]^2 + \left[\frac{\sin[q_z+(k_z'+k_z)]L/2}{[q_z+(k_z'+k_z)]L/2}\right]^2$$

$$+ \frac{\sin[q_z-(k_z'-k_z)]L/2}{[q_z-(k_z'-k_z)]L/2} \sin\frac{[q_z+(k_z'-k_z)]L/2}{[q_z+(k_z'-k_z)]L/2} 2\cos[(k_z'-k_z)L]$$

$$- \frac{\sin[q_z-(k_z'-k_z)]L/2}{[q_z-(k_z'-k_z)]L/2} \frac{\sin[q_z-(k_z'+k_z)]L/2}{[q_z-(k_z'+k_z)]L/2} 2\cos(k_zL)$$

$$- \frac{\sin[q_z-(k_z'-k_z)]L/2}{[q_z-(k_z'-k_z)]L/2} \sin\frac{[q_z+(k_z'+k_z)]L/2}{[q_z+(k_z'+k_z)]L/2} 2\cos(k_z'L)$$

$$- \frac{\sin[q_z+(k_z'-k_z)]L/2}{[q_z+(k_z'-k_z)]L/2} \frac{\sin[q_z-(k_z'+k_z)]L/2}{[q_z-(k_z'+k_z)]L/2} 2\cos(k_z'L)$$

$$- \frac{\sin[q_z+(k_z'-k_z)]L/2}{[q_z+(k_z'-k_z)]L/2} \frac{\sin[q_z+(k_z'+k_z)]L/2}{[q_z+(k_z'+k_z)]L/2} 2\cos(k_zL)$$

$$+ \frac{\sin[q_z-(k_z'+k_z)]L/2}{[q_z-(k_z'+k_z)]L/2} \quad \frac{\sin[q_z+(k_z'+k_z)]L/2}{[q_z+(k_z'+k_z)]L/2} \quad 2\cos((k_z'+k_z)L) \Bigg]$$

APPENDIX 3

EVALUATION OF THE TRANSITION RATE FOR POLAR OPTIC PHONON SCATTERING

In this appendix we evaluate the q_x integral in equation (7.20). It is easily shown that

$$G^2(q_x) = \frac{4}{a^2}\int_0^a \sin^2\frac{\pi x}{a}\, e^{iq_x x}\, dx = \frac{4\left[\frac{2\pi}{a}\right]^2 \sin^2\frac{q_x a}{2}}{a^2 q_x^2\left[q_x^2 - \left[\frac{2\pi}{a}\right]^2\right]^2} \qquad 1$$

(7.20) then takes the form

$$I = \frac{Ne^2}{L4\pi^2}\,\frac{\hbar\omega_o}{2\varepsilon_o}\left[\frac{1}{k_\infty} - \frac{1}{k_o}\right] \times \left[\frac{2\pi}{a}\right]^4 \times \frac{4}{a^2}\, k \qquad 2$$

where the integral k is given by

$$K = \int_{-\infty}^{+\infty} \frac{\sin^2(q_x a/2)\, G^2(q_y)}{q_x^2\left[q_x^2 - \left[\frac{2\pi}{a}\right]^2\right]^2\left[q_x^2 + b^2\right]}\, dq_x dq_y \qquad 3$$

with

$$b = |k-k'|^2 + q_y^2 \qquad 4$$

We can perform the q_x integration

$$\int_{-\infty}^{+\infty} \frac{(e^{iqa}-1)(e^{-iqa}-1)}{4q^2\left[q^2 - \left[\frac{2\pi}{a}\right]^2\right]^2\left[q^2+b^2\right]}\, dq \qquad 5$$

$$= \oint_{-\infty}^{+\infty} \frac{(1-e^{-iqa})\,dq}{4q^2\left[q^2 - \left[\frac{2\pi}{a}\right]^2\right]^2\left[q^2+b^2\right]} + \oint_{-\infty}^{+\infty} \frac{(1-e^{iqa})\,dq}{4q^2\left[q^2 - \left[\frac{2\pi}{a}\right]^2\right]^2\left[q^2+b^2\right]} \qquad 6$$

By changing the variable of integration from q to -q' in the second integration we see that both integrals are the same. We look at the second integral in the upper half complex plane. The integrand has poles at q=0, $q= \frac{\pm 2\pi}{a}$ and q= ±ib. We complete the contour in the upper half complex plane as $e^{iqL} \longrightarrow 0$ as $q \to i\infty$, satisfying Jordan's Lemma. This contour A, takes the form

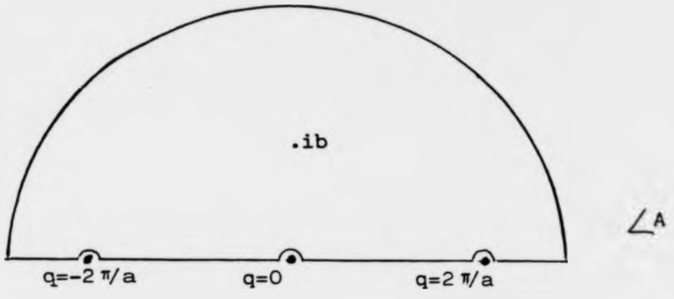

The integral around the contour A

$$\oint_A = 2\pi i \text{ Res} \left[\frac{(1-e^{iqa})}{4q^2 \left[q^2 - \left[\frac{2\pi}{a}\right]^2\right]^2 (q+b^2)} \right]_{q=ib}$$

$$= \frac{-\pi \left[1-e^{-ba}\right]}{4b^3 \left[b^2 + \left[\frac{2\pi}{a}\right]^2\right]^2}$$

We split the contour up into it's constituent elements. Schematically

$$\oint_A = \lim_{\Delta \to 0} \left[\int_{-\infty}^{\frac{-2\pi-\Delta}{a}} + \underset{q=\frac{-2\pi}{a}}{\cdot} + \int_{\frac{-2\pi+\Delta}{a}}^{-\Delta} + \underset{q=0}{\cdot} + \int_{\Delta}^{\frac{2\pi-\Delta}{a}} + \underset{q=\frac{2\pi}{a}}{\cdot} + \int_{\frac{2\pi+\Delta}{a}}^{\infty} \right]$$

we look at the contribution from the poles at q=0,

The residue at the zero pole is

$$\frac{-\pi a}{4b^2\left[\frac{2\pi}{a}\right]^4}$$

and the residue at $q=\frac{2\pi}{a}$ is equal to the residue at $q=\frac{-2\pi}{a}$

$$= \frac{-\pi a}{16\left[\left[\frac{2\pi}{a}\right]^2 + b^2\right]\left[\frac{2\pi}{a}\right]^4}$$

Hence we find that the q_y integration remaining in (3) reduces to

$$k = \int_{-\infty}^{+\infty} \left[\frac{-\pi(1-e^{-ba})}{2b^3(b^2+\left[\frac{2\pi}{a}\right]^2)^2} + \frac{\pi a}{2b^2}\left[\frac{a}{2\pi}\right]^4 + \frac{\pi a\left[\frac{a}{2\pi}\right]^4}{4\left[\left[\frac{2\pi}{a}\right]^2 + b^2\right]} \right] G^2(q_y)dq_y$$

This integral has been evaluated numerically. The results have been checked against an analytic time for large $\underline{k}-\underline{k}'$ and found to be accurate.

APPENDIX 4

THEORY OF PSEUDOPOTENTIALS

Introduction

Pseudopotentials were originally developed because experimental evidence indicated that conduction band electrons in some metals only interacted weakly with the ion cores. It was usually argued that the low resistivity of metals was due to the periodic nature of the lattice, which allowed Bloch states to exist. In some liquid metals however the resistivity is only increased by 20-30% from the value in its crystalline counterpart (Harrison (1965)) indicating a weak electron ion scattering coefficient.

With this knowledge it is natural to attempt a solution of the Schroedinger equation in terms of a simple set of free electron eigenstates. Herring (1958) gave an explanation of this based on orthogonalised plane waves. If $V(\underline{R})$ is the total self-consistent field seen by each electron then

$$H\psi_i = (T+V(R))\psi_i = E_i\psi_i \qquad 1$$

where T is the kinetic energy, $-\hbar^2k^2/2m$ and E_i is the total energy of the i'th state. Now the core states which we label with α satisfy the same equation

$$(T+V(R))\psi_\alpha = E_\alpha \psi_\alpha \qquad 2$$

The conduction band states need to have a plane wave type character away from the core and they must be orthogonal to the core states. Herring expands the conduction band wavefunction in terms of a set of orthogonalised plane waves. These are simply plane waves which have been made orthogonal to all the core states, $|\alpha\rangle$:

$$|k\rangle_{opw} = |\underline{k}\rangle - \sum_\alpha |\alpha\rangle\langle\alpha|\underline{k}\rangle = (1-P)|\underline{k}\rangle \qquad 3$$

where P is the projection operator

$$P \equiv \sum_{\alpha} |\alpha\rangle\langle\alpha| \qquad 4$$

Expanding the conduction-band eigenstates in terms of a general linear combination of OPWs

$$\psi_{\underline{k}} = \sum_{\underline{q}} a_q(k)(1-P)|k+q\rangle \qquad 5$$

when this is substituted into the Schroedinger equation (1) we obtain

$$\sum_{q} a_q(k)H(1-P)|k+q\rangle = E_k \sum_{q} a_q(k)(1-P)|k+q\rangle \qquad 6$$

If we take the terms involving P to the left hand side we have

$$T\phi_k + W\phi_k = E_k\phi_k \qquad 7$$

where W is the pseudopotential defined by

$$W = V(R) + \sum_{\alpha} (E_k - E_\alpha)|\alpha\rangle\langle\alpha| = V(R) + (E_k - H)P \qquad 8$$

and $\phi_{\underline{k}}$ is the pseudowavefunction

$$\phi_k = \sum_{q} a_{\underline{q}}(\underline{k})|\underline{k}+\underline{q}\rangle \qquad 9$$

The true wavefunction is related to the pseudowavefunction by

$$\psi_k = (1-P)\phi_k \qquad 10$$

Equation (7) is an effective Shroedinger equation which has the same eigenvalues as the true equation.

Atomic Pseudopotentials

It is usual to represent W by a sum of pseudopotentials associated with the ions in the solid. Animalu and Heine (1965) give a simple model potential for an ion which is fitted to spectroscopic data. It has the expected

coulombic tail at large distances and inside some critical radius R_c , the potential was taken to be constant, removing the coulombic singularity of the true ionic potential. The depth of the well inside the radius R_c was dependent on the angular momentum quantum number , and it was also taken to have an energy dependence. The potential takes the form,

$$V(R) = -\sum_{\ell} A\, P_{\ell} \quad , R<R_c$$

$$= \frac{-z}{4\pi\epsilon_o R} \quad , R>R_c \qquad 11$$

where P_{ℓ} is the projection operator of the l'th angular momentum component. The radial Schroedinger equation takes the form

$$\frac{\hbar^2}{m}\frac{d^2\chi(R)}{dR^2} - \left[\frac{(\ell+1)\ell\hbar^2}{R^2 m} - \left[\frac{2A_{\ell}}{2z/4\pi\epsilon_o R}\right] - 2E\right]\chi(R) = 0 \qquad 12$$

The A_{ℓ} were adjusted to fit known specroscopic values. More recently Bachelot, Hamann and Schluter have derived a set of pseudopotentials which are transferable between systems (Si molecules, Northrup E., Ihm J. and Cohen M. L. (1981) and phonon frequencies in Ge, Yin M. T. and Cohen M. L. (1980)). The Bachelot, Hamann and Schluter pseudopotentials have several advantages over the Animalu potentials. They generate the true valence wavefunction beyond some core radius and secondly inside some core radius they duplicate the scattering property of the true potential. As we are discussing electron scattering this is just what is needed.

Scattering from an Impurity Atom

The time independent pseudo-Schroedinger equation may be written as

$$(T+V(R))\psi_k = \frac{i\hbar\partial\psi_k}{\partial t} \qquad 13$$

If $V(\underline{R})$ is periodic then the eigenstates will be Bloch functions, but because $V(\underline{R})$ is weak these will approximate to plane waves to first order. These must have eigenvalues given by

$$\epsilon(k) = \frac{\hbar^2 k^2}{2m^*} \qquad 14$$

where m* is the effective mass of the electrons. We consider the scattering by a single impurity atom, which changes the pseudopotential by $\Delta V(\underline{R})$. To look at the scattering probability between eigenstate $|\underline{k}\rangle$ and $|\underline{k}+\underline{q}\rangle$, we use the time-dependent perturbation theory result.

$$P(k,k+q) = \frac{2\pi}{\hbar} |\langle k|\Delta V(R)|k+q\rangle|^2 \delta(\epsilon(k)-\epsilon(k+q)) \qquad 15$$

We are particularly interested in the scattering of electrons off isoelectronic substitutional impurities in particular aluminium in the GaAs crystal. To evaluate (15) with l dependent pseudopotentials we expand the plane-wavefunctions in terms of spherical harmonics (Harrison (1965)),

$$e^{i\underline{k}\cdot\underline{R}} = \sum_{l=0}^{\infty} (2l+1) i^l j_l(kR) P_l(\cos\theta_1) \qquad 16$$

where θ_1 is the angle between $\underline{k}$ and $\underline{R}$. The matrix element for the Animalu-Heine pseudopotentials is given by

$$\langle k+q|V_{AB}|k\rangle = \frac{4\pi}{V}(2l+1)A_l P_l(\cos\theta) \int_0^{RM} j_l(|k+q|R) j_l(|k|R) R^2 dR$$

$$- \frac{4\pi}{V} \frac{ze^2\cos q R_m}{4\pi\epsilon_0 q^2} \qquad 17$$

where θ is now the angle between $\underline{k}$ and $\underline{k}+\underline{q}$. The matrix element due to the substitution of an aluminium ion onto a Gallium site is given by

$$M_{AB} = \langle k+q| V_{AB}^{Al} - V_{AB}^{Ga} |k\rangle$$

$$= -\frac{4\pi}{V}\sum_{l}(2l+1)P_l(\cos\theta)\left[A_l^{Al}\int_0^{Rm} j_l(|k+q|R)j_l(|k|R)R^2\,dR\right.$$

$$\left. -A_l^{Ga}\int_0^{R_m} j_l(|k+q|R)j_l(|k|R)R^2dR\right|$$

$$+\frac{ze^2}{V\varepsilon_0 q^2}\left[-2\sin\frac{q(R_m^{Ga}+R_m^{Al})}{2}\sin\frac{q(R_m^{Ga}-R_m^{Al})}{2}\right] \qquad 18$$

If the arguments of the Bessel functions are small then as

$$j_l(\rho) \xrightarrow[\rho\to 0]{} \frac{\rho^l}{(2l+1)!!}$$

we find that only the l=0 component contributes to the summation (18). This type of sharply confined potential is sometimes termed an s-wave scatterer (Sernelius et al (1985)). We find

$$M_{AB} = -\frac{4\pi}{V}\left[A_o^{Al}\int_0^{R_m^{Al}} R^2dR - A_o^{Ga}\int_0^{R_m^{Ga}} R^2dR\right]$$

$$+\frac{ze^2}{V\varepsilon_0}\frac{R_m^{Al\,2} - R_m^{Ga\,2}}{2}$$

The value of M_{AH} is just equal to the volume integral of the difference between the two l=0 pseudopotentials. The values of A_o were taken from Harrison's book (Harrison (1965)).

The pseudopotentials due to Bachelot et al are expected to give better results. The l=0 pseudopotential components for Gallium and Aluminium are plotted in Figure 8.2 with the difference shown in Figure 8.2c. These graphs were obtained from a slightly modified version of a program supplied by Dr B Holland and data from Bachelot's paper. The results of the program were checked against Bachelot's silicon data. The volume integral under the difference curve was obtained numerically.

REFERENCES

Abramowitz M, Stegun I (1964), (Dover, New York)

Adachi S (1985), J Appl Phys 58, R1

Adler S L (1962), Phys Rev 126, 413

Ando T (1982), Rev Mod Phys 54, No 2

Andreoni W, Car R (1980), Phys Rev B 21, 3334

Animalu (1965), see Harrison's book

Arora V K, Awad F G (1981), Phys Rev B 23, 5570

Bachelot G B, Hamann D R, Schluter M (1982), Phys Rev B 26, 4199

Baldereschi A, Hopfield J J (1972), Phys Rev Lett 28, 171

Baldereschi A, Tosatti E (1978), Phys Rev B 17, 4710

Baldereschi A, Car R, Tosatti E (1979), Solid State Comm 32, 757

Baldereschi A, Tosatti E (1979), Solid State Comm 29, 131

Bardeen J, Shockley W (1951), Phys Rev 80, 72

Bastard G (1983), Appl Phys Lett 43, 591

Basu P K, Nag B R (1981), J Phys C 14, 1519

Basu P K, Nag B R (1983), Appl Phys Lett 7, 689

Basu P P, Chattopadlyoy D, Sarkar C K (1986), J Phys C 19, L173

Bridges R T (PhD Thesis, Warwick University)

Butcher P N (1973), Vienna IAEA

Butcher P N (1986), Vienna IAEA

Cantrell D G, Butcher P N (1985), J Phys C 18 5111

Collins S, Lowe D and Barker J R (1985), J Phys C 18 L637

DiLorenzo J V, Dingle R (1982), IEDM 82 (IEEE)

Dohler (1983), 5th Int Conf on Two-dimensional Systems, Oxford

Esaki L, Chang L L (1974), Phys Rev Lett 33 495

Fedders P A, Myles C W (1984), Phys Rev B 29 802

Fletcher K, Butcher P N (1972), J Phys C 15, 212

Freeman W L, Gettys W E (1977), Phys Rev B 17 529

Frohlich H (1937), Proc Roy Soc A160, 230

Glicksmann M, Enstrom R E (1974), Phys Rev B9, 1621

Greene P D, Wheeler S A, Adams A R (1979), Appl Phys Lett 14, 1519

Harrison W A (1965) (Benjamin W A; New York)

Harrison J W, Hauser J R (1976), J Appl Phys 47, 292

Heine V, Abarenkov I (1964), Phil Mag 9, 451

Herring C (1958), Phys Rev 110, 14

Jackson J D Classical Electrodynamics (1962) (John Wiley: New York)

Johnson L, Vassell (1984), J Phys C 17 2525

Joyce B (Phillips Research Laboratories), private communication, 1986

Kelly M J (1984), IOP meeting on localisation

Kohler M (1948), Z Phys 124, 772

Kearney M J (1986), J Phys C, 19, 5429

Lee P A, Ramakrishnan J T (1985), Rev Mod Phys 57, 287

Littlejohn M A, Hauser J R, Glisson T H, Ferry D K, Harrison J W (1978)
Solid State Electronics 21, 107

Luttinger J M, Kohn W (1955), Phys Rev 97, 869

Marsh A C, Inkson J C (1984), J Phys C 17 6561

Milsom P K, Butcher P N (1986), J Semiconductor Sci and Tech 1

Mott N F (1936), Proc Camb Phil Soc, 32, 281

Nag B R (1972), Theory of electrical transport in semiconductors (Pergamon Press: Oxford)

Nordheim L, Annalen der Physic (1931) I9 607

Northrup J E, Ihm J, Cohen M L (1981), Phys Rev Lett 47, 1910

Nye J F (1967), Physical properties of crystals OUP

Ogale S B, Madhukar A (1984), J Appl Phys 56, 388

Ogrin Yu F, Lutskii V N, Elinson M I (1966), Sov Phys JETP Lett 3 71

Okumura H, Misawa S, Yoshida S, Gonda S, Appl Phys Lett (1985) 46, 377

Palmer J F, Chomette A (1982), J Phys 43, 381

Penn D R (1962), Phys Rev 128, 2093

Riddoch F A, Ridley B K (1985), Physica 134B, 42

Ridley B K (1982a), J Phys C 15, 5899

Ridley B K (1982b), Quantum processes in semiconductors (Oxford: Clarendon Press)

Ridley B K (1983), 5th International Conference on two-dimensional systems, Oxford

Ridley B K (1985) LDS Summer School, Nottingham

Ridley B K and Watkins, Proc. Phys. Soc. (London) 78, 293, (1961)

Rode D L (1970), Phys Rev B 2, 1012

Rode D L (1975), Semiconductors and semimetals, ed R K Williardson and A C Beer (New York: Academic) Vol 10, 15-26

Rode D L, Fedders P A (1983), J Appl Phys 11, 6425

Saxena A K, Adams A R (1985), J Appl Phys 58, 2640

Seeger K (1973), Semiconductor Physics (New York Wien: Springer Verlag)

Sernelius B E, Bergren K F, Tomak M, McFadden C (1985), J Phys C 18, 225

Siggia E D, Kwok P C (1970), Phys Rev B 2, 1024

Smith A C, Janak J F, Adler R B (1967), Electronic conduction in solids (New York: McGraw-Hill)

Sondheimer E H, Howarth D J (1953), Proc Roy soc A219, 53

Stormer H L, Gossard A C, Wiegmann W (1982), Solid State Comm 41, 707

Stringfellow G B (1979), J Appl Phys 50, 4178

Tosatti E (1986), private communication

Vinter B (1982), Phys Rev B 26, 6808

Vinter B (1984), Appl Phys Lett 45, 581

Vinter B (1986), private communication

Walter J P, Cohen M (1971), Phys Rev B 4, 1877

Warren G J, Butcher P N (1986), Semiconductor Science and Technology, 1, 133

Yin M T, Cohen M L (1980), Phys Rev Lett 45, 1004

Ziman J M (1960), Electrons and Phonons (Clarendon Press; Oxford)

Zook J D (1964), Phys Rev B 136, A869

TITLE Electron Transport in Systems of Reduced Dimensionality

AUTHOR Philip Keith Milsom

University of Warwick (1987)

UNIVERSITY

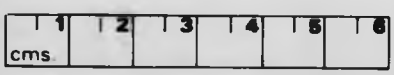

REDUCTION X 12

CAMERA 7